

COMPUTER AIDED DESIGN OF FERRO-ELECTRIC INSULATORS

BY

NIPENDU SEKHAR BISWAS

A THESIS

SUBMITTED TO THE DEPARTMENT OF ELECTRICAL AND ELECTRONIC
ENGINEERING IN PARTIAL FULFILMENT OF THE REQUIREMENTS

FOR THE DEGREE
OF

MASTER OF SCIENCE IN ENGINEERING

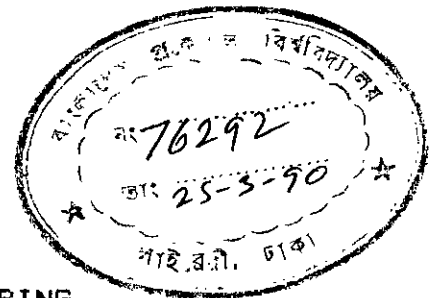
DEPARTMENT OF ELECTRICAL AND ELECTRONIC ENGINEERING
BANGLADESH UNIVERSITY OF ENGINEERING AND TECHNOLOGY

DHAKA

JANUARY 1990



#76292#



623.1937
1990
BIS

CERTIFICATE

This is to certify that this work was done by me and it has not been submitted elsewhere for the award of any degree or diploma.

Signature of the student.

Nipendu Sekhar Biswas

(NIPENDU SEKHAR BISWAS)

The thesis titled , "COMPUTER AIDED DESIGN OF FERRO-ELECTRIC INSULATORS" submitted by Nipendu Sekhar Biswas, Roll no. 861301P of Msc. Engineering, Dept of Electrical and Electronic Engineering has been accepted as satisfactory for partial fulfilment of the requirements for the degree of Master of Science in Engineering (Electrical and Electronic)

BOARD OF EXAMINERS

- 1 *m. A. Matin* 27.1.1990
Dr. Md. Abdul Matin (Supervisor)
Professor
Department of Electrical and
Electronic Engineering
BUET, Dhaka
Chairman
- 2 *m. A. Matin* 27.1.1990
Head
Department of Electrical and
Electronic Engineering
BUET, Dhaka
Member
- 3 *T. Chowdhury*
Dr. Taifur Ahmed Chowdhury
Assistant Professor
Department of Electrical and
Electronic Engineering
BUET, Dhaka
Member
- 4 *E. Basher* 27.1.1990
Dr. Enamul Basher
Associated Professor
Department of Electrical and
Electronic Engineering,
BUET, Dhaka
Member
- 5 *A. M. Zahoorul Haq*
Professor A.M. Zahoorul Haq
Plot No. 391, Road No. 6
Baitul Aman Housing Society
North Adabar
Shamoli, Dhaka
Member
(External)

ACKNOWLEDGEMENT

The author expresses his indebtedness, deep sense of gratitude and profound respect to his supervisor, Dr. Md. Abdul Matin, Professor & Head of the Department of Electrical & Electronic Engineering, BUET, Dhaka for his continuous guidance, suggestions, constant encouragement and whole-hearted supervision throughout the progress of this work.

Most of the computation works were performed at the computer center, BUET. The author is thankful to the Director and personnels of the computer center, BUET for their cooperation.

Finally the author expresses thanks to all staff and personnels of the Faculty of Electrical and Electronic Engineering for help and assistance.

ABSTRACT

Computer aided design of ferro-electric insulators is mostly a theoretical method of designing insulators. With the help of computer and some analytical techniques some of the conventional insulators are analyzed.

First the electromechanical stress distribution for ferroelectric material was calculated using finite element method. In order to formulate the finite element method, the region between two circular parallel plates has been divided into a finite number of triangular elements. An extremum function in energy density form can be developed. Then using energy minimization technique, the potential at different vertices of the elements can be calculated.

A computer program has been developed for calculating electric field and electromechanical stresses for ferro-electric material placed between two circular parallel plates. The program can be readily used for designing ferro-electric insulators subject to variable electromechanical stresses.

COMPUTER AIDED DESIGN OF
FERROELECTRIC INSULATORS

INDEX

	Page No.
CHAPTER 1 : GENERAL INTRODUCTION	
1.1 : Importance of Insulators	2
1.2 : Brief Literature Review	3
1.3 : Present State of Art of the Project	6
1.4 : Objective of the Research	6
1.5 : Research Outline.	7
CHAPTER 2 : FERRO-ELECTRICITY AND INSULATORS	
2.1 : Introduction	9
2.2 : Ferroelectricity	10
2.3 : Ferroelectric Insulators	14
2.3.1 : Pintype Insulators	15
2.3.2 : Disc type Insulators	17
2.3.3 : Post type Insulators	19
2.3.4 : Shackle Insulators	21
2.3.5 : Problems with conventional Insulators	21
2.3.6 : D.C. Insulators	25
2.4 : Discussion.	27

CHAPTER 3	: THEORETICAL ASPECTS OF DESIGNING FERROELECTRIC INSULATORS	
3.1	: Introduction	29
3.2	: Evaluation of Potential Distribution by Finite Element Method	31
3.3	: Electromechanical Stress Analysis.	41
3.4	: Electromechanical Stress Distribution in a Ferroelectric Material between Two Thin Circular Electrodes	46
3.5	: Discussion.	63
CHAPTER 4	: DESIGN OF FERROELECTRIC INSULATORS	
4.1	: Introduction	66
4.2	: Finite Element Design of a Pintype Insulator	67
4.3	: Finite Element Design of a Disc type Insulator	75
4.4	: Discussion.	85
CHAPTER 5	: GENERAL DISCUSSION AND SUGGESTION FOR FUTURE WORKS.	87
	COMPUTER PROGRAM	94
	REFERENCES	127

LIST OF PRINCIPAL SYMBOLS

\vec{E}	Electric stress or field vector (Volts/m)
\vec{D}	Electric flux density (Coulomb/m ²)
ρ	Charge density (Coulomb/m ³)
ϵ_r	Relative permittivity
ϵ_0	Permittivity of free space (Farad/m)
Φ	Potential (Volts)
J	Extremum function
S_e	Element submatrix
\hat{S}	Electromechanical stress tensor
$S_{i,j}$	Components of tensor \hat{S}
\vec{i}	Unit column vector
\vec{F}	Electro-mechanical force (Newton)
\vec{n}	Unit outward normal to a surface or contour
\vec{P}	Polarization (Coulomb/m ²)
\vec{t}	Electro-mechanical stress vector (N/m ²)
P_r	Remanant polarization (Coulomb/m ²)
ϵ_{r0}	Dielectric constant at very weak field
\vec{E}_s	Saturation electric field of ferro-electric material (Volts/m)
\vec{E}_0	Applied Electric field (Volts/m)

CHAPTER 1
GENERAL INTRODUCTION

GENERAL INTRODUCTION



1.1 Importance of Insulators:

In any typical part of power system we can see that it comprises four types of materials namely :- conductors, insulators, magnetic materials and structural materials. Undoubtedly, the most complex of the four are the insulators. Its duty is to ensure the safe operation of diverse power components as large generators, power transformers, power capacitors, circuit breakers , overhead transmission lines and underground cables. The insulator has twofold functions one for insulating and the other for giving mechanical support for the live parts of power system equipment under any possible circumstances in field such as wind, snow, rain, contamination, earthquake and so on. Therefore, it is not too much to say that reliability of power system depends upon the quality and reliability of insulators.

1.2 Brief literature review:

In order to reduce the losses in power system the trend of increasing transmission voltage is increasing day by day. So, for obtaining a reliable power system we need more reliable insulators. Increase in voltage causes increase in size of system apparatus. Improvement and compactness of design of system apparatus can reduce the cost and saving of energy resources. Moreover, the insulators are used for electrical insulating purpose as well as for mechanical support and the potential applied to it causes electrical and mechanical stresses. So for optimising and to get a reliable insulator it should be designed to withstand higher electromechanical stresses.

The insulation technology has reached the present position after a long years of study and research. In high voltage insulators space charge and its distribution can cause undesirable effects. Various effects of space charge in insulators have been summarised by Ieda [1]. He showed that the developed space charge alters the distribution profile of the field in comparison with the original field. It is known that the formation of space charge depends whether the field is uniform or non-uniform. The measurement of space charge distribution and interfacial electric fields are important for understanding the mechanism of charge build-up and decay.

The study of electric field distribution in and around insulating structures has been of considerable interest to electrical engineers for designing high voltage equipment. The peak stress value in an insulating system is an important parameter to control, because it influences discharge initiation and propagation. Compaction and miniaturization of high voltage system with resulting increased operating stress levels have made the study of electric stress distribution even more critical. Moreover physical systems are so complex that the analytical solution of Laplace's and Poisson's equations is difficult. But with the increasing availability of high speed computers ~~and~~ various numerical techniques are being extensively developed for calculating electrostatic fields in high voltage systems. Mukherjee and Roy [2] calculated fields in insulators using fictitious point charge method and they were successful in applying this method for disc insulators. Chang [3] analyzed the electric stress distribution in cavities embedded within dielectric structures and he shows that the field inside the void is enhanced by a factor ϵ_r , the relative dielectric permittivity of the insulator, in the case where no free charge is present at the void boundary. Takeshi [4] used charge simulation method in combination with the method of image to find electric fields in dielectric multilayers. Tadasu [5] successfully applied charge

simulation method to study the field behaviour at points on the boundary of two dielectrics. Takada and Sakai [6] were successful in determining electric fields at the dielectric electrode interface. Kun [7] suggests that the field distribution along the insulator surface is strongly dependent on the ρ -E characteristic as well as frequency of the operating voltage.

High tangential fields causes flashover along insulator surface. To keep tangential field below the limit required for a sustained discharge, the insulator length has to be a minimum value for a given voltage rating. Abdel-Salam [8] found that to optimize a high voltage insulator, the distribution of the tangential field component along its surface should be uniform.

Stih [9] formulated a classical approach to high voltage insulating system design using an integral equation technique for solving electric fields and optimizing the contours of the insulator.

1.3 Present state of art of the project

All porcelain or ceramic insulators used in high voltage power system as well as telephonic and telegraphic lines are ferro-electric insulators. These insulators are mostly designed by testing for mechanical breakdown stress and electrical flashover tests. No rigorous mathematical solutions for such design is available. A classical approach of designing high voltage insulators was carried by Stih [9] using integral equation techniques for solving electric stress and contour optimization. But if the hysteresis effect arising from ferro-electric property of the material is considered, a rigorous mathematical operation is needed. Begg [10] formulated the electromechanical stress analysis considering the hysteresis effect of ferro-electric materials.

1.4 Objective of the research:

The objective of this study is to evaluate the electromechanical stress distribution associated with the time periodic electric fields applied on ferro-electric insulators of finite size and to obtain an acceptable design in terms of breakdown stress, flashover voltage and electrostriction.

1.5 Research outline:

To design a high voltage insulator, electromechanical stress calculation is the first step. In doing so, the insulator region will be divided into finite nos. of triangular subregions called elements. Then the potential distribution and electromechanical stresses can be obtained using finite element method and developing an energy distribution function in variational form for the system under consideration.

CHAPTER 2
FERRO-ELECTRICITY AND INSULATORS

FERRO-ELECTRICITY AND INSULATORS

2.1 Introduction:

In dielectric material an applied electric field induces dipole moments in atoms or ions and generally displaces ions relative to each other. Consequently the dimension of a specimen undergoes slight changes. Mechanical stresses also change the dimensions of a specimen but in general such changes do not produce a dipole moment. In other words, in most materials dielectric polarization produces a mechanical distortion, but a mechanical distortion does not produce polarization. This electro-mechanical effect, which is present in all materials, is called electrostriction [13].

Ferro-electric materials are characterised by electrostriction arising from their spontaneous or residual polarization. There are various types of ferro-electric materials that are used in high voltage insulators because of their high relative permittivity. Barium titanate ($BaTiO_3$) is an important ferro-electric material that is used in fabrication of high quality AC and DC insulators used in HV power transmission.

2.2 Ferro-electricity

For the dielectric material the polarization is a linear function of the applied field. There are however, a number of substances for which the polarization of a specimen depends on its history i.e. the polarization in these materials is not a unique function of the field strength. These materials exhibit hysteresis effect, similar to those observed in ferromagnetic materials - they are therefore called ferro-electric materials [13].

An example of a hysteresis loop associated with the polarization versus electric field strength is given in fig. 2.1, when an electric field is applied to a "virgin" specimen of a ferroelectric material, the polarization increases along a curve OABC. When the field is reduced, it is observed that for $E_0 = 0$, a certain amount of remanent polarization, P_r is still present.

In other words, the material is spontaneously polarized. In order to make polarization to zero, a field in the opposite direction must be applied; this field is called the coercive field, E_c .

The direction of spontaneous polarization is generally not the same throughout the macroscopic specimen. In fact, the specimen may be considered to consist of a number of domains which are themselves spontaneously polarized but with the direction of polarization varying from one domain to another.

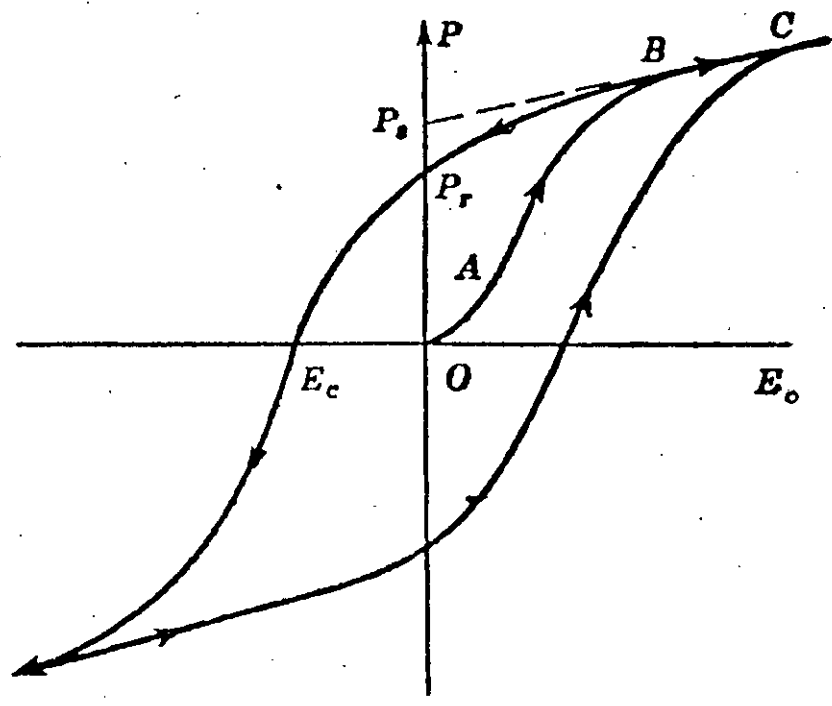


Fig: 2.1 HYSTERESIS CURVE FOR FERROELECTRIC MATERIAL

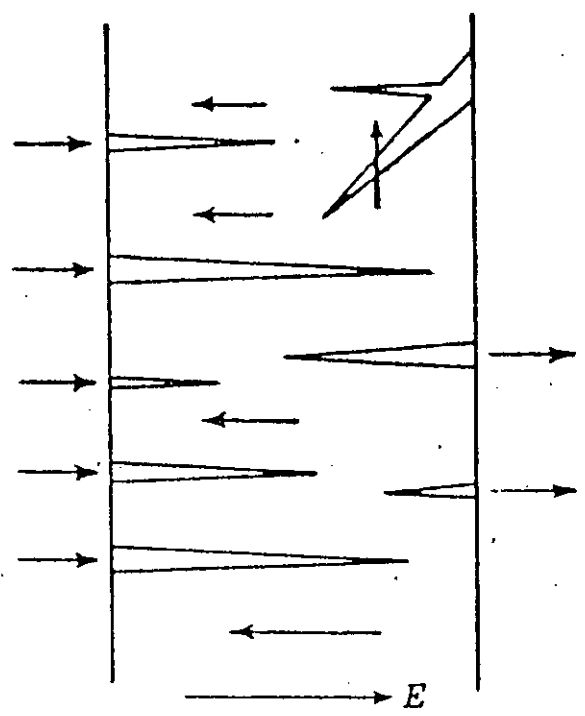


Fig: 2.2 DOMAINS SHOWING POLARIZATION

Thus a virgin macroscopic specimen may have zero polarization as a whole. Upon application of an electric field, the domains for which the polarization points along the direction of the applied field grow at the expenses of other domains for which the polarization points in the other direction (Fig 2.2).

Barium titanate (BaTiO_3) is the best known ferro-electric material commonly used in the fabrication of HV insulators/capacitors with multilayered structure. Their high permittivity enables fabrication of capacitors with high capacitance and insulators with good quality. There are three types of BaTiO_3 materials commonly used in insulators. These are NPO ($\epsilon_r = 60$), X7R ($\epsilon_r = 1800$) and ZSU ($\epsilon_r = 9000$). The permittivity of ferro-electric materials depend on the temperature. A typical temperature dependence of BaTiO_3 ceramic is shown in Fig.2.3.

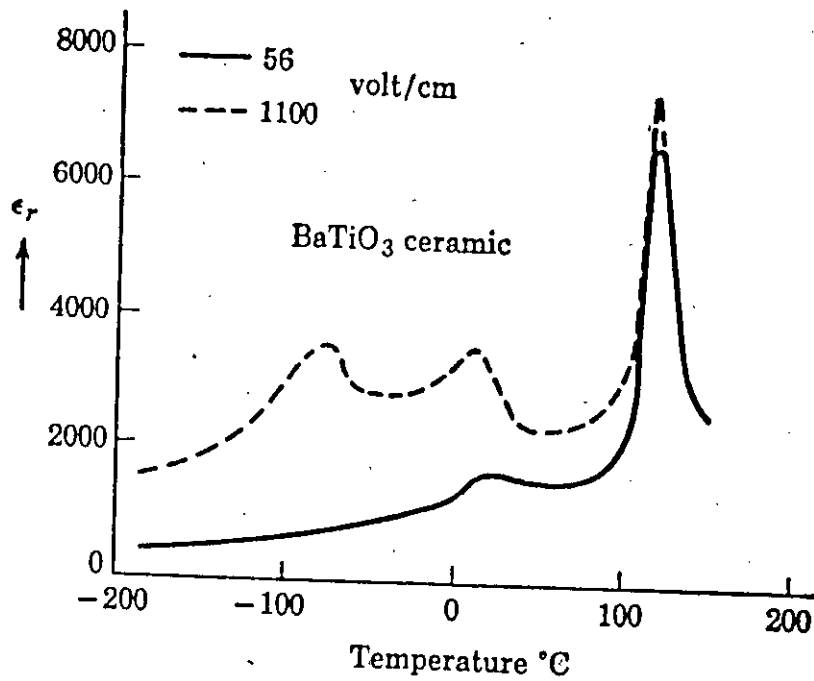


Fig. 2.3. Dielectric constant of barium titanate ceramic as a function of temperature. The fully drawn and the dashed curves correspond respectively to a peak field strength at 1 kc of 56 and 1100 volts per cm. The sharp peaks occur at the ferroelectric Curie temperature θ_f .

2.3 Ferro-electric insulators

The material most commonly used for high voltage insulators is porcelain. It has high insulating resistivity and undergoes hysteresis effect with the application of electric fields. So, we can say that most of the high voltage insulators are manufactured from ferro-electric materials. The dielectric strength of mechanically sound porcelain insulator is of the order of 12KV/mm to 28KV/mm. The ultimate strength of such insulator is for compression 275 KN and for tension 20 KN. Though the tensile strength is lower but most of the insulators are designed in such a way that it undergoes compressive stresses most of the time.

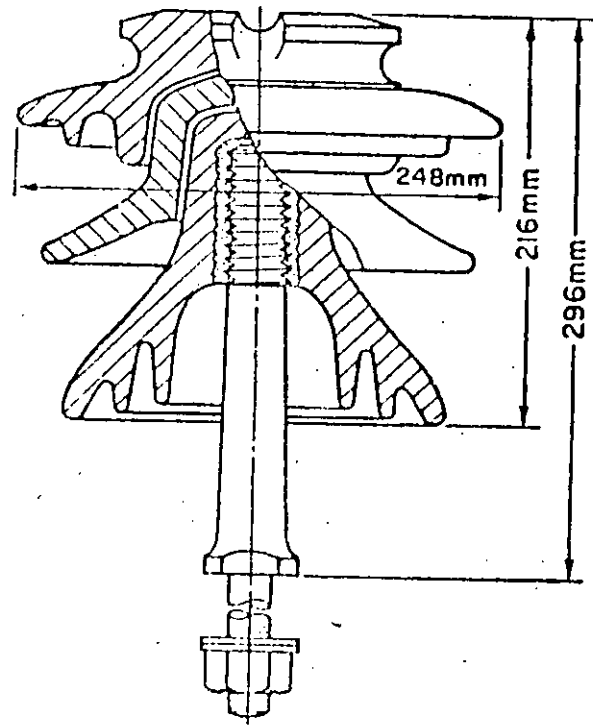
The second material that is used in manufacturing high voltage insulators is glass. Though it has higher dielectric strength, ultimate tensile strength, higher puncture voltage but due to the surface erosion and contamination problem these are not popular. In porcelain insulator these problems are overcome by suitable design.

Insulators are required to withstand both mechanical and electrical stresses. In addition to this, the surface leakage path, even when wet, must have sufficiently high resistance to prevent any appreciable current flowing to earth. So, the insulators must have enough leakage distance. For obtaining sufficient leakage distance and type of application different types of insulators are used in high voltage system. In the following articles some of them are discussed.

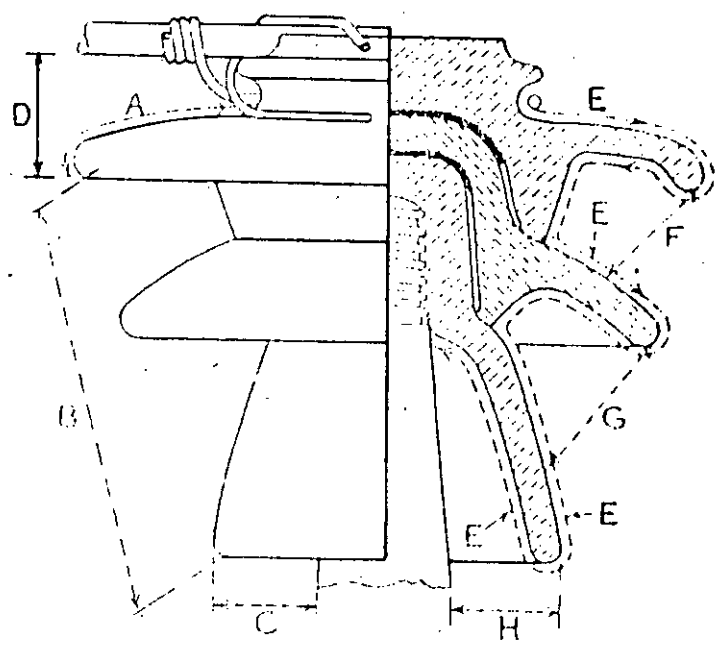
2.3.1: Pin-type Insulators.

Pin-type insulators are of one piece construction and used for operating voltages up to 33KV. As the name suggests, the pin type insulator is attached to a steel bolt or pin which is screwed to the cross arm on the pole or tower. There is a groove on the upper end of the insulator for housing the conductor. The conductor passes through this groove and it is bound by the annealed wire of the same material as the conductor. They are preferred by some users, even at voltages where multi-part insulators are available, because of the comparative absence of cement. An adequate length of leakage path is obtained by the provision of two or three sheds. There should be sufficient thickness of porcelain between the line conductor and the insulator pin to give a factor of safety of up to 10 against puncture. The insulator is designed in such a way that it will sparkover before it punctures. At wet and contaminated condition the sheds become conducting and to avoid sparkover the pin should be sufficiently long.

The insulator and its pin should be sufficiently strong mechanically to withstand resultant force due to the combined effect of weight of span, wind pressure etc. For higher voltages, the thickness of the insulator is to^{be} increased, so, it becomes un-economic. That is why pin type insulators is used up to voltage level of 33KV. A schematic diagram is shown in fig 2.4.



a) Showing pin and dimensions.



b) Showing flashover distance

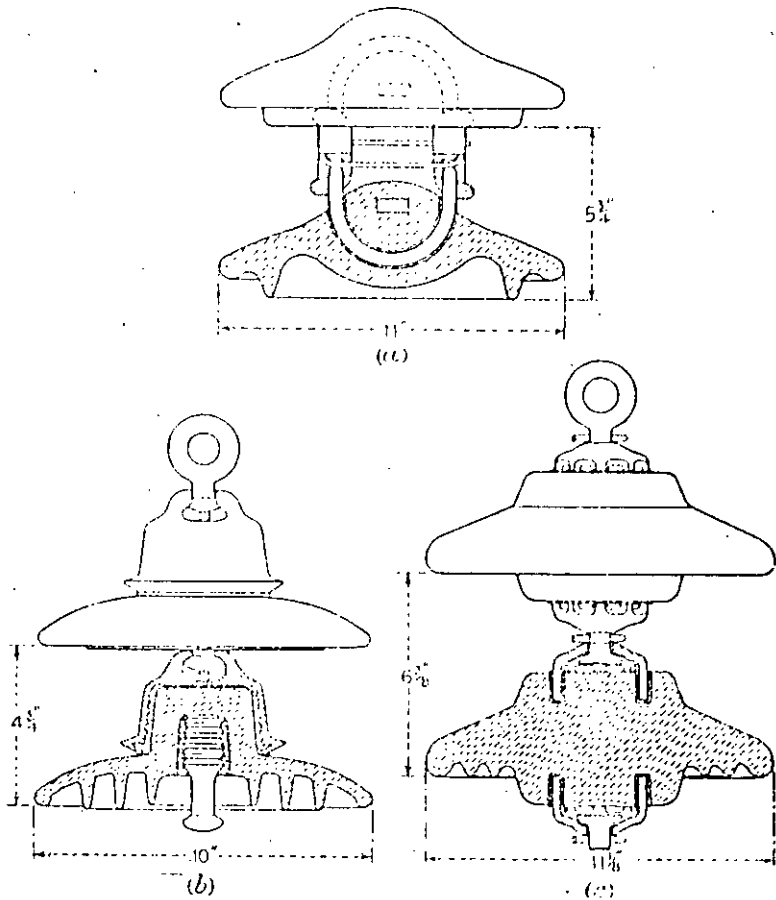
Fig: 2.4. Pin Type Insulator

2.3.2: Disc-type Insulators.

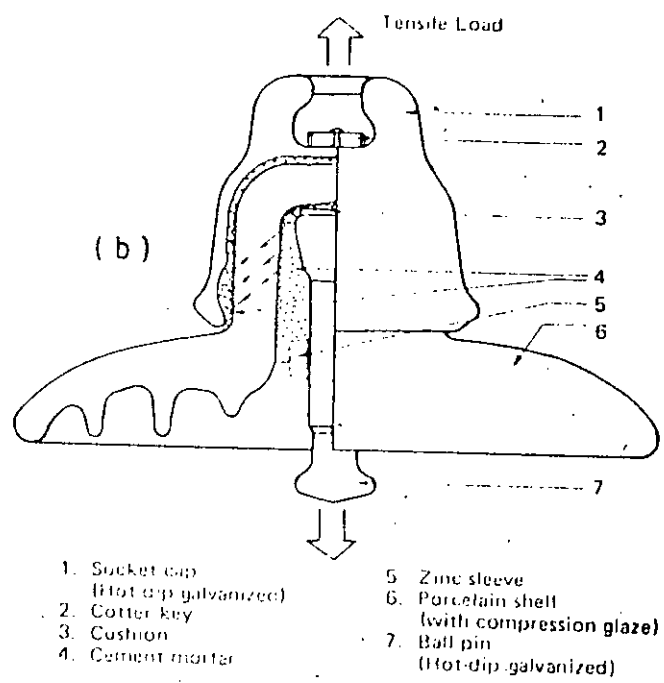
Disc-type insulators are very popular for constructing high voltage lines because of their relatively smaller size and less weight. Each disc is designed for a comparatively low working voltage and the required total insulation is obtained by using a string of suitable number of such insulators. The mechanical stresses on the insulator is less as the insulators are connected flexibly with the tower.

The first disc insulator is the Hewlt type (fig 2.5) and is characterized by great simplicity of design. Each unit consists of a single piece of porcelain, the central portion of which has two curved tunnels laying in planes at right angles to each other. The short steel strips, forming the connectors between individual units, are threaded through these tunnels and thus loop through each other, bending separated by layer of porcelain which is wholly in compression. This method of construction secures a high mechanical strength and there is no risk of breakage by the difference in expansion of conducting links and insulators.

In cap and pin type or cemented cap disc type insulators shown in fig 2.5b, each unit is covered by a metal cap cemented in place, the upper end of each cap terminating in a lug to which the pin of the unit above is fastened. The pins are also cemented in place and consecutive discs are joined together by ball and socket joints. The three materials porcelain, cement and steel



a) Hewlett type (b) Cap and pin type
 c) Core and fine type



- | | |
|---------------------------------------|--|
| 1. Socket cap
(Hot-dip galvanized) | 5. Zinc sleeve |
| 2. Cotter key | 6. Porcelain shell
(with compression glaze) |
| 3. Cushion | 7. Ball pin
(Hot-dip galvanized) |
| 4. Cement mortar | |

Fig: 2.5. Disc Type Insulator

have different co-efficients of expansion and sudden temperature change in service were sufficient to set up internal bursting stresses, which ultimately cracked the insulator. The cement material is subjected to volumetric changes depending on its moisture content and causes fracturing process. Improvements in design overcomes these troubles and cap-and pin disc insulator is giving an excellent service in all parts of the world.

Another type of disc insulator is core and tine insulator as shown in fig 2.5. Each insulator disc is symmetrical and conforms approximately the lines of electric field thus avoiding materials of different permittivities being placed in series. The metal work consists of pressed steel spiders, the legs of which are fastened into the porcelain. It is not easy to produce the necessary thick porcelain discs. That is why the core and tine insulators have fallen into disuse.

2.3.3: Post Insulators:

The post type insulators are very much important for constructing high voltage switching equipments and protection equipment. These are used in constructing the breaking chamber of MOCB, transformer and circuit breaker bushing, current transformers, potential transformer etc. In some places this type of insulators are used as line insulator up to 30KV. A schematic diagram of post type insulator is shown in fig 2.6.

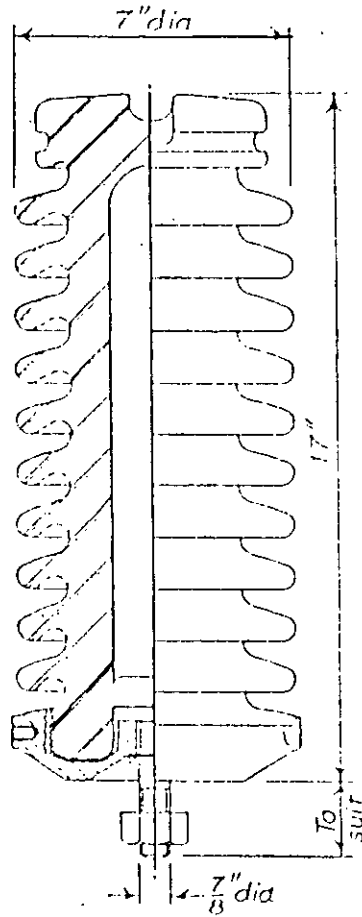


Fig: 2.6. Post Type Insulator

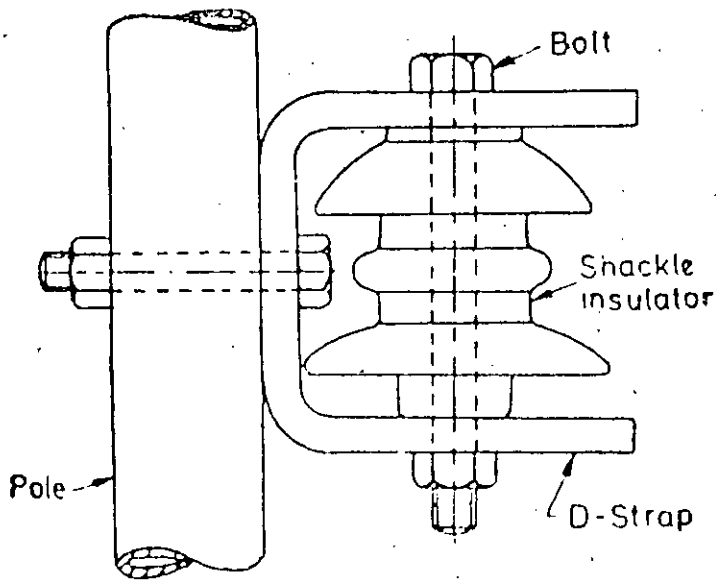


Fig :2.7. Shackle Insulator

The post type insulator is of solid core or hollow construction as per use and have a cylindrical boundary shape. All the metal work and cement is external to the porcelain. So it cannot set up bursting stress. The sheds are designed in such a way that it can be cleaned efficiently by rain. Moreover its great advantage is that if the sheds are broken off by power arc or mechanical damage, the flashover voltage of the insulator is little effected. So, this type of insulator is very useful.

2.3.4: Shackle Insulators.

Shackle Insulators are mostly used in distribution lines . Such insulators can be used either in a horizontal position or vertical position. They can be fixed directly on the pole as shown in fig 2.7. The conductor is fixed in the groove with a soft binding wire.

2.3.5: Problems With Conventional Insulator

The safety and reliability of transmission lines depend on the long term performance of insulators. Insulators must electrically and mechanically remain stable for a long period of service under harsh environmental conditions such as contamination, wind, rain, snow and so on. So, the insulators must be designed in such a way that it must cope with harsh environmental conditions. Some special designs against different causes of insulator deterioration are discussed bellow:

a) Aging of insulating material:

Poor manufacturing technique causes internal defects in the insulating material, resulting in cracking or shattering due to mechanical or electrical stress concentration on the defects during a long term use. The porosity of porcelain occurs due to improper firing technique and reduces electrical and mechanical strength. Improved manufacturing technique together with good quality of insulating material can reduce this problem .

b) Contamination and Erosion of Insulating Material:

A drastic reduction can be seen in withstand or flash-over voltage when the insulator surface is contaminated and wetted. The pollutant accumulation, cleaning of polluted surface, wetted of pollutant layer, leakage current and occurrence of flashover are influenced by the insulator shape, dimensions, atmospheric conditions, voltage stress, pollution source etc. This contamination problem is severe in the coastal and desert area. In heavy contaminated environment, the surface deterioration of insulating material occurs due to surface erosion, in the worst case, resulting complete failure of insulating material. The erosion is caused by leakage current on the insulators.

The anti-contaminated insulators are designed to provide less contaminant accumulation on surface, to keep surface dry and to increase the leakage distance. There are some anticontaminated designs of disc type insulators namely aerodynamic or profile type and fog type insulators as shown in fig 2.8. In aerodynamic type insulators the leakage distance is 300 to 400 mm and the shape is such that the contamination is cleaned by the wind. In fog type insulators, inner skirts are long enough to provide long creepage distance and remain dry and less contaminated condition as these are covered by the top skirts.

c) Cement Growth Failure.

In cap-and-pin disc insulator the cap and the pin is fitted to the insulator by cement. The cement is usually dried and hardened after curing, resulting in shrinkage but it sometimes causes also expansion of its volume by enough water. Moreover, its properties changes with time. Accordingly, the cement changes and expands with time and a high mechanical stress is applied to the material of the suspension insulators. This in turn causes radial cracks in the pin hole. Laboratory tests on various insulators support the mechanism for cement growth as being mainly due to excessive gypsum present in the cement. Not all the cements used in the assembly of insulators exhibit this long term expansion.

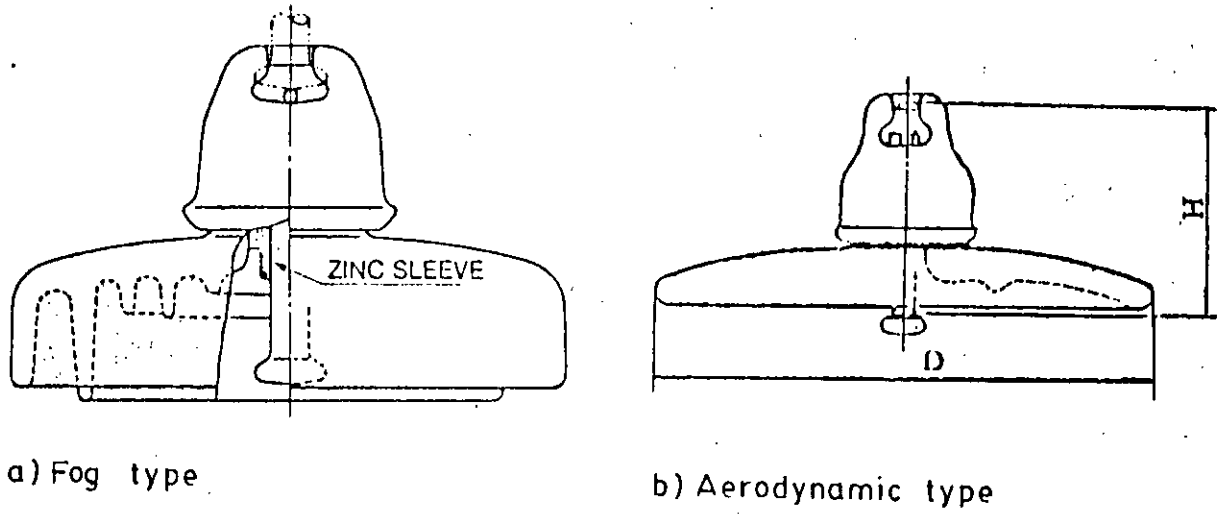


Fig: 2.8. Anticontaminated Insulators

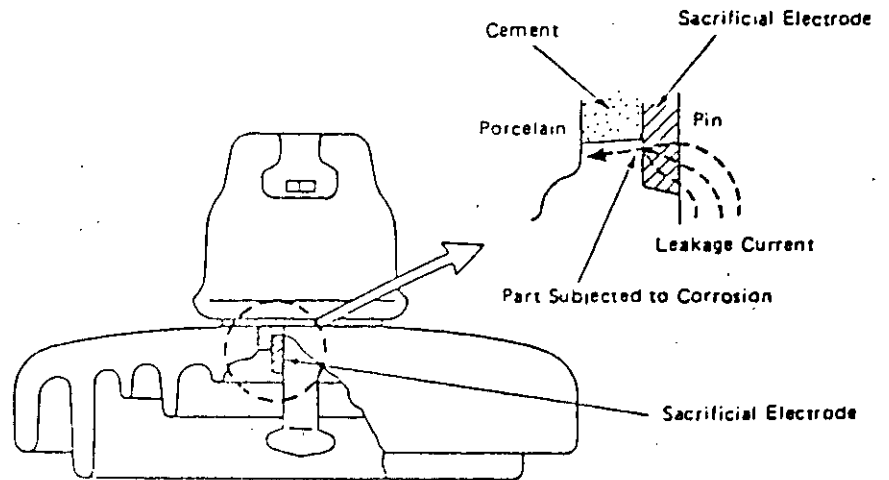


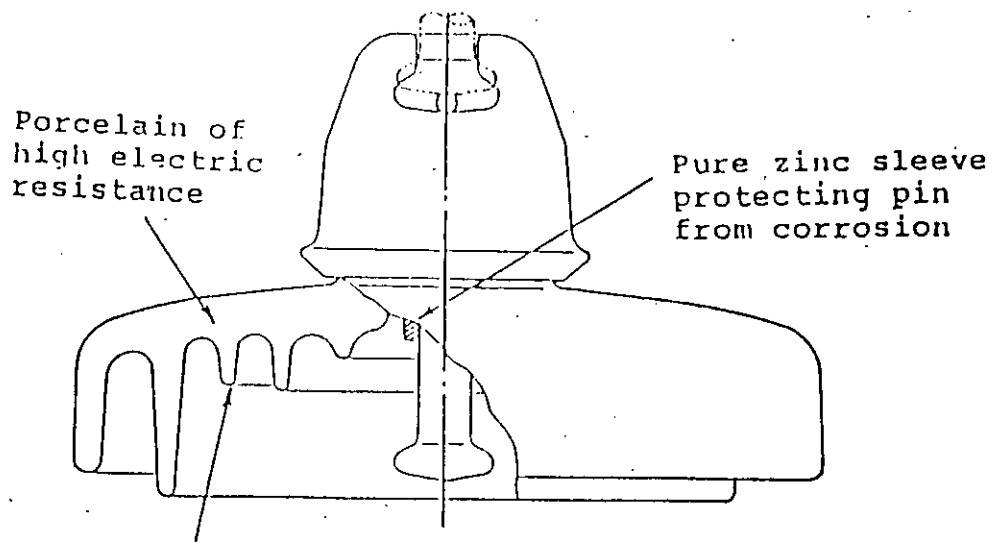
Fig: 2.9. Hardware Corrosion of Disc Type Insulator

d) Hardware corrosion.

The hardware of suspension insulators also suffers from corrosion during long term use in contaminated areas. In both AC and DC lines, this corrosion presents due to the electrochemical reaction (electrolytic corrosion) because of the flow of leakage current as shown in fig 2.9. Among hardware of suspension insulators, pin corrosion is serious problem because of reduction in mechanical strength of the corroded pin or breakage of insulator caused by expansion of pin body. The pin can be protected against electrolytic corrosion by attaching a sacrificial electrode (Zinc Sleeve) to the pin close to cement boundary as in fig 2.9.

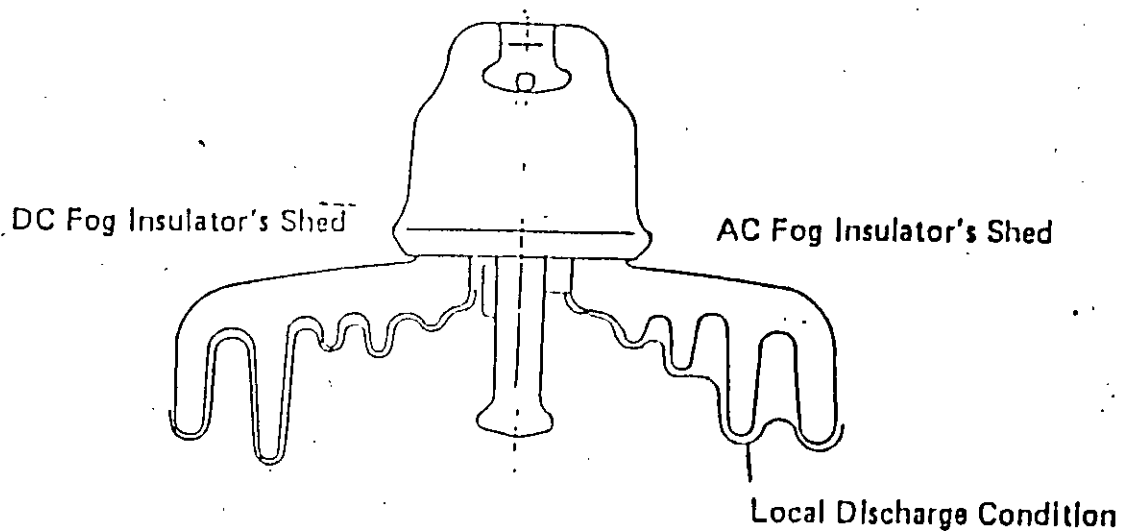
2.3.6: D.C Insulators:

Recently, DC transmission line became popular due to the availability of DC converting equipment and for long distance transmission of bulk power. As the DC flashover mechanism is different from AC ones, so the insulators used in DC line should be of different shape than AC ones, otherwise fault rate will increase. The insulator under DC voltage is more contaminated than under AC voltage due to the dust collecting effect of DC voltage. Moreover the local discharge effect is more effective in DC insulators. So it is clear that the surface erosion, pin corrosion and flashover problems are more severe than AC insulators.



Alternate long and short ribs
(High DC contamination withstand voltage)

a) Insulator Unit Showing Different parts



b) Showing Discharge

Fig 2.10. D.C Insulators

In order to cope with the above problems, the DC insulators are usually manufactured by high electric resistance porcelain putting a zinc sleeve around the pin shank and for obtaining high withstand voltage the shed is designed with alternate long and short ribs, keeping long distance between rib lips and long leakage distance as shown in fig. 2.10. The DC insulators are designed to provide 10-20% higher withstand voltage than AC insulator with same leakage distance.

2.4 Discussion

From the above discussion we can say that the ferroelectric insulators are the widely used and most popular insulator. In both AC and DC power system they are most reliable. Glass insulator, the other material used in manufacturing HV insulator, presents high local discharge of contaminated condition, which in turn causes surface erosion and pin corrosion and lowers the mechanical strength. In ferroelectric insulators this is not so prominent. Due to the high insulating resistance the local discharge is less in this type of insulators. The ferro-electric materials have high compressive stress and low tensile stress. For that most of the ferroelectric insulators are designed to bear high compressive and low tensile stress. Disc insulators, the widely used insulators, are designed taking this into consideration.

CHAPTER 3

THEORETICAL ASPECTS OF DESIGNING
FERRO-ELECTRIC INSULATORS

THEORETICAL ASPECTS OF DESIGNING FERRO-ELECTRIC INSULATORS

3.1 Introduction:

Physical system comprises of different types of dielectrics, such as solid, liquid and gaseous dielectrics and in almost every instance a combination of at least two of these components is involved. Another observation is that the dielectric must frequently serve as a structural material as well as an insulating material. Liquid and gaseous dielectric may also serve as coolants. These double or sometimes triple functions causes mechanical and thermal stresses in addition to electrical stress and place severe constraints on the designer, which greatly reduce his freedom of choice. This is because he has to consider a multiple system of stresses, such as electrical, mechanical and thermal stresses.

The electrical stress on the insulation of a power system component is perhaps the easiest to quantify. Firstly, there is stress due to the steady state power frequency voltage. Depending upon the particular component involved, this may range from a few Kv up to 800 Kv, with higher voltages in contemplation. Because of the geometry of most power system components, the electric fields that voltages give rise to, are more often than not quite non-uniform.

In addition to the power frequency fields, system insulation is subjected to transient overvoltages caused by switching operations and intrusion of lightning into the power system. Those are of variable duration, magnitude and wave form. Rapidly changing transient voltages can temporarily cause further extremely non-uniform distributions of stress.

So, the study of electric field distribution in and around insulating structures has been of considerable interest to electrical engineers for designing equipment that operate at very high voltage levels. The peak stress value in an insulating system is an important parameter to control because it influences discharge initiation and propagation. Compaction and miniaturization of high voltage system, with the resulting increased operating stress levels, have made the study of electric stress distribution even more critical.

Mechanical stress occurs due to mechanical deformation under the application of electric fields. Thermal Stresses occur due to the thermal gradients, which ^{are} present in insulators due to the ohmic losses in the conducting parts.

Unfortunately, the excessive electrical, mechanical and thermal stresses often occur simultaneously. And as thermal stress is not so prominent, then electro-mechanical stress analysis is very important for an insulating system design.

Our present analysis is, however, motivated to the calculation of electro-mechanical stress developed in a ferroelectric material. But electro-mechanical stress analysis of such media has not been reported. Only the electro-mechanical stress in ether, a hypothetical medium has been widely discussed by stratton [11]. Taking this analysis into consideration as valid for dielectric, we extended that analysis for ferroelectric materials.

3.2 Evaluation of Potential Distribution by Finite Element Method.

The basic principle used for developing finite element method of finding potential distribution is the solution of Laplace's equation. Laplace's equation is written as

$$\nabla^2 \Phi = 0 \quad \dots (3.1)$$

where Φ = potential

Physical systems are so complex that the analytical solution of Laplace's equation is very difficult, though not impossible. As such, with the increasing availability of high speed digital computers, two numerical methods are being extensively used in the calculation of electrostatic fields in high voltage systems.

The first method is based on the difference technique employing Laplace's and Poisson's equations in the space where the field is to be determined. This is done by dividing the whole space into small meshes.

The second approach to the computation of fields is to integrate Laplace's or Poisson's equation either by employing discrete charges, or by dividing the electrode surface into sub-sections with charges. This method of computation is known as the charge simulation method. In this method fictitious point, line or ring charges are assumed outside the space in which the field is to be computed. The magnitude and position of these charges are such that their integrated effect together with the field of those charges existing inside the space, satisfies the boundary conditions. This method is very successful for many high voltage field problems.

Finite element numerical technique is now being extensively used to find solution of Laplace's equation encountered in problems related to civil, mechanical and electrical engineering, Chang et al [3] used finite element method to calculate electrical stress distribution within dielectric cavities. The finite element method is a powerful numerical technique that can be precisely used to solve boundary value problem by piecewise linearization of the potential function over a large number of discrete spatial elements. In this chapter we are formulating the finite element method of solving Laplace's equation to obtain electrical stress distribution.

The basic requirement of the development of finite element equation is to find an extremum function which can be written in energy density form. As a first step in the development of this method, a uniform surface is considered which is completely filled with homogeneous and isotropic dielectric.

The extremum function for electrostatic field can be written as, [10]

$$J(\Phi) = \frac{1}{2} \iiint |\nabla\Phi|^2 ds \quad \dots (3.2)$$

The finite element method employs a set of algebraic functions defined over a subsection of the whole crosssection. These subsections may be polygonal in shape and are called elements. Thus in the finite element method the entire domain over which the operator is defined is divided into a finite number of elements on each of which the actual node function is approximated by a set of continuous algebraic functions which are only defined over the particular element under consideration and are linearly dependent on the values of Φ at the vertices of the element.

Hence, if an element has n vertices (for triangular element $n=3$), the potential Φ within it may be approximated by [10]

$$\Phi(x,y) = \sum_{m=1}^n N_m(x,y) \Phi_m \quad \dots (3.3)$$

Where Φ_m is the value of Φ at the vertex m and $N_m(x,y)$ is a predetermined algebraic function which is uniquely defined and differentiable over the element and which reduces to zero outside the element.

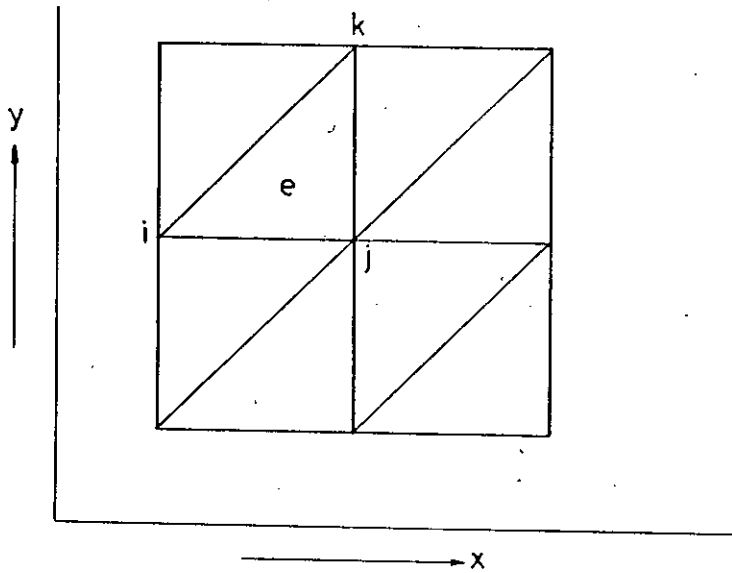


Fig 3.1 : division into triangular elements

Let us consider triangular elements as shown in fig 3.1. A typical element (the e th element) is described by the vertices i, j and k in cyclic order. Let Φ_i, Φ_j and Φ_k be the corresponding values of Φ at the vertices. For the element e the functional dependence of $\Phi(x, y)$ can be written as [10]

$$\Phi^e(x, y) = \alpha_0 + \alpha_1 x + \alpha_2 y \quad \dots \quad (3.4)$$

where α_0, α_1 and α_2 are to be determined.

If $(x_1, y_1), (x_2, y_2)$ and (x_3, y_3) are the coordinates of the vertices i, j and k , then solving for α_0, α_1 and α_2 , we obtain, [10]

$$\begin{aligned} \Phi(x, y) = & \frac{1}{2A} (a_1 + b_1 x + c_1 y) \Phi_i^e + \frac{1}{2A} (a_2 + b_2 x + c_2 y) \Phi_j^e \\ & + \frac{1}{2A} (a_3 + b_3 x + c_3 y) \Phi_k^e \quad \dots \quad (3.5) \end{aligned}$$

Where $2A$ is the determinant of the matrix,

$$\begin{bmatrix} 1 & x_1 & y_1 \\ 1 & x_2 & y_2 \\ 1 & x_k & y_k \end{bmatrix}$$

A = area of the triangular element.

$$a_1 = x_1 \cdot y_k - x_k \cdot y_1$$

$$b_1 = y_2 - y_k$$

$$c_1 = x_k - x_2$$

Here a_i, b_i, c_i, \dots are the cofactors of the above square matrix.

From (3.5) we get ,

$$\frac{\partial \Phi^e}{\partial x} = \frac{1}{2A} (b_1 \Phi_1^e + b_2 \Phi_2^e + b_k \Phi_k^e) \quad \dots \quad (3.6)$$

$$\frac{\partial \Phi^e}{\partial y} = \frac{1}{2A} (c_1 \Phi_1^e + c_2 \Phi_2^e + c_k \Phi_k^e) \quad \dots \quad (3.7)$$

Now from equation (3.2) for eth element,

$$J = \frac{1}{2} \iint [\left(-\frac{\partial \Phi}{\partial x} \right)^2 + \left(-\frac{\partial \Phi}{\partial y} \right)^2] dx \cdot dy$$

$$= \frac{1}{8A^2} \iint [(b_1 \Phi_1^e + b_2 \Phi_2^e + b_k \Phi_k^e)^2 + (c_1 \Phi_1^e + c_2 \Phi_2^e + c_k \Phi_k^e)^2] dx \cdot dy$$

Since $\frac{1}{2} \iint dx \cdot dy = A$

$$J = \frac{1}{8A} [(b_1 \Phi_1^e + b_2 \Phi_2^e + b_k \Phi_k^e)^2 + (c_1 \Phi_1^e + c_2 \Phi_2^e + c_k \Phi_k^e)^2] \dots (3.8)$$

If there are in all M vertices, then from (3.2)

$$J(\Phi) = F(\Phi_1, \Phi_2, \Phi_3, \Phi_4, \dots, \Phi_M) \dots (3.9)$$

The optimum value of a set of Φ_m for a certain functional form of $Nm(x,y)$ may be obtained by minimizing the function given by (3.9) with respect to each of m i.e. equating,

$$\frac{\partial J}{\partial \Phi_m} = 0 ; \text{ for } m = 1, 2, 3 \dots M (3.10)$$

However, in the vicinity of boundaries where constant potentials are specified.

$$J \rightarrow \frac{1}{2} \Phi_b^2$$

So that at the boundary, $\frac{\partial J}{\partial \Phi} \rightarrow \Phi_b$

where Φ_b is the value of the potential at the boundary.

Using equation (3.10) for the minimization of J function over the element e.

$$\frac{\partial J}{\partial \Phi_i} = \frac{1}{4A} [b_i (b_i \Phi_i + b_j \Phi_j + b_k \Phi_k) + c_i (c_i \Phi_i + c_j \Phi_j + c_k \Phi_k)]$$

$$\frac{\partial J}{\partial \Phi_j} = \frac{1}{4A} [b_j (b_i \Phi_i + b_j \Phi_j + b_k \Phi_k) + c_j (c_i \Phi_i + c_j \Phi_j + c_k \Phi_k)]$$

$$\frac{\partial J}{\partial \Phi_k} = \frac{1}{4A} [b_k (b_i \Phi_i + b_j \Phi_j + b_k \Phi_k) + c_k (c_i \Phi_i + c_j \Phi_j + c_k \Phi_k)]$$


In matrix form for the element with nodes i, j and k

$$\begin{bmatrix} \frac{\partial J^e}{\partial \Phi_i} \\ \frac{\partial J^e}{\partial \Phi_j} \\ \frac{\partial J^e}{\partial \Phi_k} \end{bmatrix} = \frac{1}{4A} \begin{bmatrix} b_i^2 + c_i^2 & b_i \cdot b_j + c_i \cdot c_j & b_i \cdot b_k + c_i \cdot c_k \\ b_i \cdot b_j + c_i \cdot c_j & b_j^2 + c_j^2 & b_j \cdot b_k + c_j \cdot c_k \\ b_i \cdot b_k + c_i \cdot c_k & b_j \cdot b_k + c_j \cdot c_k & b_k^2 + c_k^2 \end{bmatrix} \begin{bmatrix} \Phi_i^e \\ \Phi_j^e \\ \Phi_k^e \end{bmatrix}$$

or, $\frac{\partial J}{\partial \Phi^e} = [S^e] [\Phi^e] \dots (3.11)$

Where S^e is the element sub-matrix and Φ^e is a column matrix. S^e is a square symmetric matrix such that $S_{ij} = S_{ji}$. The above equation can be applied to obtain elemental submatrices for all the elements of the domain. The resultant matrix will be the sum of all the element submatrices generated by all the elements. Then inverting this matrix and multiplying it with the boundary values we can get the potentials of the nodes of each element

The potential distribution for parallel circular thin plate as shown in fig 3.2 can be easily determined by using the above analysis.

Let the upper plate be kept at a certain potential $V = 11\text{KV}$ and the lower plate is maintained at zero potential. The space on one side of Y-axis between the two plates is divided into 64 numbers of elements and 45 nodes. Assuming linear variation of potential over elements, taking permittivity is constant over the region and considering the procedure discussed earlier we get 45 linear algebraic equations. Solving these equations we get potentials at different nodes. The results are plotted in fig 3.3. From the plot it is clear that the potential is constant about the level $Y = h/2$, the potential from the top plate decreases gradually and become constant function of x at the level $Y = h/2$ i.e. $\Phi = 5.5\text{KV}$. Similarly from the bottom plate the potential gradually increases and becomes a constant function of x at $Y = h/2$ i.e. $\frac{\partial \Phi}{\partial x} = 0$ indicates that no lateral field exists. Rather the field is entirely vertical at the midlevel between the two plates. This is expected because  the electric lines of forces emanating from the top plate will turn towards the bottom plate after reaching vertically at the mid level.

This also indicates that half of the energy is stored in the upper half region as is expected in a parallel plate capacitor or in the case of dipole.

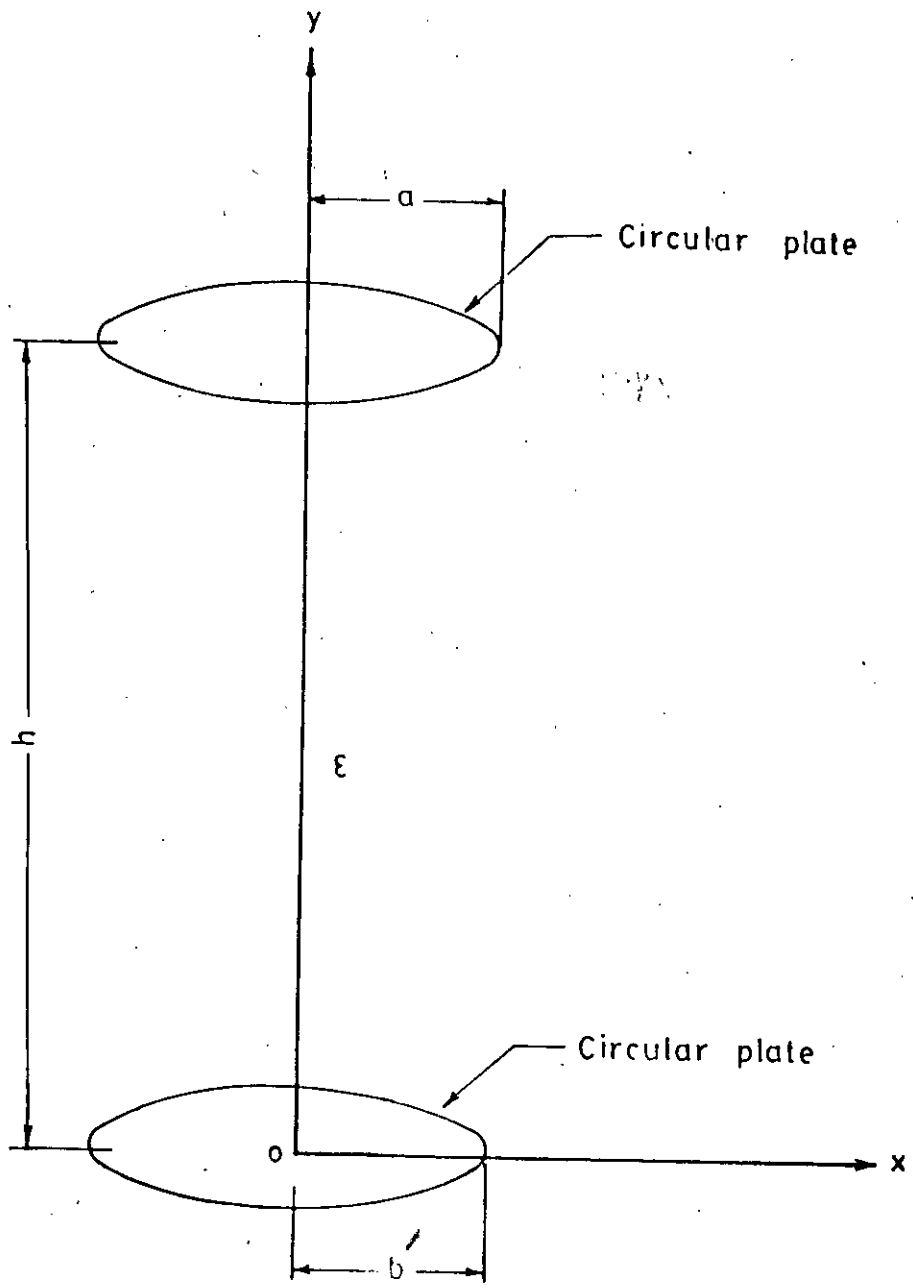


Fig. 3.2. Coordinate system of the problem

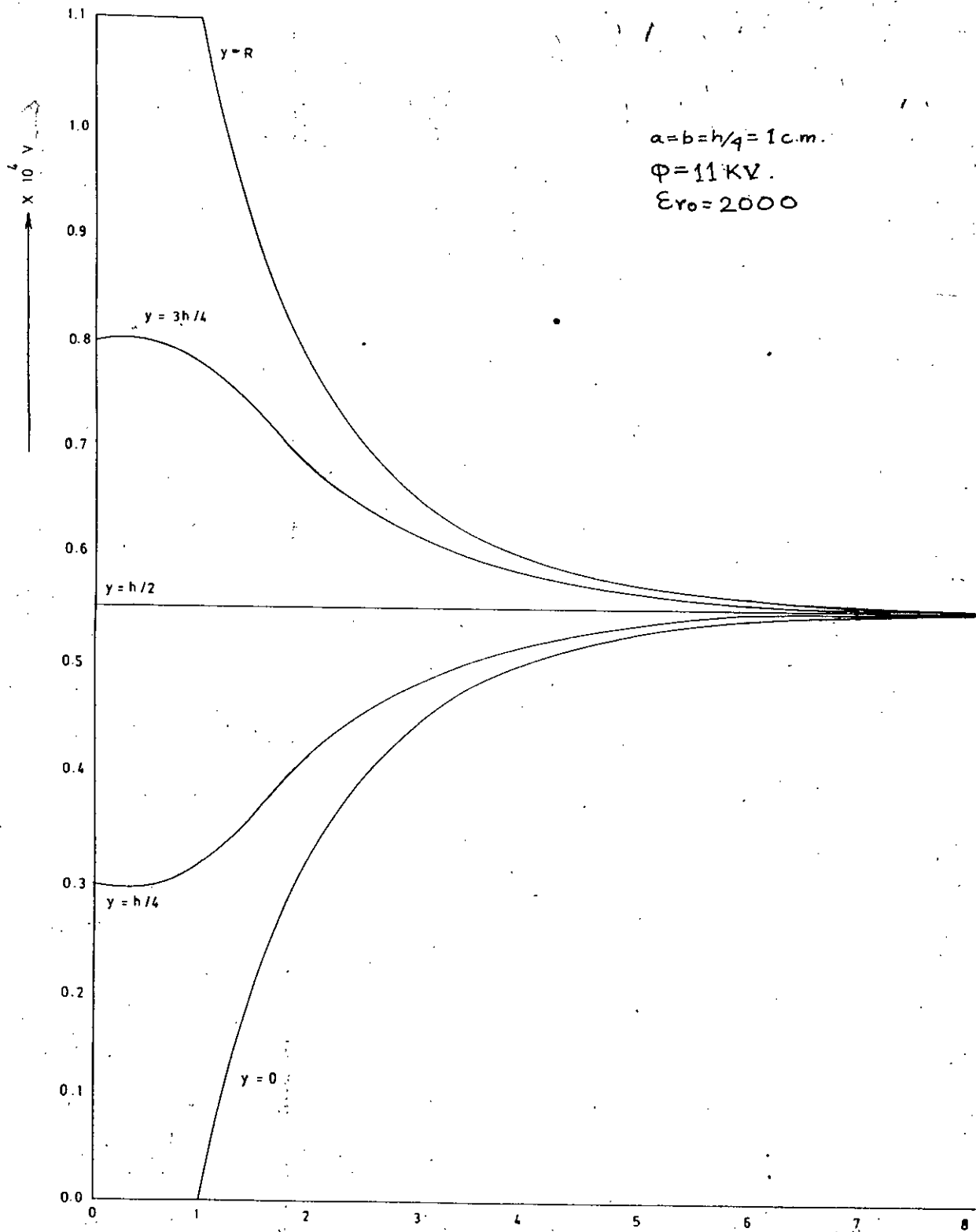


FIG. 3.3 POTENTIAL DISTRIBUTION AT DIFFERENT LEVELS IN BETWEEN PLATES

3.3 Electromechanical Stress Analysis

The theory of Maxwell-Faraday on electromechanical stress in "ether" has been widely discussed by Stratton [11]. Emphasizing their validity for dielectric materials, the following analysis has been done.

Let us suppose that a certain bounded region of space contains charge distribution. The field is produced in part by the charges within the region and in part by the sources which are exterior to it. Then at every interior point we get,

$$\bar{E} = -\nabla\Phi$$

Then $\nabla \times \bar{E} = 0$. . . (3.12)

and $\nabla \cdot \bar{E} = \frac{\rho}{\epsilon}$. . . (3.13)

Let equation (3.12) be multiplied vectorically by $\bar{D} = \epsilon_0 \epsilon_r \bar{E}$, ^{Hence} we get,

$$(\nabla \times \bar{E}) \times \bar{D} = 0 \quad . . . (3.14)$$

or,

$$\left[\begin{array}{ccc} \bar{a}_x & \bar{a}_y & \bar{a}_z \\ \frac{\partial E_x}{\partial y} & \frac{\partial E_y}{\partial z} & \frac{\partial E_z}{\partial x} \\ \frac{\partial E_x}{\partial z} & \frac{\partial E_z}{\partial x} & \frac{\partial E_y}{\partial x} \\ \frac{\partial E_y}{\partial x} & \frac{\partial E_x}{\partial y} & \frac{\partial E_z}{\partial y} \\ D_x & D_y & D_z \end{array} \right] = 0$$

The x, y and z components of the vector (3.14) are given by,

$$[(\nabla \times \bar{E}) \times \bar{D}] \cdot \bar{a}_x = D_x \left(\frac{\partial E_x}{\partial z} - \frac{\partial E_z}{\partial x} \right) - D_y \left(\frac{\partial E_y}{\partial x} - \frac{\partial E_x}{\partial y} \right) = 0 \quad \dots (3.15)$$

$$[(\nabla \times \bar{E}) \times \bar{D}] \cdot \bar{a}_y = D_x \left(\frac{\partial E_y}{\partial x} - \frac{\partial E_x}{\partial y} \right) - D_z \left(\frac{\partial E_z}{\partial y} - \frac{\partial E_y}{\partial z} \right) = 0 \quad \dots (3.16)$$

$$[(\nabla \times \bar{E}) \times \bar{D}] \cdot \bar{a}_z = D_y \left(\frac{\partial E_z}{\partial y} - \frac{\partial E_y}{\partial z} \right) - D_x \left(\frac{\partial E_x}{\partial z} - \frac{\partial E_z}{\partial x} \right) = 0 \quad \dots (3.17)$$

The above equations can be arranged by adding equal quantities on both sides. i.e.,

$$D_x \left(\frac{\partial E_x}{\partial z} - \frac{\partial E_z}{\partial x} \right) - D_y \left(\frac{\partial E_y}{\partial x} - \frac{\partial E_x}{\partial y} \right) + E_x \nabla \cdot \bar{D} = E_x \nabla \cdot \bar{D} \quad \dots (3.18)$$

$$D_x \left(\frac{\partial E_y}{\partial x} - \frac{\partial E_x}{\partial y} \right) - D_y \left(\frac{\partial E_z}{\partial y} - \frac{\partial E_y}{\partial z} \right) + E_y \nabla \cdot \bar{D} = E_y \nabla \cdot \bar{D} \quad \dots (3.19)$$

$$D_x \left(\frac{\partial E_y}{\partial x} - \frac{\partial E_x}{\partial y} \right) - D_y \left(\frac{\partial E_z}{\partial y} - \frac{\partial E_y}{\partial z} \right) + E_z \nabla \cdot \bar{D} = E_z \nabla \cdot \bar{D} \quad \dots (3.20)$$

The above three equations can be arranged in tensor form,

$$\nabla \cdot \hat{S} \bar{i} = \bar{E} \nabla \cdot \bar{D} \quad \dots (3.21)$$

where \hat{S} is the tensor expressed as follows:

$$\hat{S} = \begin{bmatrix} S_{11} & S_{12} & S_{13} \\ S_{21} & S_{22} & S_{23} \\ S_{31} & S_{32} & S_{33} \end{bmatrix} \quad \dots (3.22)$$

and \vec{I} is the column vector expressed as,

$$\vec{I} = \begin{bmatrix} \vec{a}_x \\ \vec{a}_y \\ \vec{a}_z \end{bmatrix}$$

For an isotropic dielectric the elements S_{ij} are shown in Table 3.1.

Table 3.1 : Components S_{ij} of the tensor \hat{S} in free space

j/k	1	2	3
1	$\epsilon_0 \epsilon_r E_x^2 - \frac{\epsilon_0 \epsilon_r}{2} E^2$	$\epsilon_0 \epsilon_r E_x E_y$	$\epsilon_0 \epsilon_r E_x E_z$
2	$\epsilon_0 \epsilon_r E_y E_x$	$\epsilon_0 \epsilon_r E_y^2 - \frac{\epsilon_0 \epsilon_r}{2} E^2$	$\epsilon_0 \epsilon_r E_y E_z$
3	$\epsilon_0 \epsilon_r E_z E_x$	$\epsilon_0 \epsilon_r E_z E_y$	$\epsilon_0 \epsilon_r E_z^2 - \frac{\epsilon_0 \epsilon_r}{2} E^2$

Equation (3.21) is a relation through which the forces exerted on elements can be expressed in terms of the vector \vec{D} . As $\nabla \cdot \vec{D}$, is the charge density is in coulomb/m^3 , the force distribution given by the right hand side of (3.21) will be in Newton/m^3 . Let us now integrate the identity over a volume V to obtain the force,

$$\vec{F} = \int \nabla \cdot \hat{S} \vec{I} dv = \int \vec{E} \nabla \cdot \vec{D} dv \quad \dots (3.23)$$

Let \vec{n} be the unit outward normal at a point on the boundary surface. Then by divergence theorem.

$$F = \oint (\hat{S} \vec{I}) \cdot \vec{n} da = \int \vec{E} \nabla \cdot \vec{D} dv \quad \dots (3.24)$$

Thus the quantity $(\hat{S}\bar{I}) \cdot \bar{n}$ comes out in the form of force per unit area or as mechanical stress. That means $(\hat{S}\bar{I}) \cdot \bar{n}$ represents a mechanical stress developed with application of electric stress \bar{E} . In vector notation the electromechanical stress is given by

$$\bar{t} = (\hat{S}\bar{I}) \cdot \bar{n} \quad \dots (3.25)$$

Hence the stress components can be given as,

$$t_x = (S_{11}\bar{n}_x + S_{12}\bar{n}_y + S_{13}\bar{n}_z)$$

$$t_y = (S_{21}\bar{n}_x + S_{22}\bar{n}_y + S_{23}\bar{n}_z)$$

$$t_z = (S_{31}\bar{n}_x + S_{32}\bar{n}_y + S_{33}\bar{n}_z)$$

Referring to Fig.3.2 the electric field between the two circular parallel plates has x and y components only. Now if we desire to calculate stress in the xz plane then \bar{n} will be in the y direction such that $\bar{n}_x = 0$, $\bar{n}_y = 1$ and $\bar{n}_z = 0$.

Then

$$t_x = S_{12} = \epsilon_0 \epsilon_r E_x E_y \quad \dots (3.26)$$

$$\begin{aligned} t_y = S_{22} &= \epsilon_0 \epsilon_r \left(E_y^2 - \frac{1}{2} E^2 \right) \\ &= \frac{\epsilon_0 \epsilon_r}{2} (E_y^2 - E_x^2) \quad \dots (3.27) \end{aligned}$$

$$t_z = S_{32} = 0 \quad \dots (3.28)$$

Hence the magnitude of the stress is given by,

$$\begin{aligned}
 t &= \sqrt{t_x^2 + t_y^2} \\
 &= \epsilon_0 \epsilon_r \sqrt{(E_x E_y)^2 + \frac{1}{4} (E_y^2 - E_x^2)} \\
 &= \frac{\epsilon_0 \epsilon_r}{2} (E_x^2 + E_y^2) \\
 &= \frac{\epsilon_0 \epsilon_r}{2} E^2
 \end{aligned}$$

or,
$$t = \frac{1}{2} \bar{D} \cdot \bar{E} \quad \dots (3.29)$$

The angle of the mechanical stress is then given by

$$\theta_m = \tan^{-1} \left(\frac{t_y}{t_x} \right) \quad \dots (3.30)$$

In general $\frac{1}{2} \bar{D} \cdot \bar{E}$ represents the magnitude of the electro-mechanical stress in the dielectric.

3.4 Electromechanical Stress Distribution in Ferroelectric Material between Two Thin Circular Parallel Electrodes.

In order to obtain the electromechanical stress distribution in ferroelectric material between two thin circular parallel electrodes by finite element method, first we have to calculate the applied field distribution between the electrodes. The applied field can be expressed as,

$$\bar{E}_o = \bar{a}_x \cdot E_{ox} + \bar{a}_y \cdot E_{oy} \quad \dots (3.31)$$

The field components E_{ox} and E_{oy} can be easily obtained by dividing the region between the electrode into finite number of triangular elements and applying equations(3.6) and (3.7) we get,

$$E_{ox} = \frac{1}{2A} [b_1 \Phi_1^e + b_2 \Phi_2^e + b_n \Phi_n^e] \quad \dots (3.32)$$

$$E_{oy} = \frac{1}{2A} [c_1 \Phi_1^e + c_2 \Phi_2^e + c_n \Phi_n^e] \quad \dots (3.33)$$

For satisfying the ^{mean} hysteresis curve (Fig. 2.1) the magnitude of the electric flux density as a function of electric field can be well approximated as,

$$D = \epsilon_0 (\epsilon_{r0} E_0 - KE_0^3) \quad \dots (3.34)$$

Where $\epsilon_0 \epsilon_{r0} = \left. \frac{dD}{dE_0} \right|_{E_0=0}$

Hence, ϵ_{r0} is the dielectric constant at very weak field, K is a constant.

When ferroelectric material is placed between two electrodes, major portion of the electrical energy is spent in polarizing the molecules. After polarizing the dielectric, a portion of the supplied energy remains to link the two electrodes. These phenomena are explained by Lorentz equation.

$$\bar{D} = \bar{D}_0 + \bar{P} \quad \dots (3.35)$$

Where,

\bar{P} is the polarized portion,

and $\bar{D}_0 = \epsilon_0 \bar{E}_0$ is the macroscopic flux density that remains as an unpolarized portion of the net flux density \bar{D} . The purpose of electrical insulation is to keep this unpolarized flux density to a minimum. As $\nabla \cdot \bar{D}_0 = 0$ in the dielectric region, then $\bar{E}_0 = -\nabla \Phi$, where Φ is the potential satisfying Laplace's equation and can be obtained by the finite element method discussed earlier.

Now from (3.34) and (3.35) we get

$$P = \epsilon_0 [(\epsilon_{r0} - 1)E_0 - KE_0] \quad \dots (3.36)$$

The effective relative permittivity ϵ_r is obtained from

$$\epsilon_0(\epsilon_r - 1) = \frac{dP}{dE_0} \dots (3.37)$$

Substituting (3.36) in (3.37) we get

$$\begin{aligned} \epsilon_0(\epsilon_r - 1) &= \epsilon_0 [(\epsilon_{r0} - 1) - 3 K E_0^2] \\ \epsilon_r &= \epsilon_{r0} - 3 K E_0^2 \dots (3.38) \end{aligned}$$

From Fig. [2.1]

We get flux density corresponding to the two curves of Fig.

2.1

$$D1 = \epsilon_0 [\epsilon_{r0} (E_0 + E_c) - K (E_0 + E_c)^3] \dots (3.39)$$

$$D2 = \epsilon_0 [\epsilon_{r0} (E_0 - E_c) - K (E_0 - E_c)^3] \dots (3.40)$$

At $E_0 = E_s$ the polarization saturates and we get $D1 = D2$ i.e.

$D1 - D2 = 0$. Hence

$$\epsilon_0 [2 \epsilon_{r0} E_c - K \{ (E_s + E_c)^3 - (E_s - E_c)^3 \}] = 0$$

$$\therefore K = \frac{2 \epsilon_{r0} E_c}{(E_s + E_c)^3 - (E_s - E_c)^3}$$

$$\text{or, } K = \frac{2 \epsilon_{r0} E_c}{2 E_c [(E_s + E_c)^2 + (E_s - E_c)^2 + E_s^2 - E_c^2]}$$

$$K = \frac{\epsilon_{r0}}{3E_s^2 + E_c^2} \dots (3.41)$$

After saturation the field leaks out into the medium surrounding the ferroelectric material, and flashover takes place around the insulator with the air breakdown at which the field strength is, $E_s = 2 \times 10^6$ v/m. We choose $E_c = 1/2 E_s = 10^6$ v/m and $\epsilon_{r0} = 2000$ for ceramic at 100°C (the extreme condition).

Now from equation (3.34) we can also write the x and y components of flux density as,

$$D_x = \epsilon_0 (\epsilon_{rx} E_{ox} - K E_{ox}^3) \quad \dots (3.42)$$

$$D_y = \epsilon_0 (\epsilon_{ry} E_{oy} - K E_{oy}^3) \quad \dots (3.43)$$

Again for any dielectric, the internal field developed is given by [11],

$$\bar{E} = \bar{E}_o + \bar{E}_p$$

where \bar{E}_o = applied field

\bar{E}_p = field due to polarization

For ferroelectric material we have $\bar{E}_p = \frac{\gamma \bar{P}}{\epsilon_0}$, where \bar{P} is the polarization vector.

Therefore,

$$\bar{E} = \bar{E}_o + \frac{\gamma \bar{P}}{\epsilon_0} \quad \dots (3.44)$$

γ is a constant, for $BaTiO_3$ the coefficient of expansion $\lambda = 3 \times 10^{-5}$ per degree and the observed curie constant $1/\lambda \gamma \cong 10^9$. Hence $\gamma \cong 1/3$ [13].

Again for ferroelectric material the polarization is expressed as, [13]

$$\frac{\partial P}{\partial E_o} = \epsilon_0 (\epsilon_r - 1) \quad \dots (3.45)$$

Where ϵ_r is the relative permittivity of the material. For polarization in x and y direction we can write,

$$\frac{\partial P_x}{\partial E_{ox}} = \epsilon_0 (\epsilon_{rx} - 1) \quad \dots (3.46)$$

$$\frac{\partial P_y}{\partial E_{oy}} = \epsilon_0 (\epsilon_{ry} - 1) \quad \dots (3.47)$$

where ϵ_{rx} and ϵ_{ry} are the relative permittivities for fields in x and y direction respectively. Now by definition of relative permittivity,

$$\epsilon_p = \frac{1}{\epsilon_0} \frac{\partial D}{\partial E_0} \dots (3.48)$$

Hence substituting the values of flux density components from equations (3.42) and (3.43) we get,

$$\epsilon_{rx} = (\epsilon_{r0} - 3KE_{0x}^2) \dots (3.49)$$

$$\epsilon_{ry} = (\epsilon_{r0} - 3KE_{0y}^2) \dots (3.50)$$

Substituting equations (3.49) and (3.50) into equations (3.46) and (3.47) respectively we get,

$$\frac{\partial P_x}{\partial E_{0x}} = \epsilon_0 (\epsilon_{r0} - 1 - 3KE_{0x}^2) \dots (3.51)$$

$$\frac{\partial P_y}{\partial E_{0y}} = \epsilon_0 (\epsilon_{r0} - 1 - 3KE_{0y}^2) \dots (3.52)$$

Hence by integrating we get,

$$P_x = \epsilon_0 [(\epsilon_{r0} - 1)E_{0x} - KE_{0x}^3] \dots (3.53)$$

$$P_y = \epsilon_0 [(\epsilon_{r0} - 1)E_{0y} - KE_{0y}^3] \dots (3.54)$$

Now substituting equations (3.53) and (3.54) in equation (3.44) we get the components of the field as,

$$E_x = [\gamma (\epsilon_{r0} - 1) + 1] E_{0x} - KE_{0x}^3 \dots (3.55)$$

$$E_y = [\gamma (\epsilon_{r0} - 1) + 1] E_{0y} - KE_{0y}^3 \dots (3.56)$$

Therefore the magnitude and angle of the field are

$$E = \sqrt{E_x^2 + E_y^2} \quad \dots (3.57)$$

$$\text{and } \theta_e = \tan^{-1} \left(\frac{E_y}{E_x} \right) \quad \dots (3.58)$$

The magnitude of the mechanical stress according to eqn. (3.29) is given by,

$$t = \frac{1}{2} \bar{D} \cdot \bar{E}$$

$$t = \frac{1}{2} (D_x \cdot E_x + D_y \cdot E_y)$$

$$t^2 = \frac{1}{4} (D_x \cdot E_x + D_y \cdot E_y)^2 \quad \dots (3.59)$$

The stress t can be divided into x and y components,

$$t^2 = t_x^2 + t_y^2 = D_x D_y E_x E_y + \frac{1}{4} (D_y \cdot E_y - D_x \cdot E_x)^2$$

$$t_x = \sqrt{D_x D_y E_x E_y} \quad \dots (3.60)$$

$$\text{and } t_y = \frac{1}{2} (D_y \cdot E_y - D_x \cdot E_x) \quad \dots (3.61)$$

$$t = \sqrt{t_x^2 + t_y^2} \quad \dots (3.62)$$

$$\text{and angle } \theta_m = \tan^{-1} \left(\frac{t_y}{t_x} \right) \quad \dots (3.63)$$

Hence from equation (3.62) and (3.63) we can readily determine the magnitude and angle of mechanical stress developed in ferro-electric material under application of electric field.

For alternating fields experiencing hysteresis effect, the electric field components in the above expression must be changed as $E_0 \pm E_c$ respectively for alternation from negative maximum to positive maximum and from positive maximum to negative maximum. The coercive field E_c can be assumed $E_s/2$, where E_s is the saturation field.

Both the electric and equivalent mechanical stresses have been calculated for ferro-electric material between two circular parallel plates. For electrostatic case Fig. 3.4 and 3.5 illustrate the plots of electric and equivalent mechanical stress magnitudes as functions of radial distance from the axis of the electrodes. Plots are shown for different levels $y=h$, $3h/4$, $h/2$ and $h/4$. The peak values of the stresses occur at the edges of the electrodes and the stress value drops rapidly for distances away from the edge. The electric and equivalent mechanical stress curves have almost similar shape.

From the angle distribution of electromechanical stress shown in table 3.2, it can be checked that the upper half of the ferro-electric material experiences compressive stresses and the lower half of the material experiences tensile stresses.

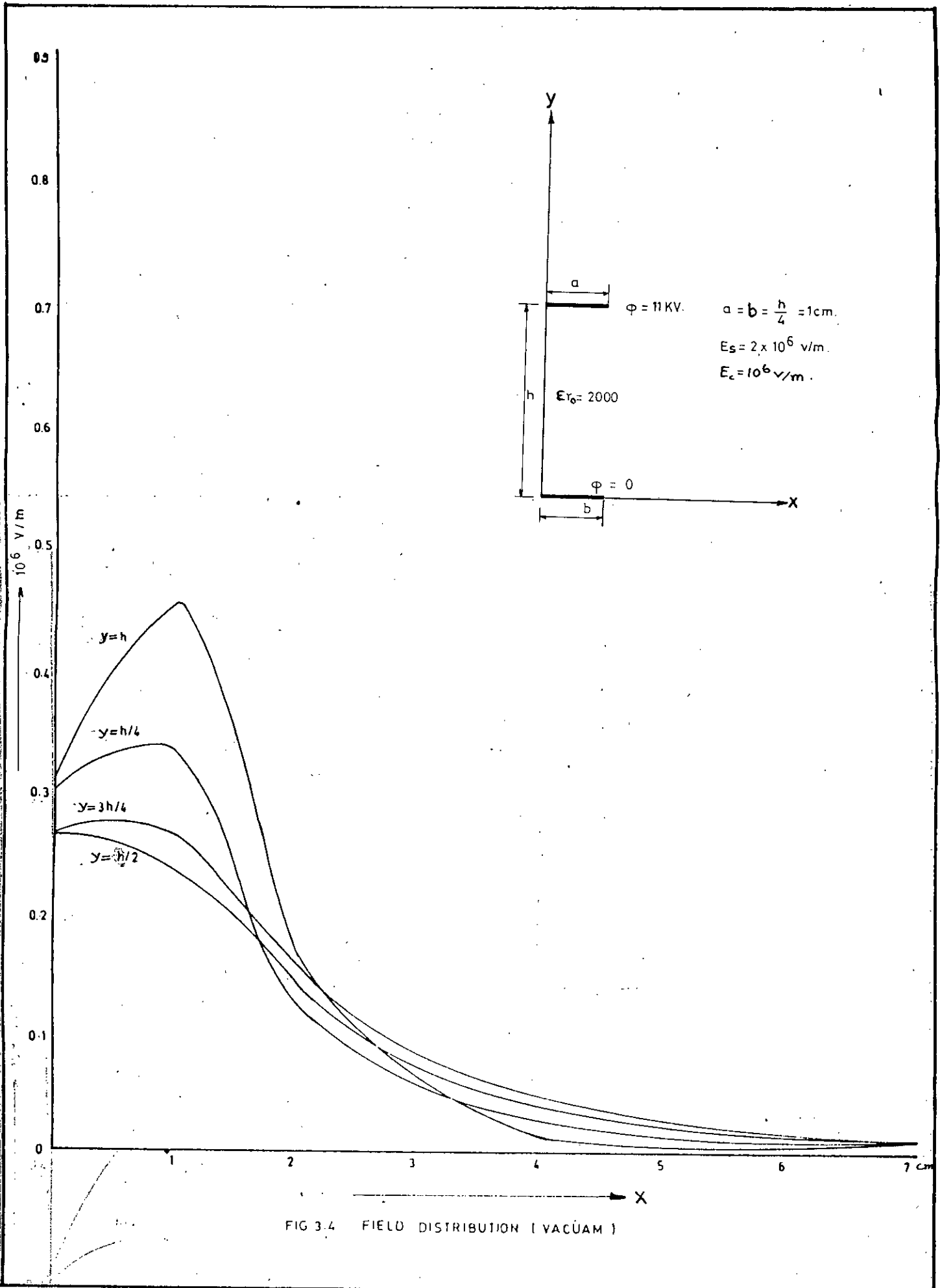


FIG 3.4 FIELD DISTRIBUTION (VACUUM)

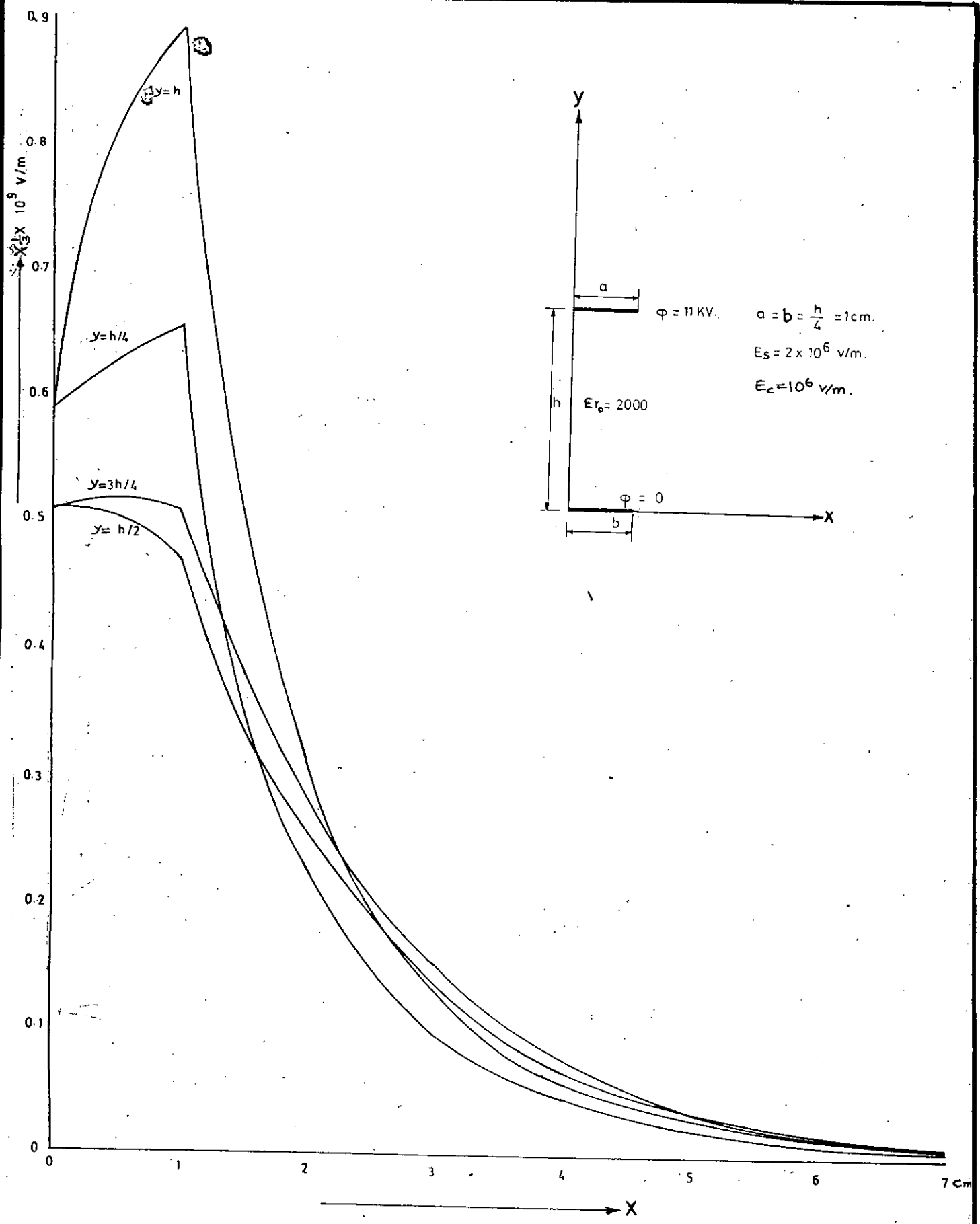


FIG. 3.4.1 DISTRIBUTION OF ELECTRIC STRESS FOR FERROELECTRIC MATERIAL (STATIC CASE)

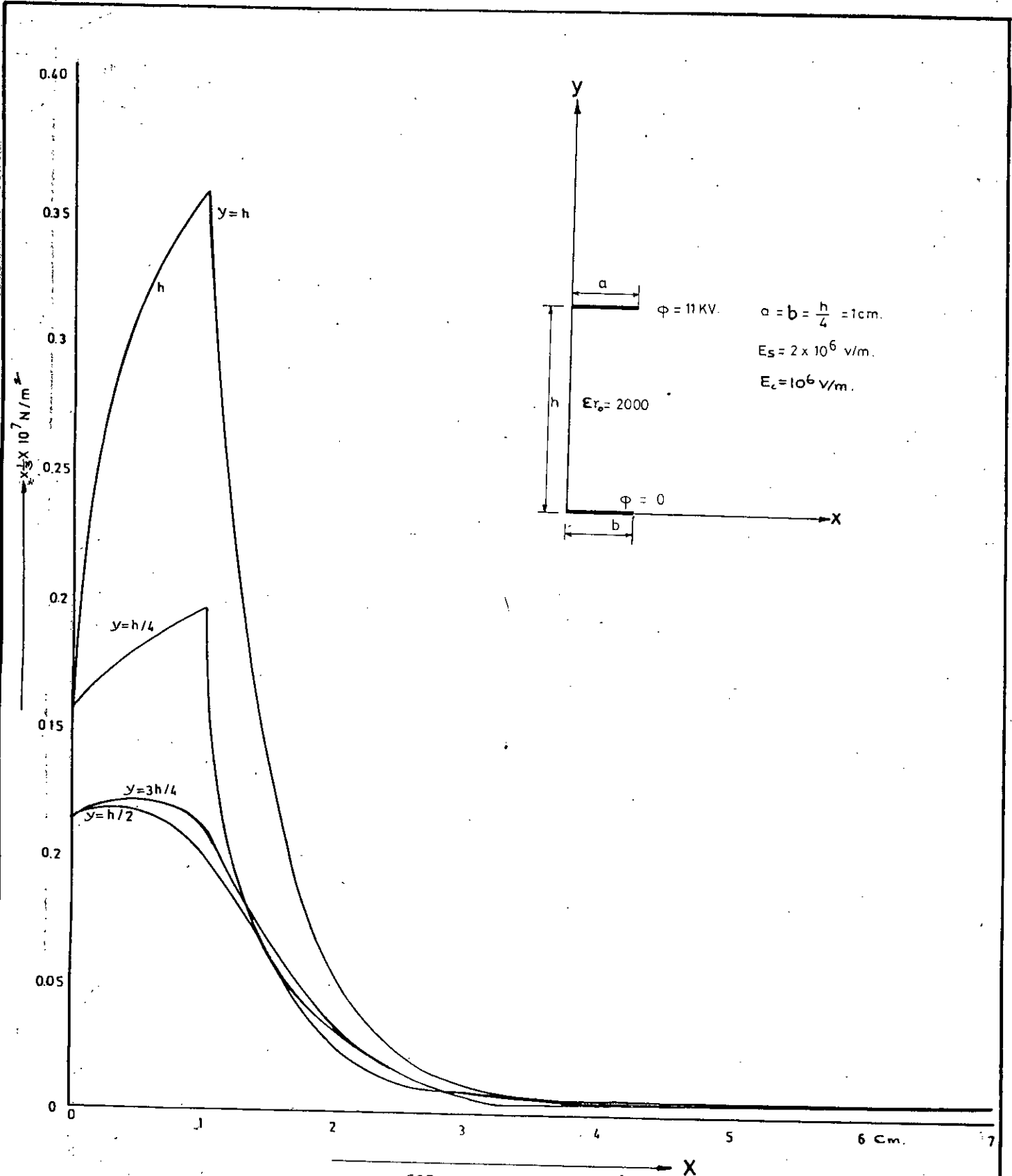


FIG 3.5: DISTRIBUTION OF MECHANICAL STRESS FOR FERROELECTRIC MATERIAL (STATIC CASE)

Table - 3:2

Electromechanical stress angle variation of ferroelectric material

(Staticase)

X (C.m.) Y (C.m.)		0	1	2	3	4	5	6	7
		4	θ_e -90	-44.57	-37.39	-32.96	-30.91	-30.62	-33.43
	θ_m +90	-179.153	-164.78	+155.92	-151.83	-151.25	-156.86	-165.28	
3	θ_e - 85.41	- 66.48	- 63.64	- 62.80	- -2.62	- 63.74	- 65.89	- 77.25	
	θ_m + 99.17	+137.02	+142.71	+144.39	+144.75	+143.72	+138.20	+115.49	
2	θ_e - 90.00	- 89.99	- 89.99	- 89.99	- 89.99	- 89.99	- 89.99	- 90.00	
	θ_m + 90.00	+ 90.00	+ 90.00	+ 90.00	+ 90.00	+ 90.01	+ 90.00	+ 90	
1	θ_e - 93.96	-107.96	-124.16	-133.90	-138.29	-139.47	-136.70	-118.48	
	θ_m + 82.074	+ 54.08	+ 21.69	+ 2.19	+ 6.59	- 8.94	- 3.40	+ 33.02	
0	θ_e -90	-163.07	-164.21	-164.75	-164.83	-164.11	-160.15	-135.00	
	θ_m +90	- 56.139	- 58.435	- 59.507	- 59.66	- 58.23	- 50.31	- 0.01	

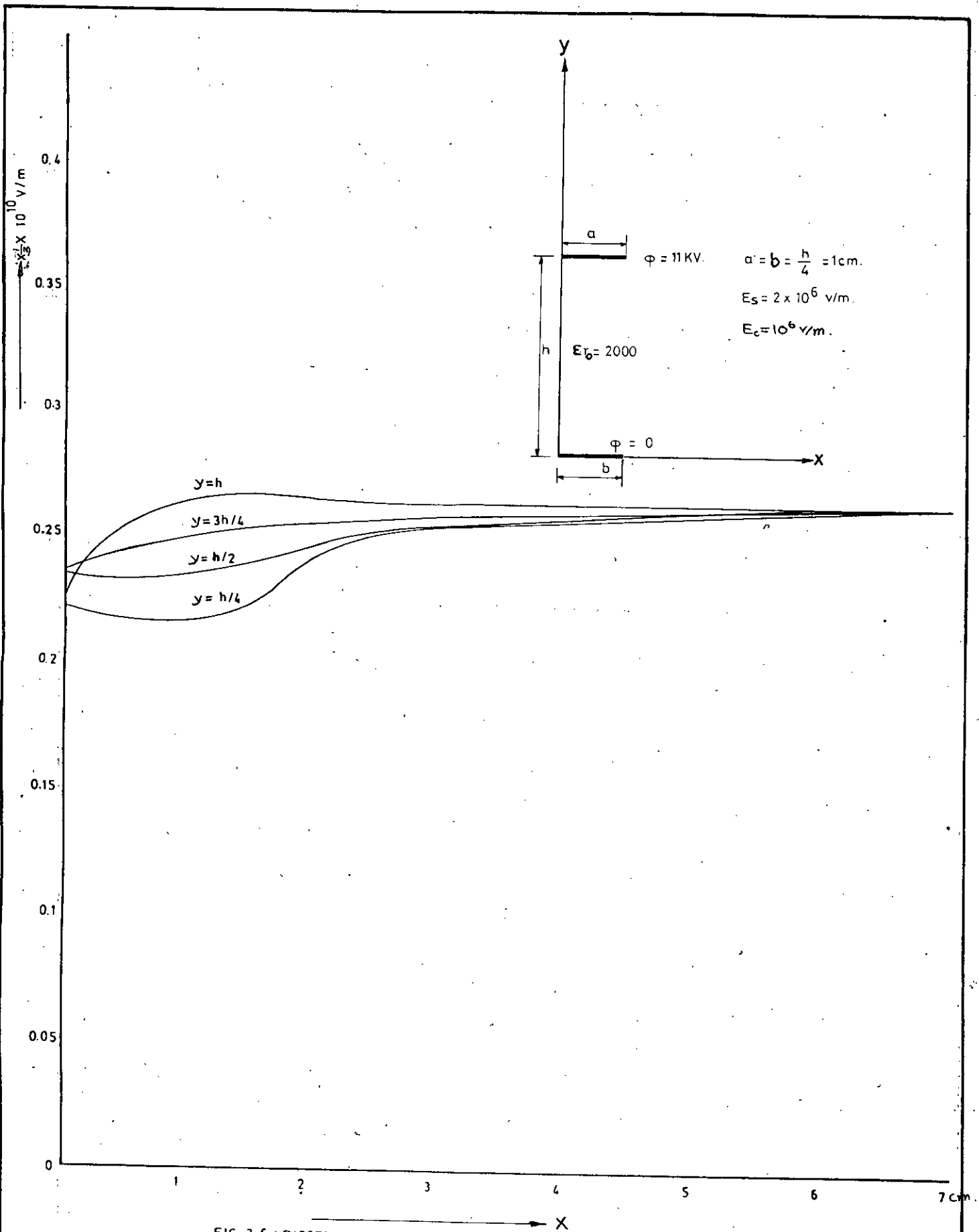


FIG. 3.6 : DISTRIBUTION OF ELECTRIC STRESS FOR FERROELECTRICAL MATERIALS
 (ALTERNATING CASE WHEN POTENTIAL VARIES FROM NEGATIVE MAXIMUM TO
 POSITIVE MAXIMUM)

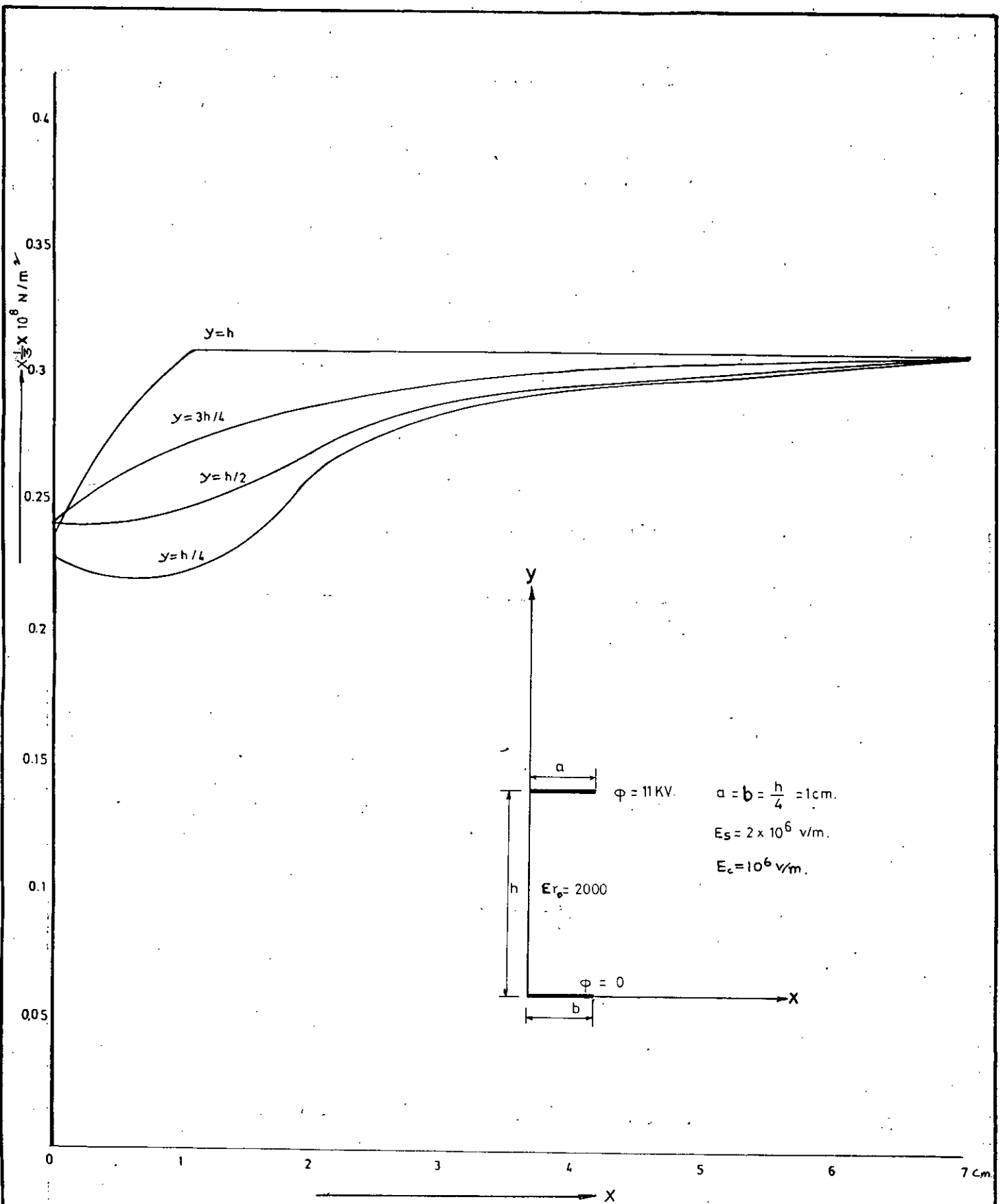


FIG. 3.7 : DISTRIBUTION OF MECHANICAL STRESS FOR FERROELECTRIC MATERIAL (ALTERNATING CASE WHEN POTENTIAL VARIES FROM NEGATIVE MAXIMUM TO POSITIVE MAXIMUM)

Table -33

Electromechanical stress angle variation of ferroelectric material

(Negative maximum to positive maximum)

Y (C.m.)	X (C.m.)	0	1	2	3	4	5	6	7
		4	θ_e	+35.10	29.98	+39.79	+42.85	+44.04	44.56
	θ_m	-17.42	-30.03	-10.44	- 4.28	- 1.90	- 0.87	- 0.39	- 0.15
3	θ_e	+37.23	+36.20	+40.03	+42.52	+43.80	+44.43	+44.73	+44.87
	θ_m	-15.52	-17.59	- .93	- 4.95	- 2.38	- 1.13	- 0.53	- 0.25
2	θ_e	+37.70	+38.38	+41.51	+43.32	+44.20	+44.62	+44.81	+44.89
	θ_m	-14.59	-13.23	- 6.97	- 3.35	- 1.59	- 0.75	- 0.37	- 0.20
1	θ_e	+36.75	+38.05	+44.16	+44.96	+45.04	+45.02	+45.00	+44.98
	θ_m	-16.48	-13.88	- 1.67	- 0.06	- 0.09	- 0.05	- 0.01	- 0.03
0	θ_e	+35.55	+52.24	+47.44	+46.00	+45.44	+45.19	45.07	45.00
	θ_m	-18.89	-14.49	- 4.88	- 2.01	- 0.89	- 0.39	- 0.15	0

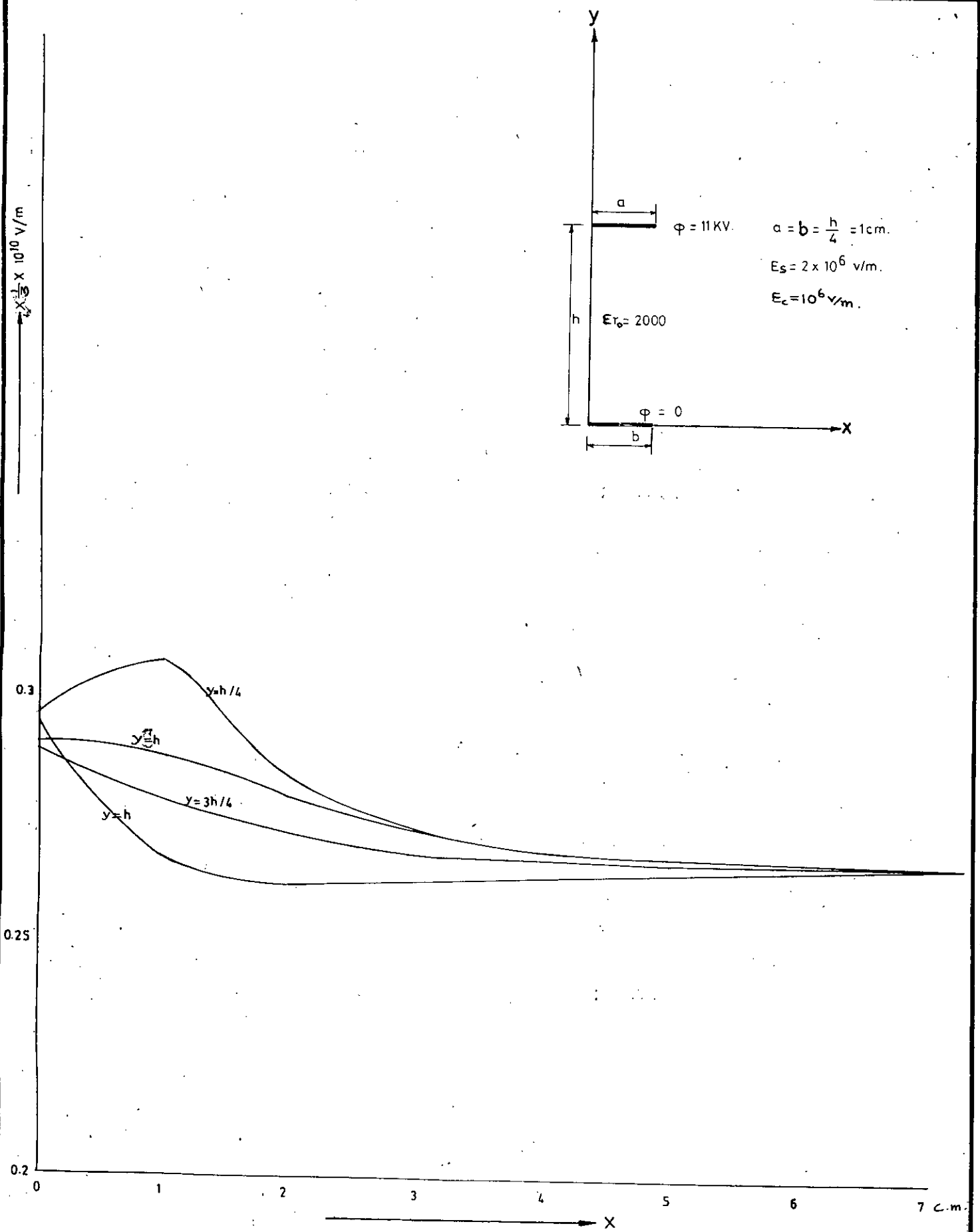


FIG. 3B. DISTRIBUTION OF ELECTRICAL STRESS FOR FERROELECTRIC MATERIAL
 (ALTERNATING CASE WHEN POTENTIAL VARIES FROM POSITIVE MAXIMUM
 TO NEGATIVE MAXIMUM)

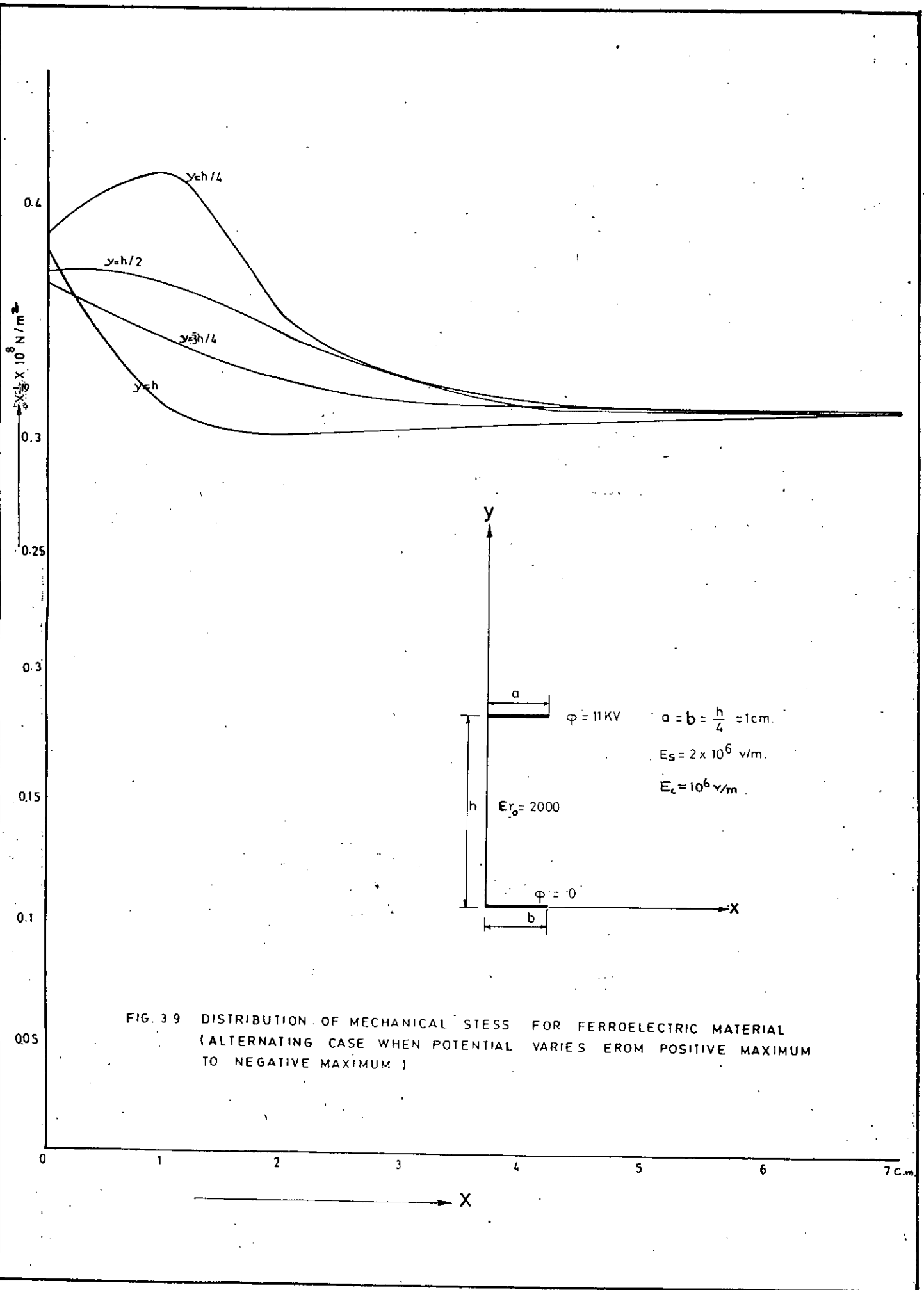


FIG. 3.9 DISTRIBUTION OF MECHANICAL STRESS FOR FERROELECTRIC MATERIAL (ALTERNATING CASE WHEN POTENTIAL VARIES FROM POSITIVE MAXIMUM TO NEGATIVE MAXIMUM)

Table - 3-4

Electromechanical stress angle variation of ferroelectric material

(Positive maximum to negative maximum)

X (C.m.) Y (C.m.)		Y							
		0	1	2	3	4	5	6	7
4	θ_e	-129.29	-119.55	-129.55	-132.79	-134.03	-134.56	-134.80	-134.92
	θ_m	+ 11.41	+ 30.22	+ 10.89	+ 4.40	+ 1.93	+ 0.87	+ 0.39	+ 0.15
3	θ_e	-129.44	-127.71	-130.48	-132.63	-133.85	-134.43	-134.73	-134.87
	θ_m	+ 11.20	+ 14.57	+ 9.02	+ 4.73	+ 2.33	+ 1.12	+ 0.53	+ 0.25
2	θ_e	-129.93	-130.26	-132.11	-133.47	-134.23	-134.62	-134.81	-134.89
	θ_m	+ 10.13	+ 9.46	+ 5.76	+ 3.05	+ 1.52	+ 0.74	+ 0.36	+ 0.20
1	θ_e	-129.76	-131.21	-134.33	-134.96	-135.04	-135.02	-135.00	-134.98
	θ_m	+ 10.47	+ 5.57	+ 1.32	+ 0.06	+ 0.08	+ 0.05	+ 0.01	+ 0.03
0	θ_e	-128.98	-175.95	-136.93	-135.91	-135.42	-135.19	-135.07	- 45.00
	θ_m	+ 12.02	+ 7.91	+ 3.86	+ 1.82	+ 0.85	+ 0.38	+ 0.15	+ 0

76292

For alternating field a different nature of stress curve is observed. In the cycle when applied voltage alternates from negative maximum to positive maximum, the stress distribution takes the shape as in Fig. 3.6 and 3.7 and their angle variation is as in Table 3.3. In this case the maximum stress occurs at the edge of the upper plate and the minimum stress occurs at the lower plate. The stress curves attain a constant value with the increase in x . The stress angles in table 3.3 indicate that in this half-cycle the material is subject to laterally expanding stress.

When the applied voltage alternates from positive maximum to negative maximum, the stress distribution takes the shape as in Fig. 3.8 and 3.9 and their angle variation is as in Table 3.4. In this case the maximum stress occurs at the edge of the lower plate and minimum stresses at the upper plate, the stress curves attain constant value with the increase in x . In this case also, the material is subject to laterally expanding stresses as can be checked from the angle distribution shown in table 3.4.

3.5 Discussion.

The above study gives the distribution of electric and equivalent mechanical stresses developed in a ferro-electric material placed between two circular parallel electrodes.

We calculated stresses for both static and alternating fields. In all cases shapes of the electric stress distribution curves resemble those of the equivalent mechanical stress distribution curves.

For static case the peak stress occurs at the edge of the top plate and minimum stress at the bottom plate. At $y = h/2$ or i.e. in the mid-level the electromechanical stress has only normal components but the edge of the top plate is subjected to compressive lateral stress only. In general the lower half of the material is subject to expanding stress, the upper half to compressive stresses for a static applied field.

For an a.c. field as the applied potential varies from negative maximum to positive maximum, the peak stress occurs at the edge of the top plate and its magnitude is higher than that of the static stress. The angle variation (Table 3.3) in this case is such that the insulator inside the plates are subject to laterally expanding stresses.

For applied potential varying from positive maximum to negative maximum, the peak stress occurs at the bottom plate and its magnitude is higher than that of the above two cases. So, the greatest maximum stress occurs at the bottom plate. The angle variation (Table 3.4) in this case is such that the insulator inside the plate suffers from laterally expanding stresses.

CHAPTER 4

DESIGN OF FERRO-ELECTRIC INSULATORS

DESIGN OF FERRO-ELECTRIC INSULATORS

4.1 Introduction:

The most obvious objective in insulating system design is to obtain suitable system elements (electrodes and insulators) which will withstand electrical and equivalent mechanical stresses at normal operating conditions and occasional faults. In order to get reliable insulating system, the peak value of the stresses must be less than the allowable stress. The continuously increasing voltage level of HV devices imposes the need for better space utilization. For this purpose it is necessary to apply electrode and insulator contour optimization in insulating system design. This contour optimization of field distribution and its application in insulating system design is widely discussed by Stih [9]. The same method was discussed by Itaka and Hara [12] for three dimensional field problems. In order to produce high quality insulator, it is necessary to follow some noticed points which are as follows:

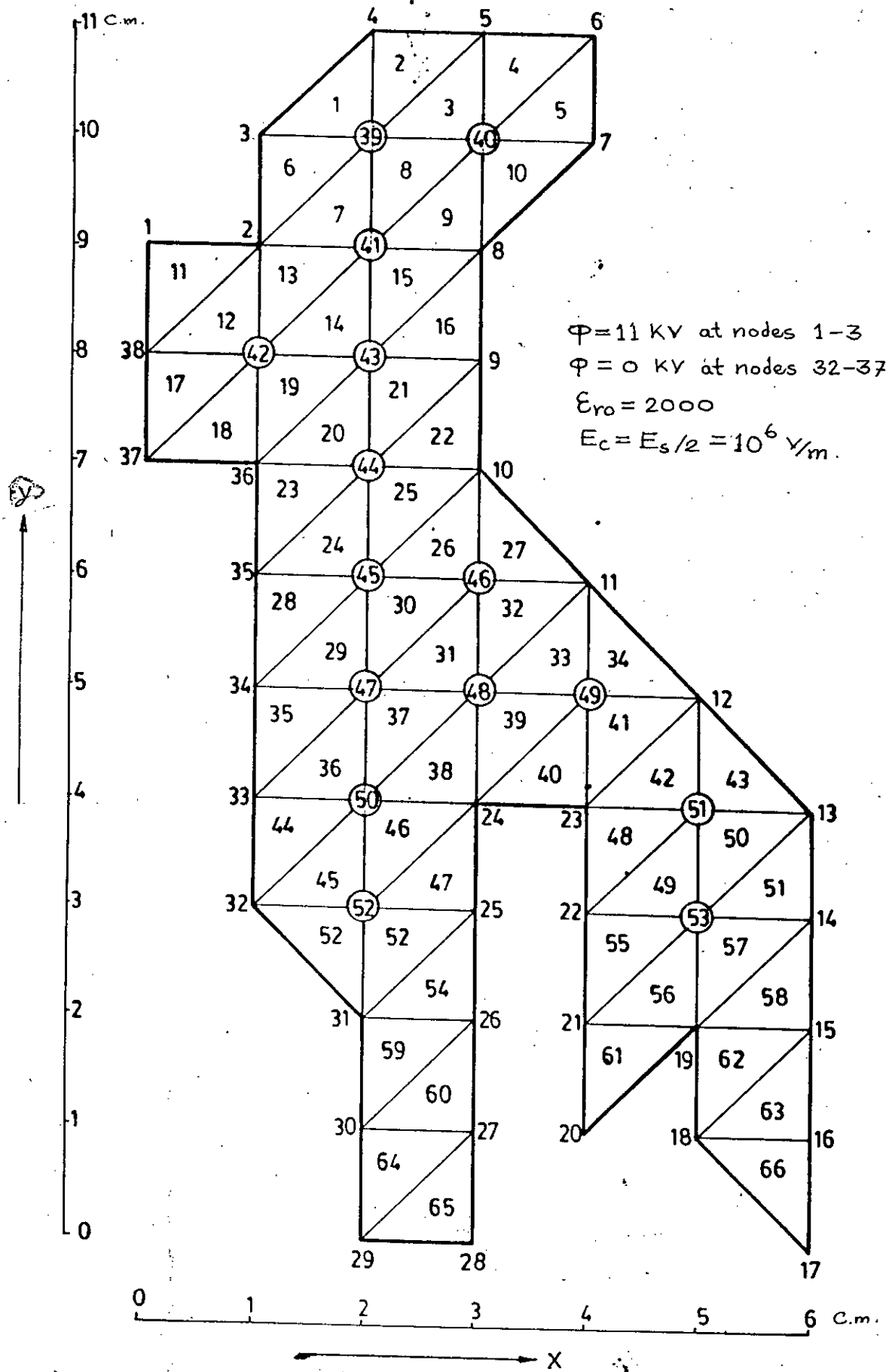
- Selection of high quality materials
- High manufacturing technique
- Strict quality control
- Suitable design engineering

The mechanical strength of porcelain depends upon its raw material. So, the raw material must be free of ferrous particles, the size and pores should be less and the amount of crystal should be more. Then using high manufacturing technique and strict quality control we can produce good quality of insulators with the application of suitable engineering design. The electro-mechanical stress analysis of ferro-electric material gives an idea about the stress distribution, magnitude of peak stress and angle of action.

4.2 Finite Element Design of a Pin-Type Insulator:

Pin type insulators are used in distribution lines for voltage ranges upto 33 kV. It is usually a one-piece construction and fitted with pin to the tower. The finite element design of this type of insulator can be performed using the electromechanical stress analysis for ferro-electric materials studied in chapter 3.

The pin-type insulator is symmetrical about its axis. So we take half portion of it divided into 66 nos. of triangular elements as in fig. 4.1. The 66 no. of elements produces 53 nodes. Then taking 11 kV at nodes 1,2 and 3 and considering the pin at nodes 33-37 and applying the analysis of article 3.4 we get electric stress and equivalent mechanical stress distribution for static and alternating cases. The distributions are plotted in figs. 4.2-4.5.



4.1. Finite element division of pint-type Insulator.

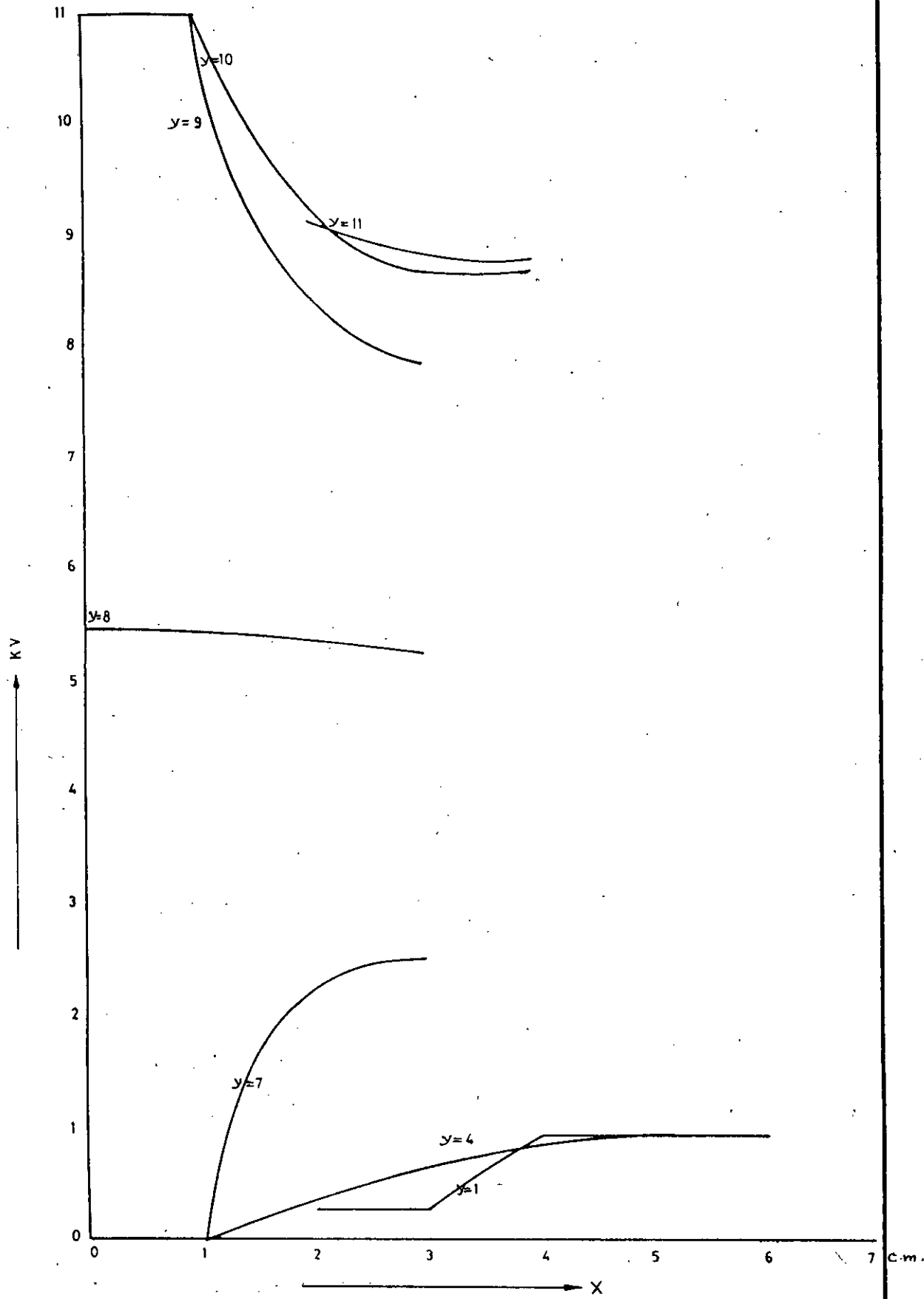


FIG. 42. POTENTIAL DISTRIBUTION FOR PIN TYPE INSULATOR

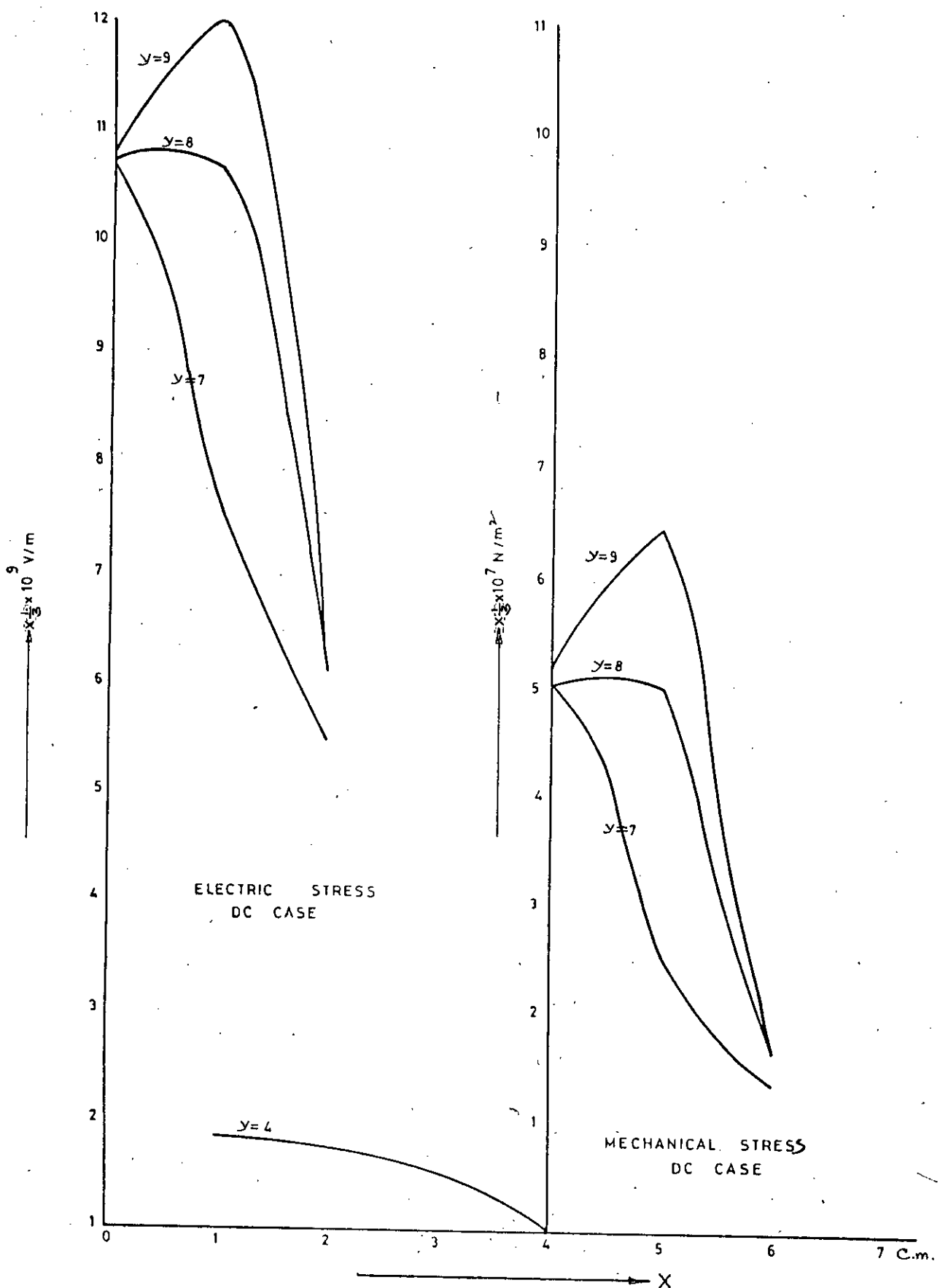


FIG. 4.3. ELECTRO-MECHANICAL STRESS DISTRIBUTION IN PIN TYPE INSULATOR

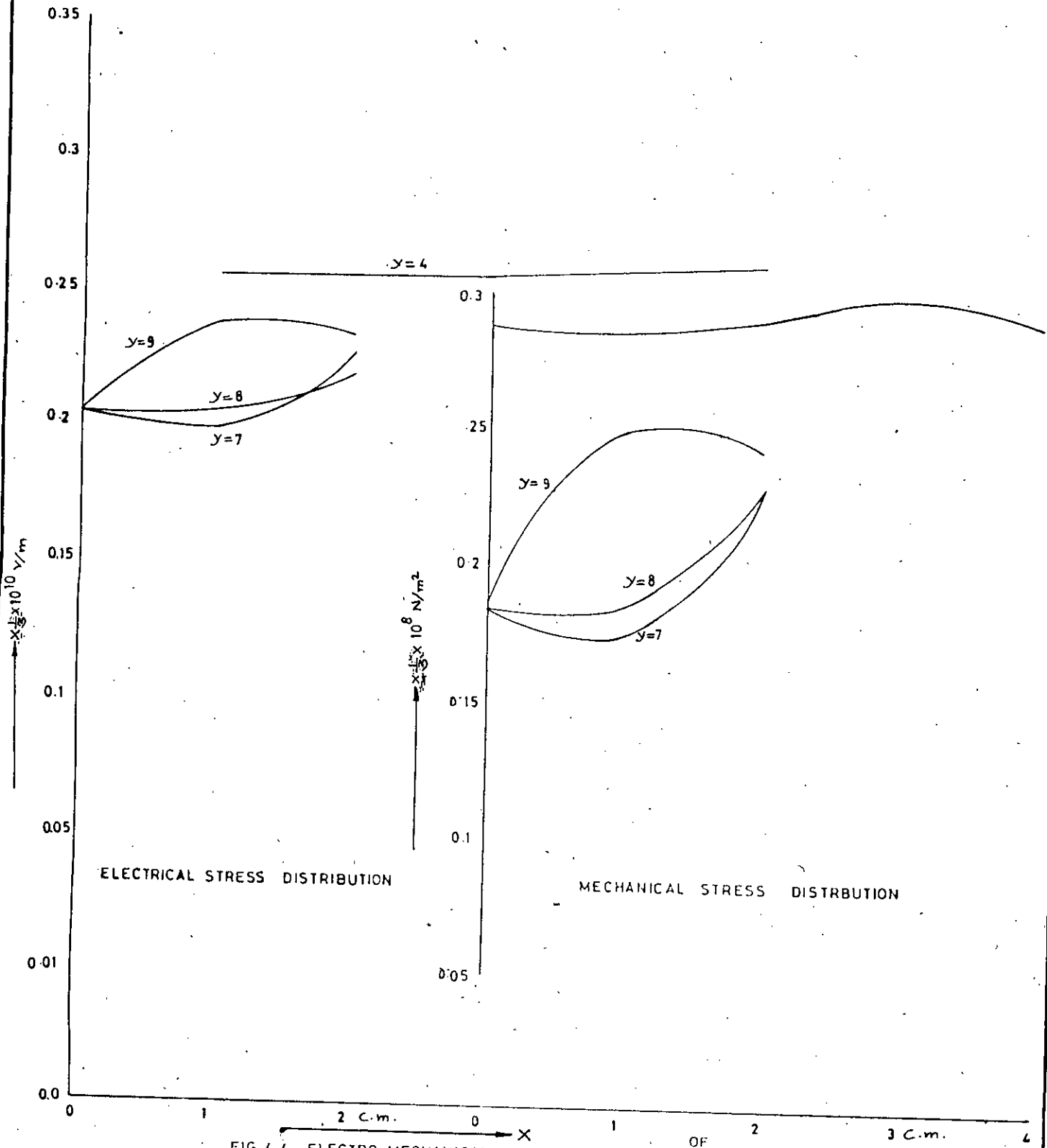


FIG. 4.4. ELECTRO MECHANICAL STRESS DISTRIBUTION ON A PIN-TYPE INSULATOR WHEN POTENTIAL VARIES FROM NEGATIVE MAXIMUM TO POSITIVE MAXIMUM.

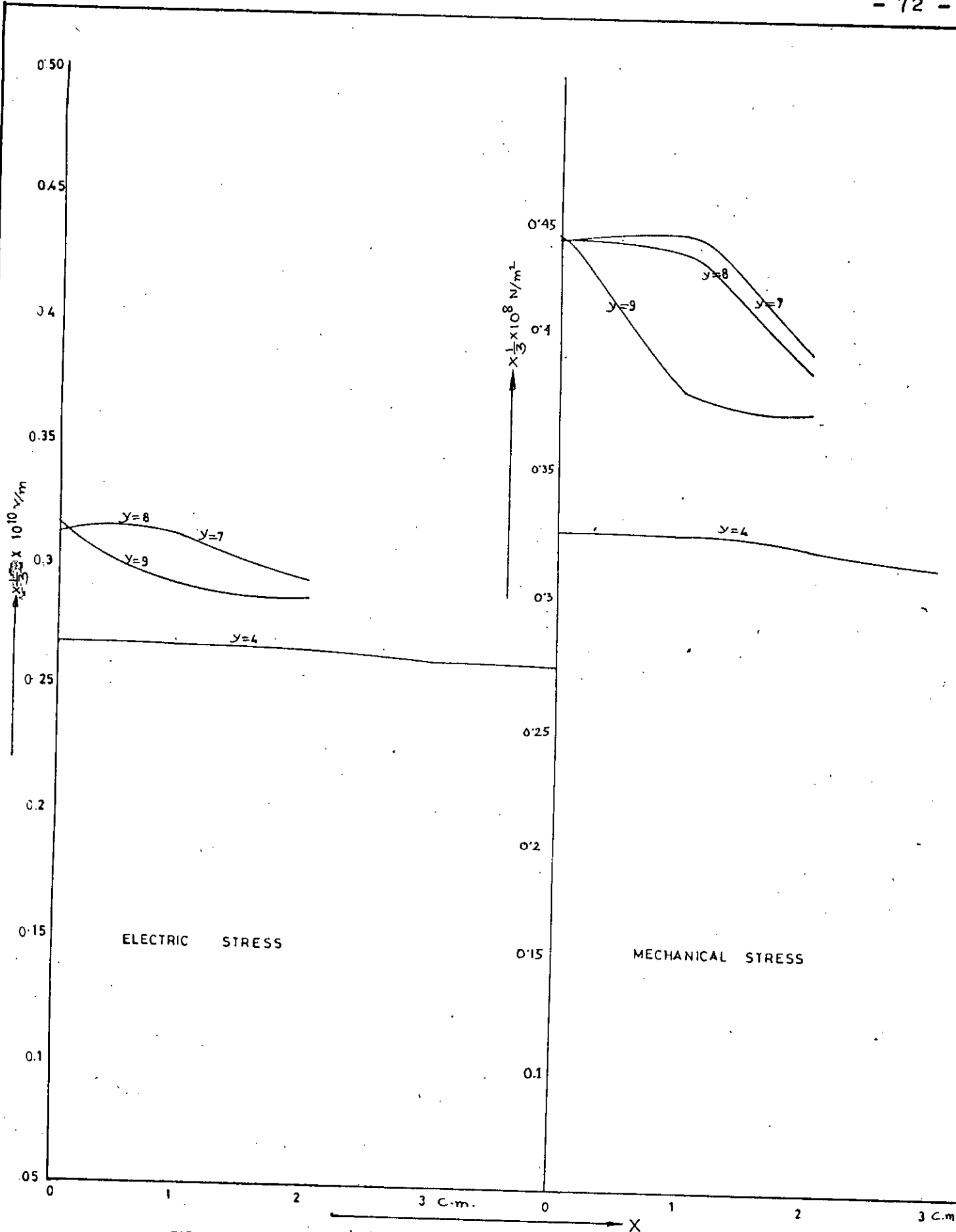


FIG. 4.5. ELECTRO MECHANICAL STRESS DISTRIBUTION OF PIN - TYPE INSULATOR WHEN POTENTIAL VARIES FROM POSITIVE MAXIMUM TO NEGATIVE MAXIMUM.

TABLE 4.1

Table showing average vertical stresses at different regions of
the Pin-Type insulator considered in Fig. 4.1

Region considered	Type of field applied	Working Load (KN)	Average Stress in Y-direction (KN/m ²)	Type of Stress
Top region, (elements 1 - 10)	DC	- 0.54	-34.39	Compressive
	AC (negative maximum to positive maximum)	-12.20	-776.95	Compressive
	AC (positive maximum to negative maximum)	12.02	765.48	Tensile
Between Conductor and Pin (elements 11 - 22)	DC	8.75	744.24	Tensile
	AC (negative maximum to positive maximum)	-28.53	-2524.77	Compressive
	AC (positive maximum to negative maximum)	34.79	3078.98	Tensile
Body region (elements 28 - 43)	DC	-0.035	-1.14	Compressive
	AC (negative maximum to positive maximum)	-1.414	-46.00	Compressive
	AC (positive maximum to negative maximum)	1.414	45.67	Tensile
Outer Skirt (elements 55 - 66)	DC	0.00003	-0.0005	Compressive
	AC (negative maximum to positive maximum)	0.071	1.18	Tensile
	AC (positive maximum to negative maximum)	-0.071	-1.18	Compressive

From the figures and numerical results we observe that the potentials of the nodes decreases as its distance increases from the potential plate and becomes zero at the pin i.e. at the ground plate.

From study of the average vertical component of stresses at different regions of the insulator as shown in Table 4.1, the following phenomena are observed:

(i) For d.c., the material between the pin and the conductor is subjected to a tensile stress and the remaining portion undergoes compressive stress. However, the insulator as whole is subjected to tensile stress.

(ii) For a.c. when the cycle varies from negative maximum to positive maximum the material above the pin undergoes compressive stress and the remaining portion undergoes tensile stress, but as a whole the insulator is subjected to compressive stress.

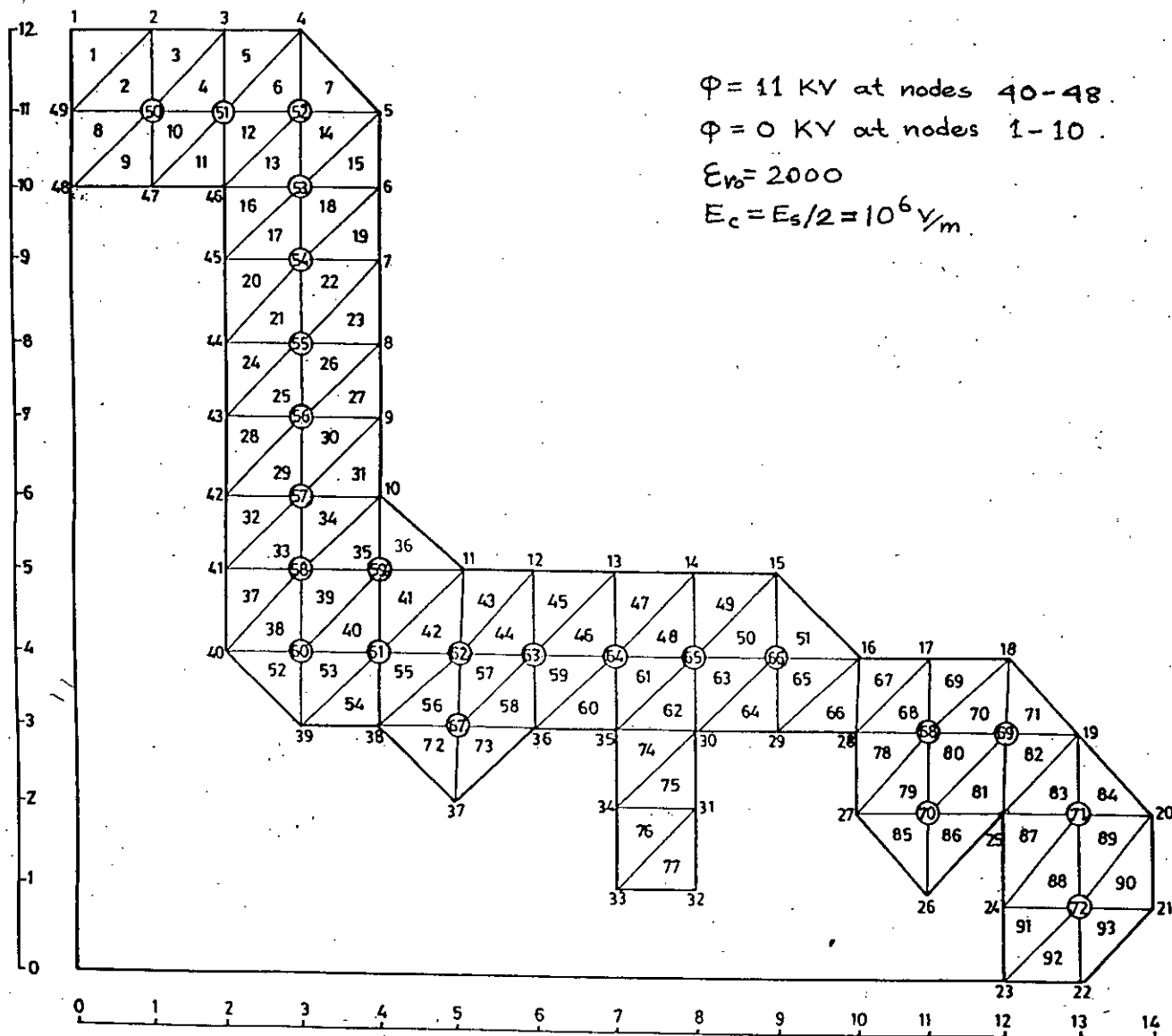
(iii) For a.c. when the cycle varies from positive maximum to negative maximum, the material above the pin undergoes tensile stress and the remaining portion undergoes compressive stress but as a whole the insulator is subjected to tensile stress.

In all cases the average lateral component of stress is very high compared to the vertical component. It is tensile in nature and of the order of 10^7 N/m². However, for the proposed design the magnitude of electromechanical stress is greatly reduced compared with the case of hypothetically infinite lateral extent of the material as discussed in Chapter 3.

4.3 Finite Element Design of a Disc type Insulator:

The Disc type insulators are used in constructing HV transmission lines. Usually this type of insulators are designed at a lower voltage say 11 kV and used as string for HV (132KV, 230KV, 400KV etc) transmission lines. The finite element design of this type of insulator is performed applying the electro-mechanical stress analysis for ferro-electric materials in chapter 3. In doing so, the axially symmetric insulator is divided into 93 numbers of triangular elements as shown in fig. 4.6 which results 72 nos. of nodes. As the cap of the insulator remains at ground potential, we take the potentials of the nodes 1 to 10 as zero. As the conductor hangs with a steel pin fitted inside the insulator, we take 11 kV at the nodes 40 to 48 considering that each disc is designed for 11 kV). Now, applying the method developed in section 3.4 we get the distributions of electric and equivalent mechanical stresses developed within the insulator. The distributions are plotted in figs. 4.7-4.12.

From the figures and numerical results we found that the potentials of the nodes decreases as the distance from the pin increases and becomes zero at the cap.



4.6 Finite element division of disc-type Insulator

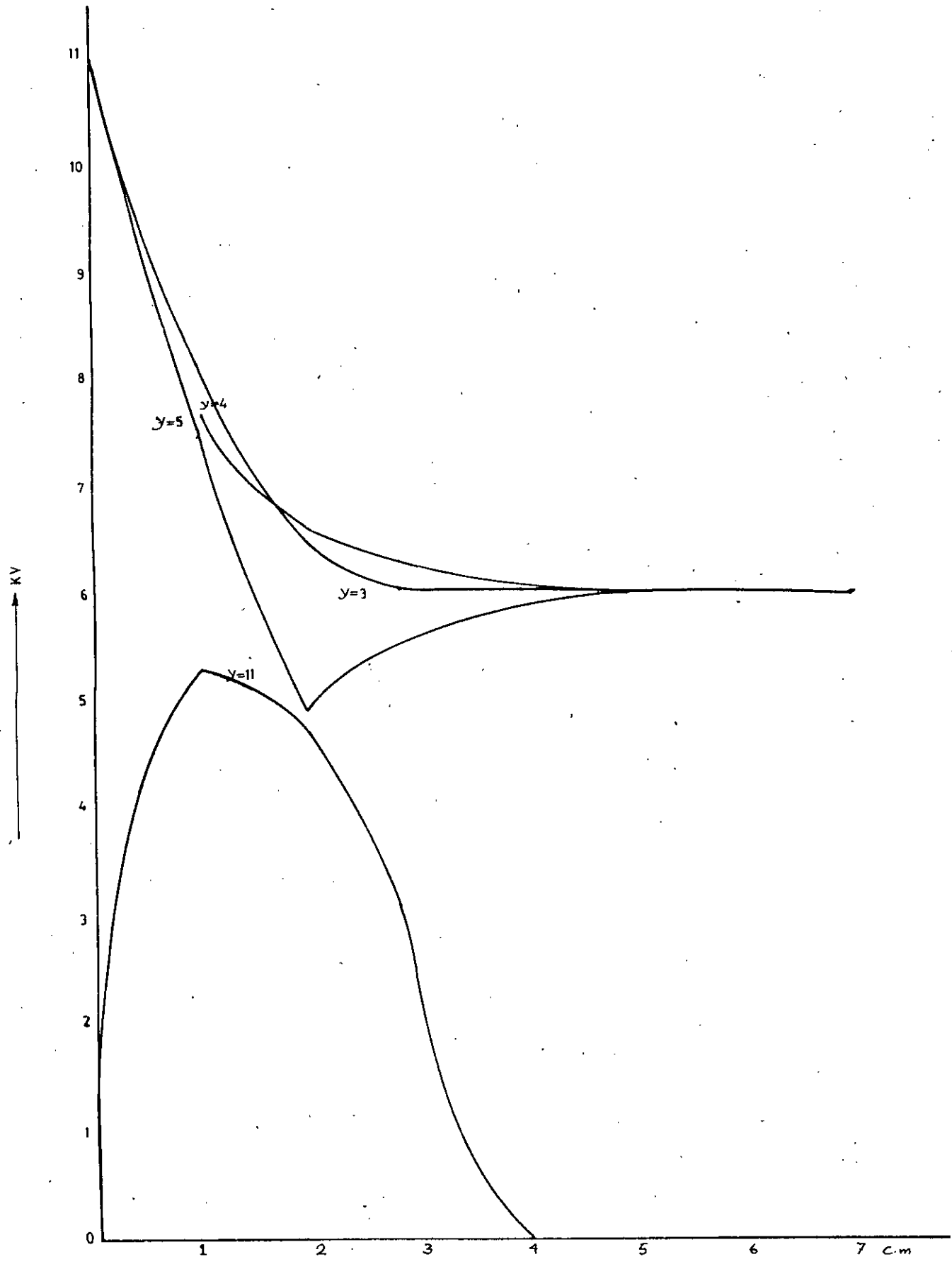


FIG. 4.7 POTENTIAL DISTRIBUTION IN HORIZONTAL PLANE IN DISC TYPE INSULATOR

—————→ x

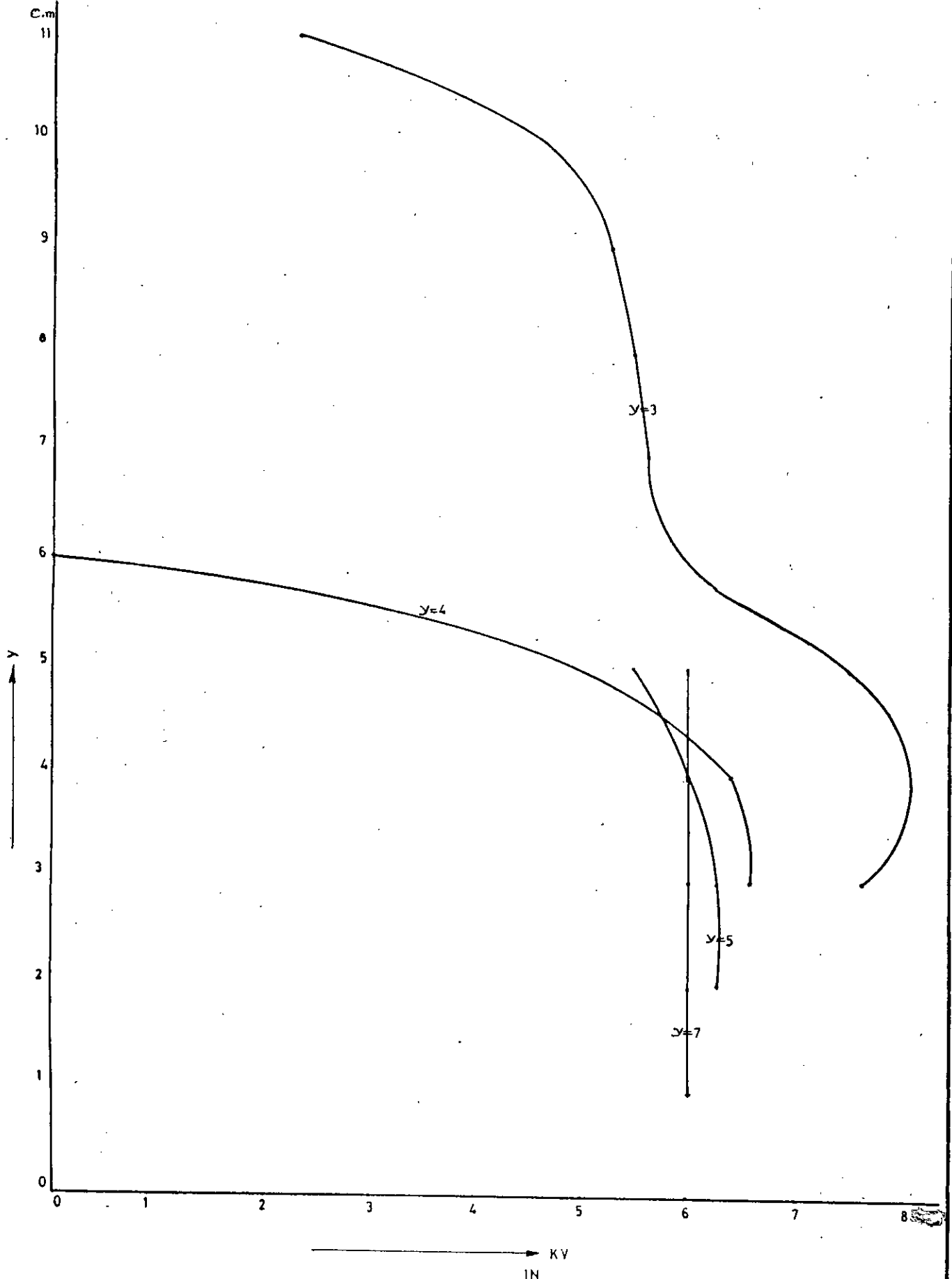


FIG. 4.8 POTENTIAL DISTRIBUTION VERTICAL PLANE OF DISC TYPE INSULATOR

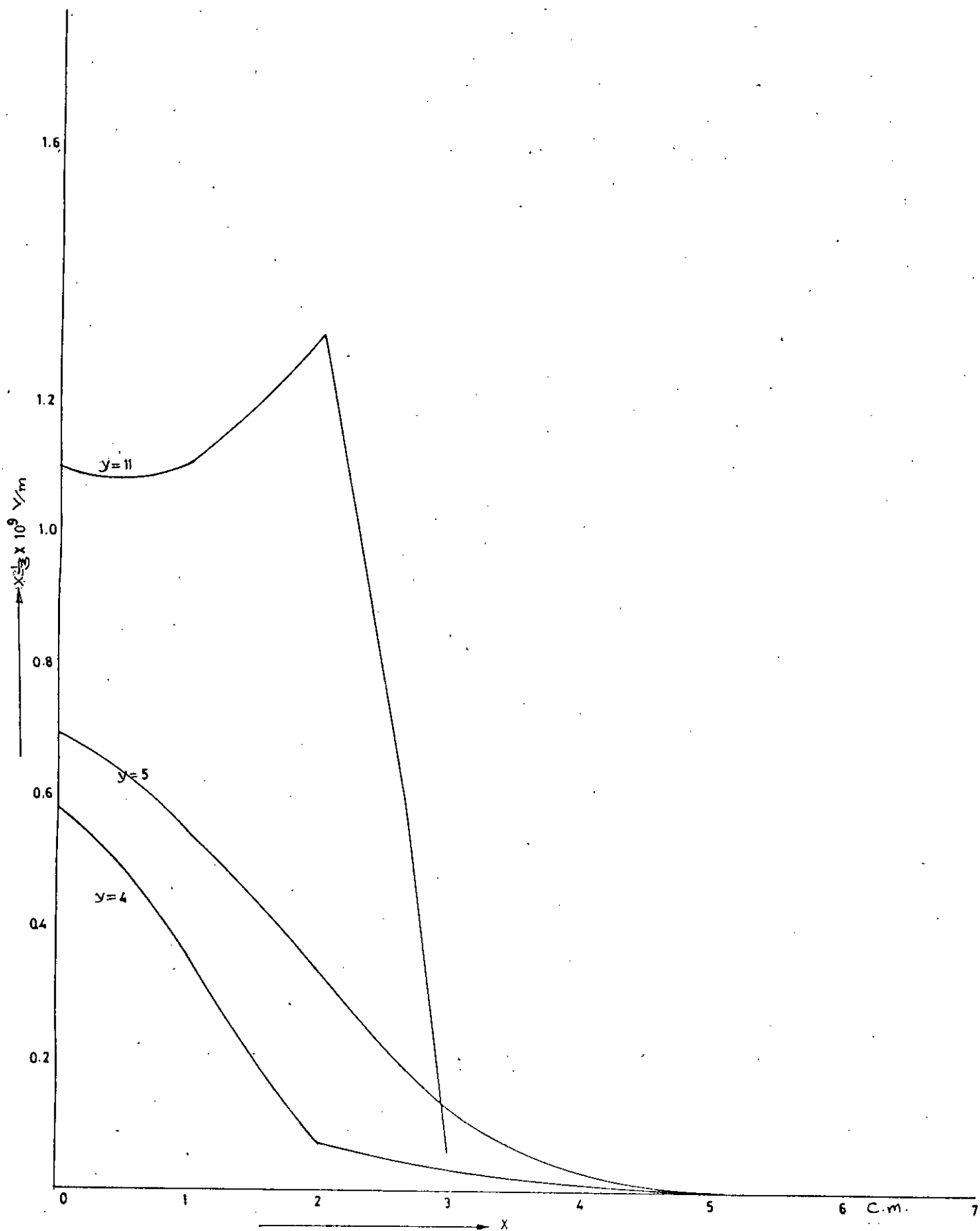


FIG. 4. 9 DISTRIBUTION OF ELECTRIC STRESS IN DISC TYPE INSULATOR (STATIC CASE)

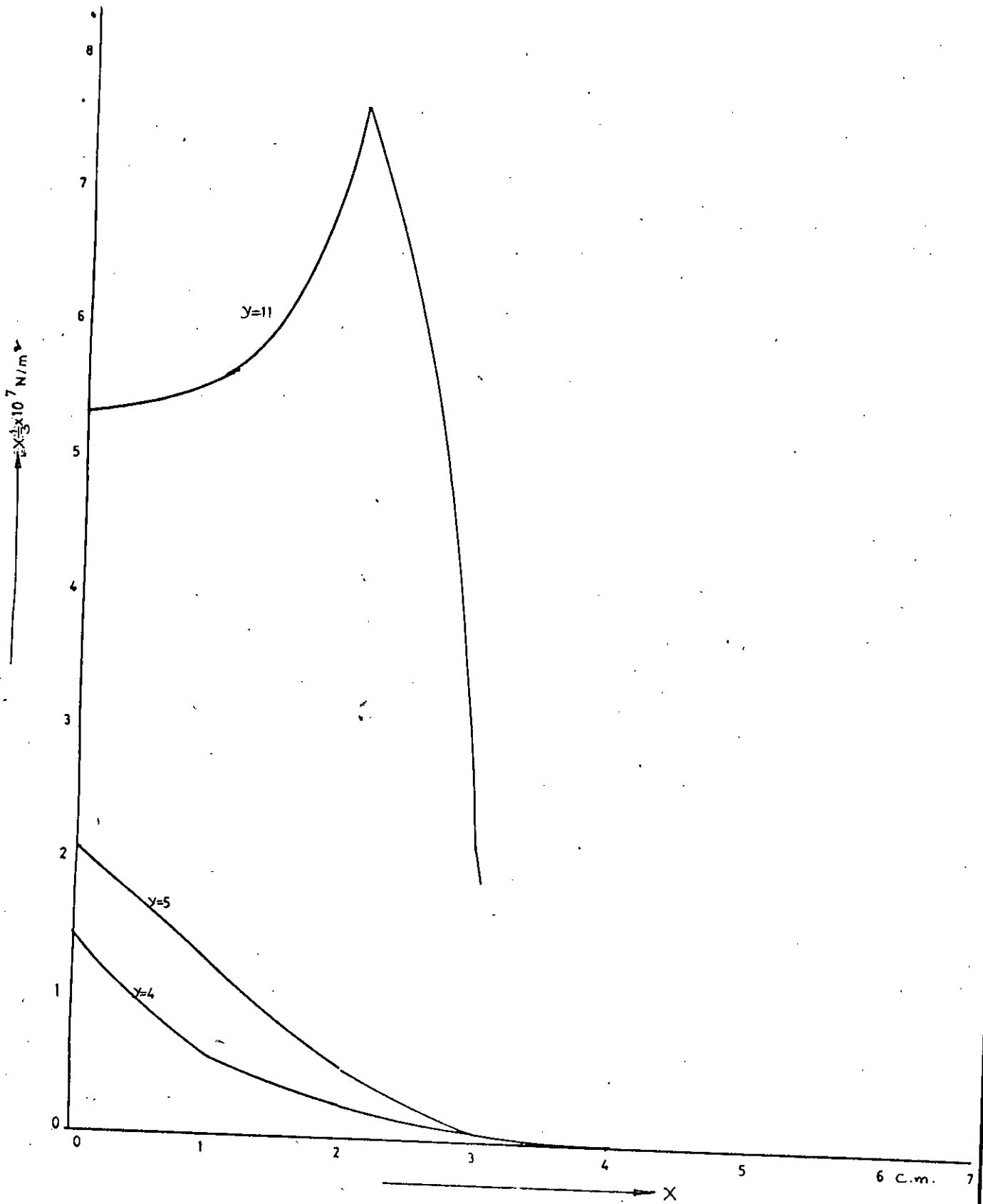


FIG. 4.10 DISTRIBUTION OF MECHANICAL STRESS IN DISC TYPE INSULATOR (STATIC CASE)

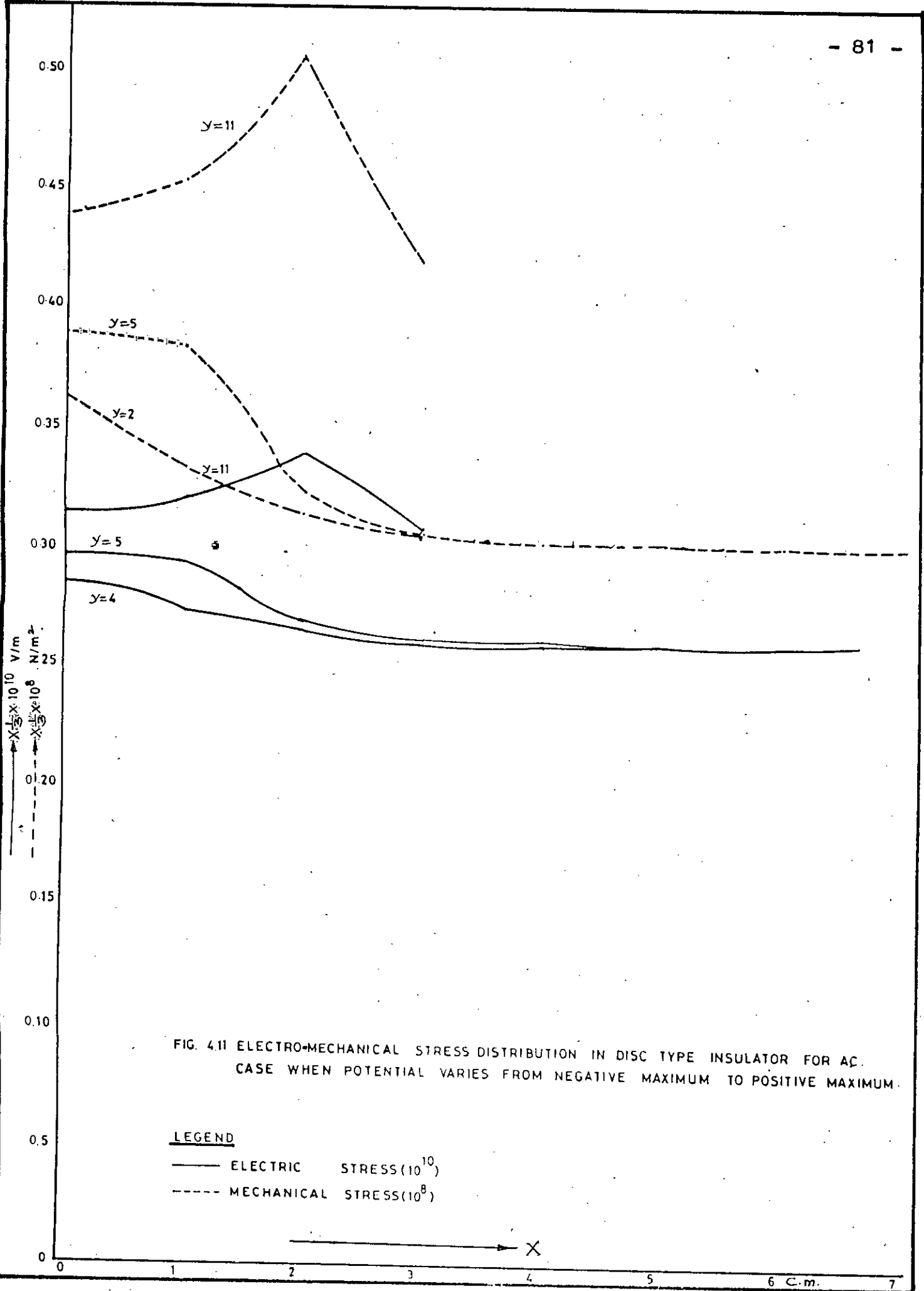


FIG. 4.11 ELECTRO-MECHANICAL STRESS DISTRIBUTION IN DISC TYPE INSULATOR FOR AC. CASE WHEN POTENTIAL VARIES FROM NEGATIVE MAXIMUM TO POSITIVE MAXIMUM.

LEGEND
—— ELECTRIC STRESS (10^{10})
- - - MECHANICAL STRESS (10^8)

X

6 C.m.

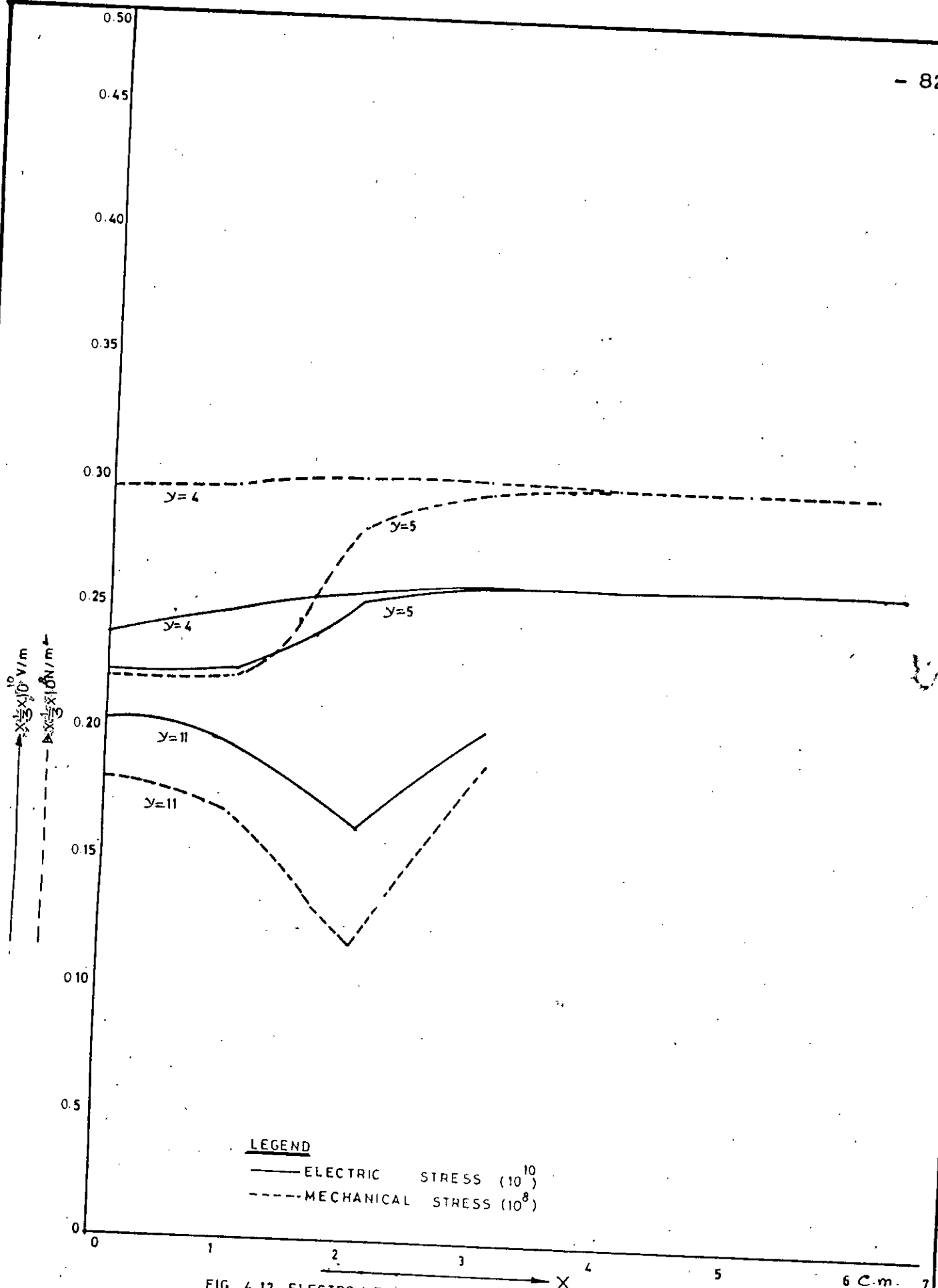


FIG. 4.12 ELECTRO MECHANICAL STRESS DISTRIBUTION IN DISC TYPE INSULATOR FOR A.C CASE WHEN POTENTIAL VARIES FROM NEGATIVE MAXIMUM TO POSITIVE MAXIMUM.

TABLE 4.2

Table showing average vertical stresses at different regions of the Disc-type insulator considered in Fig. 4.6

Region considered	Type of field applied	Working Load (KN)	Average Stress in Y-direction (KN/m ²)	Type of Stress
Top circular portion (elements 1 - 15)	DC	7.82	437.36	Compressive
	AC (negative maximum to positive maximum)	18.64	1042.51	Compressive
	AC (positive maximum to negative maximum)	-16.25	-908.84	Tensile
Cap portion (elements 16 - 36)	DC	-52.75	-1301.51	Tensile
	AC (negative maximum to positive maximum)	-127.90	-3150.68	Tensile
	AC (positive maximum to negative maximum)	111.71	2756.23	Compressive
Body region (elements 37 - 71)	DC	-3.58	-23.40	Tensile
	AC (negative maximum to positive maximum)	-12.20	-79.73	Tensile
	AC (positive maximum to negative maximum)	11.03	72.09	Compressive

From the study of the average vertical component stress at different regions of the insulator as shown in Table 4.2. the following phenomena are observed:

(i) For d.c. the material of the top circular portion undergoes compressive stress and the remaining portion undergoes tensile stress. However, the insulator as a whole undergoes tensile stress.

(ii) For a.c. when the cycle varies from negative maximum to positive maximum, the material of the top circular portion undergoes compressive stress and the remaining portion undergoes tensile stress. However, the insulator as a whole undergoes tensile stress.

(iii) For a.c. when the cycle varies from positive maximum to negative maximum, the material of the top circular portion undergoes tensile stress and the remaining portion undergoes compressive stress. However, the insulator as a whole undergoes compressive stress.

In all cases the average lateral component of stress is very high compared to the vertical component. It is tensile in nature and is of the order of 10^7 N/m². However, for the proposed design the magnitude of electromechanical stress is greatly reduced compared with the case of hypothetically infinite lateral extent of the material as discussed in Chapter 3.

4.4 Discussion:

The design obtained in this section for pin type and disc - type insulators are performed on the basis of finite numbers of elements and by analyzing the electromechanical stress for ferroelectric materials filling those elements. From the Table 4.1. and 4.2. it can be observed that the portion of the insulator which remains in contact with the conductor undergoes the maximum stress. Moreover, for a.c. the insulator is subjected to alternate compressive and tensile stresses with the alternation of cycle.

To check the validity of the present calculation we made a comparison with the electromechanical test data of disc-type insulator carried out by Swedish State Power Board materials Laboratory [19], when the insulator is subjected to 60 KV A.C. the observed average electromechanical load is 105.5 KN. According to the present calculation the average electromechanical load at 60 KV becomes 119.52 KN. This agrees reasonably well with the test result. It may be mentioned that the difference in the working load is due to the value of internal field constant which we take $1/3$ for $BaTiO_3$ and this value may perhaps be slightly different.

CHAPTER 5

GENERAL DISCUSSION AND SUGGESTION
FOR FUTURE WORKS

GENERAL DISCUSSION AND SUGGESTION
FOR FUTURE WORK

Computer Aided design of ferro-electric insulators is carried over by calculating the electromechanical stress distribution in ferro-electric material by finite element method. Firstly, a Computer Program has been developed for calculating the electromechanical stress distribution in ferro-electric material of infinite extent and then it is modified to calculate the electromechanical stress distribution for the ferro-electric insulator of finite size.

To get an idea about the electromechanical stress over a region, it is first necessary to know the potential distribution over the region. The space between two circular parallel plates has been divided into a finite number of triangular elements. Then assuming linear dependence of potential over the elements Laplace's equation has been solved to get potential at different nodes. It is observed that for dielectric between two circular parallel plates, the potentials at different nodes converge to half of the applied potential at the midlevel between the parallel plates as the distance from the axis of parallel plates increases. The potential distribution has been plotted in Fig. 3.3.

Since ferro-electric materials are extensively used in fabrication of high voltage insulators because of their high relative permittivity, a study has been given to the electro-mechanical stress distribution in such materials in section 3.3. and 3.4. Because of the non-linearity in the medium, the stresses cannot be calculated in a direct manner. The finite element method enables us to linearize the medium in a piecewise manner and evaluate the effective non-linear characteristics. In view of the hysteresis curve of polarization of ferro-electric materials, three cases were investigated. These are :-

- (1) insulator subjected to d.c. voltage
- (2) insulator subjected to a.c. voltage and the applied voltage goes from negative maximum to positive maximum, and
- (3) insulator subjected to a.c. voltage and the applied voltage goes from the positive maximum to negative maximum.

The magnitude of the electric and equivalent mechanical stresses for the above three cases for material of infinite extent are plotted in Figs. 3.4, 3.5, 3.6, 3.7, 3.8 and 3.9 respectively.

For static case (Figs. 3.4-3.5) the peak stress occurs at the edge of the plate and the stress value drops rapidly for distance away from the edge. From the angle distribution shown in table 3.2, it is clear that half of the ferro-electric material experiences compressive stresses and the rest half experiences tensile stresses.

For alternating current when potential goes from negative maximum to positive maximum, the maximum stress occurs at the upper plate and the minimum stress occurs at the lower plate (Figs. 3.6 and 3.7). The stress curves attain a constant value as the distance increases from the axis of the plates. From the angle distribution (Table 3.3) it is clear that the material in between the plates is subjected to laterally expanding stress.

For alternating current, when potential goes from positive maximum to negative maximum, the maximum stress occurs at the edge of the lower plate and minimum stress at the upper plate (Figs. 3.8 and 3.9). The stress curves attain a constant value with the increase in distance from the plate. From the angle distribution (Table 3.4), it is clear that the material is subjected to laterally expanding stress. The greatest peak stress occurs in this case at the bottom plate.

The electromechanical stress analysis for ferro-electric material of infinite extent developed in chapter 3 is applied for designing ferro-electric insulators of finite size. In doing so, we divided the insulator region into a finite number of elements (Figs 4.1 and 4.6) and applying the above analysis we get the results discussed below:

For the design of pin-type insulator (Fig. 4.1) the insulator region is divided into 66 numbers of elements comprising 53 nodes. The width of each element is taken as 1 cm. The potentials of different nodes decreases as its distance increases from the conductor and becomes zero at the pin. For d.c., the material between the pin and the conductor undergoes tensile stress and the remaining portion undergoes compressive stress. However, the insulator as a whole is subjected to compressive stress. For a.c. when the cycle varies from negative maximum to positive maximum, the material above the pin undergoes compressive stress and the remaining portion undergoes tensile stress. However, the insulator as a whole is subjected to compressive stress. For a.c. when the cycle varies from positive maximum to negative maximum, the materials above the pin undergoes tensile stress and the remaining portion undergoes compressive stress. However, the insulator as a whole is subjected to compressive stress.

For the design of Disc-type insulator (4.6), the insulator region is divided in 93 numbers of elements comprising 72 nodes. The width of each element is taken as 1 cm. The potentials at different nodes decreases as the distance from the pin increases and becomes zero at the cap. For d.c., the material of the top circular portion undergoes compressive stress and the remaining portion undergoes tensile stress. However, the insulator as a whole is subjected to tensile stress. For a.c. when the potential varies from negative maximum to positive maximum, the material in the top circular region undergoes compressive stress and the remaining portion undergoes tensile stress. However, the insulator as a whole is subjected to tensile stress. For a.c. when the cycle varies from positive maximum to negative maximum, the material in the top circular portion undergoes tensile stress and the remaining portion undergoes compressive stress. However, the insulator as a whole is subjected to compressive stress. Therefore, the insulator is subjected to alternate compressive and tensile stresses with the alternation of cycle.

An interesting feature is that a severe lateral component of the electromechanical stress can be observed in the two ferro-electric insulators designed in the present work. It is of the order of 10^7 N/m² for a.c. and 10^6 N/m² for d.c. with an 11 KV applied potential. Such lateral phenomenon seems to have not been studied extensively in experimental design of ferro-electric insulators.

The finite element design of pin-type and Disc-type insulator performed in this thesis can be a very useful technique for designing ferro-electric insulators. Hence the analysis may be extended to get optimum design of ferro-electric insulators.

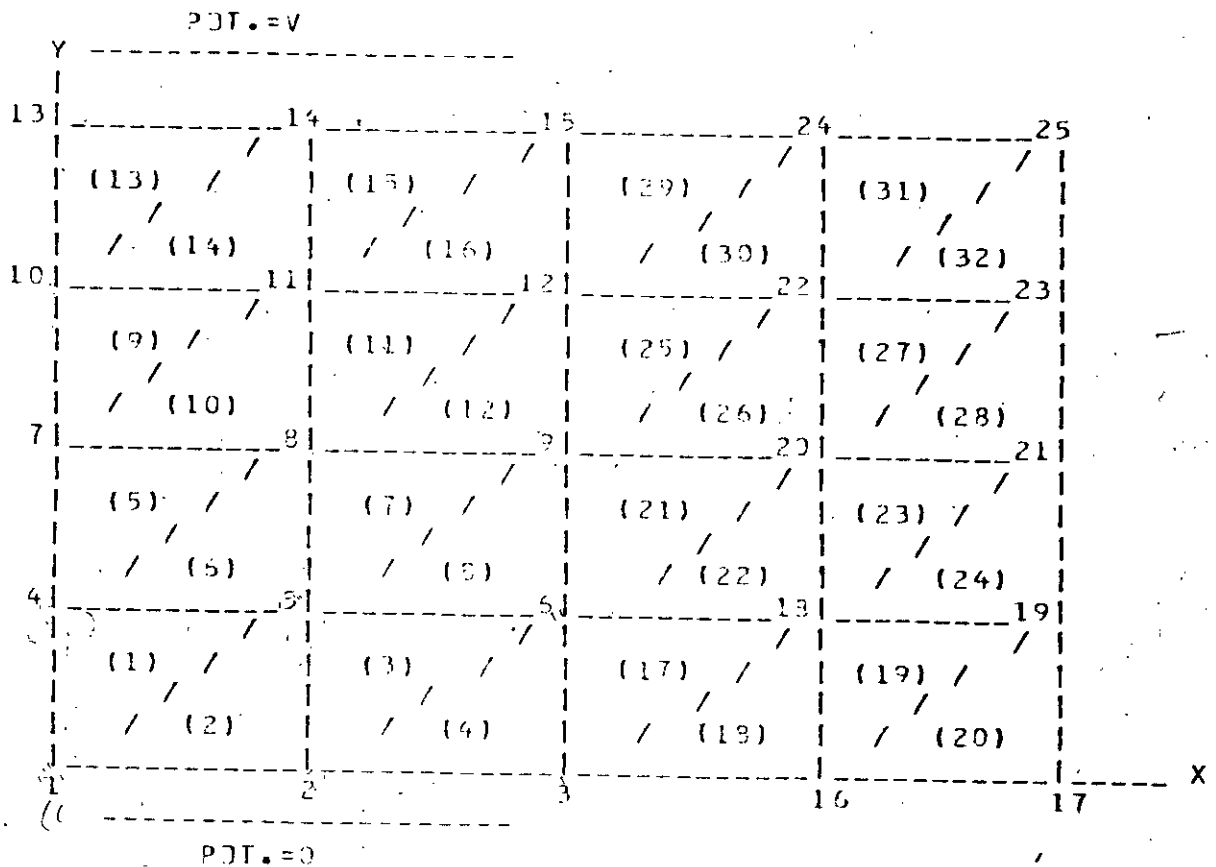
The electrothermal stress analysis and frequency response of insulators may be subjects of further research.

COMPUTER PROGRAM

PDT.=V

PDT.=0

TWO PARALLEL PLATES



DIVISION INTO TRIANGULAR ELEMENTS
 () INDICATES ELEMENTS
 NUMBERS INDICATE NODES

MAIN PROGRAM

REAL KA

DIMENSION V(45,45),C(45,45),MI(64),YJ(64),XK(64),YI(64),YJ(64),YK
 +(64),I(64),J(64),K(64),ZA(45,20),Z1(45,45),VD(45),XA(45),HX1(64),
 +HY1(64),B1(80),B2(80),B3(80),C1(80),C2(80),C3(80),B4(80),B5(80),
 +B6(80),C5(80),C6(80),C4(80)

OPEN(UNIT=5,FILE='IN',STATUS='OLD')

```
OPEN(UNIT=3,FILE='DUT',STATUS='NEW')
```

```
VJ(1)=0.0
```

```
VJ(2)=0.0
```

```
VJ(3)=0.0
```

```
VJ(13)=11000.0
```

```
VJ(14)=11000.0
```

```
C VJ(15)=0.0
```

```
DD 8 MV=4,12
```

```
VJ(MV)=0.0
```

```
B CONTINUE
```

```
DD 71 M5=15,45
```

```
VJ(M5)=0.0
```

```
71 CONTINUE
```

```
C
```

```
R=1
```

```
NML=64
```

```
NQY=45
```

```
DD 10 IA=1,NQY
```

```
DD 10 JA=1,NQY
```

```
V(IA,JA)=0.0
```

```
10 CONTINUE
```

```
DATA I/4,2,5,3,7,5,3,5,10,9,11,9,13,11,14,12,6,3,16,15,9,6,20,18,15
```

```
+2,9,22,20,15,12,24,22,19,17,30,26,31,27,32,28,21,19,34,30,35,31,36
```

```
+32,23,21,38,34,39,35,40,36,25,23,42,38,43,39,44,40/
```

```
DATA J/1,5,2,6,4,8,5,9,7,11,8,12,10,14,11,15,3,16,19,17,6,18,18,19
```

```
+9,20,20,21,12,22,22,23,17,26,26,27,27,28,28,29,19,30,30,31,31,32,
```

```
+32,33,21,34,34,35,35,36,36,37,23,38,38,39,39,40,40,41/
```

```
DATA K/5,1,5,2,3,4,2,5,11,7,12,8,14,10,15,11,18,18,18,19,20,20,21,
```

```
+21,22,22,23,23,24,24,25,25,30,30,31,31,32,32,33,33,34,34,35,35,36,
```

```
+36,37,37,38,38,39,39,40,40,41,41,42,42,43,43,44,44,45,45/
```

```
DATA XI/0.0,1.0,1.0,2.0,0.0,1.0,1.0,2.0,0.0,1.0,1.0,2.0,0.0,1.0,1
```

```
+0,2.0,2.0,2.0,3.0,3.0,2.0,2.0,3.0,3.0,2.0,2.0,3.0,3.0,2.0,2.0,3.0
```

```
+3.0,4.0,4.0,5.0,5.0,6.0,6.0,7.0,7.0,4.0,4.0,5.0,5.0,6.0,6.0,7.0,7
```

```
+0,4.0,4.0,5.0,5.0,6.0,6.0,7.0,7.0,4.0,4.0,5.0,5.0,6.0,6.0,7.0,7.0
```

```
+/
```

```
DATA XJ/0.0,1.0,1.0,2.0,0.0,1.0,1.0,2.0,0.0,1.0,1.0,2.0,0.0,1.0,1
```

```
+0,2.0,2.0,3.0,4.0,4.0,2.0,3.0,3.0,4.0,2.0,3.0,3.0,4.0,2.0,3.0,3.0
```

```
+4.0,4.0,5.0,5.0,6.0,6.0,7.0,7.0,3.0,4.0,5.0,5.0,6.0,6.0,7.0,7.0,8
```

```
+0,4.0,5.0,5.0,6.0,6.0,7.0,7.0,3.0,4.0,5.0,5.0,6.0,6.0,7.0,7.0,8.0
```

```
+/
```

```
DATA XK/1.0,0.0,2.0,1.0,1.0,3.0,2.0,1.0,1.0,0.0,2.0,1.0,1.0,0.0,2
```

```
+0,1.0,3.0,3.0,3.0,4.0,3.0,3.0,4.0,4.0,3.0,3.0,4.0,4.0,3.0,3.0,4.0
```

```
+4.0,5.0,5.0,6.0,6.0,7.0,7.0,3.0,4.0,5.0,5.0,6.0,6.0,7.0,7.0,8.0,8
```

```
+0,5.0,5.0,6.0,6.0,7.0,7.0,3.0,4.0,5.0,5.0,6.0,6.0,7.0,7.0,8.0,8.0
```

```
+/
```

```
DATA YI/1.0,0.0,1.0,0.0,2.0,1.0,2.0,1.0,3.0,2.0,3.0,2.0,4.0,3.0,4
```

```
+0,3.0,1.0,0.0,0.0,2.0,1.0,2.0,1.0,3.0,2.0,3.0,2.0,4.0,3.0,4.0
```

```
+2.0,1.0,0.0,1.0,0.0,1.0,0.0,1.0,0.0,2.0,1.0,2.0,1.0,2.0,1.0,2.0,1
```

```
+0,3.0,2.0,3.0,2.0,3.0,2.0,3.0,2.0,4.0,3.0,4.0,3.0,4.0,3.0,4.0,3.0
```

```
+/
```

```
DATA YJ/0.0,1.0,0.0,1.0,1.0,2.0,1.0,2.0,2.0,3.0,2.0,3.0,3.0,4.0,3
```

```
+0,4.0,0.0,0.0,1.0,0.0,1.0,1.0,1.0,1.0,2.0,2.0,2.0,2.0,3.0,3.0,3.0
```

```
+3.0,0.0,0.0,0.0,0.0,0.0,0.0,0.0,0.0,0.0,1.0,1.0,1.0,1.0,1.0,1.0,1
```

```
+0,2.0,2.0,2.0,2.0,2.0,2.0,2.0,2.0,3.0,3.0,3.0,3.0,3.0,3.0,3.0,3.0
```

```
+/
```

DATA YK/1.0,0.0,1.0,0.0,2.0,1.0,2.0,1.0,3.0,2.0,3.0,2.0,4.0,3.0,4.0,3.0,1.0,1.0,1.0,1.0,1.0,2.0,2.0,2.0,2.0,3.0,3.0,3.0,3.0,4.0,4.0,4.0,4.0,0SE

*,4.0,1.0,1.0,1.0,1.0,1.0,1.0,1.0,1.0,1.0,2.0,2.0,2.0,2.0,2.0,2.0,2.0,2.0,2SE

*,0,3.0,3.0,3.0,3.0,3.0,3.0,3.0,3.0,4.0,4.0,4.0,4.0,4.0,4.0,4.0,4.0,4.0,4.0,4.0SE

*/ WRITE(3,11) SE:

11 FORMAT(4X,'ELEMENTS OF MATRIX'//) SE:

DO 20 JJ=1,NML SE:

DO 30 IJ=1,NJN SE:

DO 30 JJ=1,NJN SE:

C(IJ,JJ)=0.0 SE:

30 CONTINUE SE:

XI1=XI(JJ) SE:

XJ1=XJ(JJ) SE:

XK1=XK(JJ) SE:

YI1=YI(JJ) SE:

YJ1=YJ(JJ) SE:

YK1=YK(JJ) SE:

I1=I(JJ) SE:

J1=J(JJ) SE:

K1=K(JJ) SE:

BI=YJ1-YK1 SE:

BJ=YK1-YI1 SE:

BK=YI1-YJ1 SE:

CI=XK1-XJ1 SE:

CJ=XI1-XK1 SE:

CK=XJ1-XI1 SE:

C(I1,I1)=(BI*BI+CI*CI)*R SE:

C(J1,J1)=(BJ*BJ+CJ*CJ)*R SE:

C(K1,K1)=(BK*BK+CK*CK)*R SE:

C(I1,J1)=(BI*BJ+CI*CJ)*R SE:

C(I1,K1)=(BI*BK+CI*CK)*R SE:

C(J1,K1)=(BJ*BK+CJ*CK)*R SE:

C(J1,I1)=C(I1,J1) SE:

C(K1,J1)=C(J1,K1) SE:

C(K1,I1)=C(I1,K1) SE:

DO 22 IV=1,NJN SE:

DO 22 JV=1,NJN SE:

V(IV,JV)=V(IV,JV)+C(IV,JV) SE:

22 CONTINUE SE:

20 CONTINUE SE:

DO 17 IP=1,2 SE:

DO 17 JP=1,NJN SE:

V(IP,JP)=0.0 SE:

17 CONTINUE SE:

DO 18 IJ=13,14 SE:

DO 18 JI=1,NJN SE:

V(IJ,JI)=0.0 SE:

18 CONTINUE SE:

DO 19 IR=1,2 SE:

V(IR,IR)=1.0 SE:

19 CONTINUE SE:

V(13,13)=1.0 SE:

V(14,14)=1.0 SE:


```

C      TT1=SQRT(TX1**2+TY1**2)
C      S3=1000000.0
C      S4=EX0+S3
C      S5=EY0+S3
C      DX2=E0*(E0*S4-10*S4**3)
C      DY2=E0*(E0*S5-10*S5**3)
C      EZ2=SQRT(DX2**2+EY2**2)
C      EA2=ATAN(EY2/DX2)*(180.0/PI)
C      EX2=((E0-1.0)/3.0)+1.0)*S4-(40/3.0)*S4**3
C      EY2=((E0-1.0)/3.0)+1.0)*S5-(40/3.0)*S5**3
C      TY2=(DY2*EY2-DX2*EX2)*0.5
C      TX2=SQRT(DX2**2+DY2**2)*EY2
C      TT2=SQRT(TX2**2+TY2**2)
C      ANG2=ATAN(TY2/TX2)*(180.0/PI)
C      S6=EX0-S3
C      S7=EY0-S3
C      DX3=E0*(E0*S6-10*S6**3)
C      DY3=E0*(E0*S7-10*S7**3)
C      EZ3=SQRT(DX3**2+EY3**2)
C      EA3=ATAN(EY3/DX3)*(180.0/PI)
C      EX3=((E0-1.0)/3.0)+1.0)*S6-(40/3.0)*S6**3
C      EY3=((E0-1.0)/3.0)+1.0)*S7-(40/3.0)*S7**3
C      TY3=(DY3*EY3-DX3*EX3)*0.5
C      TX3=SQRT(DX3**2+DY3**2)*EY3
C      TT3=SQRT(TX3**2+TY3**2)
C      ANG3=ATAN(TY3/TX3)*(180.0/PI)
C      IF(EX1.EQ.0.)EAI=-99.
C      IF(EY1.EQ.0.)ANG1=99.
C      IF(EX1.EQ.0.)GO TO 200
C      EAI=ATAN(TY1/EX1)*(180.0/PI)
C      IF(EX1.LT.0.)EAI=EAI-180.
C      ANG1=ATAN(TY1/TX1)*(180.0/PI)
C200  WRITE(3,132)M,TT1,ANG1,TT2,ANG2,TT3,ANG3
C132  FORMAT(1X,I2,1X,F10.4,1X,F7.2,1X,F10.4,1X,F7.2,1X,F10.4,1X,F7.2/)
C      IF(EX0.EQ.0.)EAD=-99.
C      IF(EY0.EQ.0.)GO TO 200
C      EAD=ATAN(EY0/EX0)*(180./PI)
C 200  WRITE(3,132)M,EZ1,EAI,EZ2,EA2,EZ3,EA3
C 132  FORMAT(1X,I2,1X,F10.4,1X,F7.2,1X,F10.4,1X,F7.2,1X,F10.4,1X,F7.2/)
C +E10.4,2X,F5.2/)
C 37  CONTINUE
C
C      STOP
C      END
C      SUBROUTINE TO OBTAIN INVERSE OF A MATRIX
C      SUBROUTINE INVERT(ZA,N,ZI)
C      DIMENSION ZA(45,90),ZI(45,45)
C      M=N+N
C      M2=N+1
C      DO 24 LI=1,N
C      DO 24 LJ=M2,M
C24   ZA(LI,LJ)=0.0
C      DO 81 K=1,N
C      I2=K+N
C81   ZA(K,I2)=1.0

```


ELECTROMECHANICAL STRESS ANALYSIS OF FERROELECTRIC MATERIAL

NODE POTENTIAL AT DIFF NODE(V)

1	0.00
2	0.00
3	3204.12
4	2953.16
5	3156.38
6	4172.45
7	5499.92
8	5499.91
9	5499.87
10	8046.71
11	7843.48
12	6827.32
13	11000.00
14	11000.00
15	7795.69
16	4471.59
17	5023.42
18	4829.41
19	5173.80
20	5499.84
21	5499.82
22	6170.28
23	5825.82
24	6528.11
25	5975.21
26	5274.50

27 5389.45
 28 5439.00
 29 5452.79
 30 5342.56
 31 5422.16
 32 5456.83
 33 5466.58
 34 5499.79
 35 5499.78
 36 5499.77
 37 5499.77
 38 5657.02
 39 5577.39
 40 5542.67
 41 5532.97
 42 5725.10
 43 5610.11
 44 5560.55
 45 5546.76

	TT1	ANG1	TT2	ANG2	TT3	ANG3
1	0.5108E+06	82.07	0.7579E+07	-16.48	0.1273E+08	10.48
2	0.5797E+05	90.00	0.7607E+07	-18.90	0.1272E+08	12.03
3	0.6406E+05	54.08	0.6767E+07	-13.88	0.1358E+08	7.58
4	0.5524E+05	-56.14	0.6773E+07	14.50	0.1358E+08	-7.92
5	0.3794E+05	90.00	0.8043E+07	-14.60	0.1222E+08	10.14
6	0.3242E+05	80.05	0.8023E+07	-12.28	0.1222E+08	8.52
7	0.3218E+05	90.00	0.8193E+07	-13.24	0.1205E+08	9.47

8	0.1647E+06	15.11	0.8140E+07	-1.76	0.1205E+08	1.26
9	0.3819E+06	80.83	0.8214E+07	-15.52	0.1205E+08	11.11
10	0.3213E+06	90.00	0.8193E+07	-13.24	0.1205E+08	9.47
11	0.3827E+06	42.97	0.9053E+07	-17.59	0.1121E+08	14.58
12	0.1038E+06	90.00	0.8980E+07	-6.97	0.1119E+08	5.76
13	0.5085E+06	90.00	0.7749E+07	-17.43	0.1256E+08	11.42
14	0.5322E+06	32.53	0.7777E+07	-19.80	0.1255E+08	12.99
15	0.1177E+07	-0.85	0.1030E+08	-30.03	0.1022E+08	30.23
16	0.1152E+06	-2.75	0.1013E+08	-9.44	0.1005E+08	9.50
17	0.3081E+05	21.67	0.8723E+07	-1.67	0.1144E+08	1.32
18	0.1022E+06	-58.44	0.8729E+07	4.38	0.1144E+08	-3.87
19	0.1457E+05	2.19	0.9483E+07	-0.07	0.1066E+08	0.06
20	0.1932E+05	-59.51	0.9484E+07	2.02	0.1066E+08	-1.82
21	0.1038E+06	90.00	0.8980E+07	-6.97	0.1119E+08	5.76
22	0.5202E+05	1.16	0.8966E+07	-0.07	0.1119E+08	0.06
23	0.2554E+05	90.00	0.9513E+07	-3.36	0.1064E+08	3.05
24	0.1329E+05	-3.14	0.9510E+07	0.09	0.1063E+08	-0.03
25	0.1293E+06	37.29	0.9535E+07	-9.93	0.1065E+08	9.03
26	0.2554E+05	39.99	0.9513E+07	-3.36	0.1064E+08	3.05
27	0.3355E+05	35.60	0.9803E+07	-4.96	0.1035E+08	4.73
28	0.5279E+04	89.99	0.9797E+07	-1.59	0.1034E+08	1.52
29	0.1500E+06	-15.22	0.1034E+08	-10.44	0.9847E+07	10.90
30	0.3306E+05	-32.84	0.1033E+08	-4.74	0.9825E+07	4.95
31	0.2555E+05	-24.08	0.1024E+08	-4.28	0.9912E+07	4.40
32	0.8345E+04	-42.82	0.1023E+08	-2.33	0.9908E+07	2.40
33	0.3019E+04	-6.59	0.9803E+07	0.09	0.1034E+08	-0.09
34	0.3998E+04	-59.67	0.9803E+07	0.89	0.1034E+08	-0.85
35	0.6481E+03	-8.94	0.9946E+07	0.06	0.1019E+08	-0.05

36	0.8440E+03	-58.23	0.9946E+07	0.40	0.1019E+08	-0.39
37	0.1344E+03	-3.40	0.1001E+08	0.01	0.1013E+08	-0.01
38	0.1639E+03	-50.32	0.1001E+08	0.15	0.1013E+08	-0.15
39	0.2445E+02	33.02	0.1005E+08	-0.04	0.1009E+08	0.04
40	0.2248E+02	-0.02	0.1005E+08	0.00	0.1009E+08	0.00
41	0.5279E+04	89.99	0.9797E+07	-1.59	0.1034E+08	1.52
42	0.3143E+04	-4.05	0.9797E+07	0.05	0.1034E+08	-0.05
43	0.1461E+04	89.99	0.9938E+07	-0.76	0.1020E+08	0.74
44	0.7303E+03	-1.45	0.9938E+07	0.01	0.1020E+08	-0.01
45	0.3559E+03	89.99	0.1000E+08	-0.37	0.1014E+08	0.37
46	0.1799E+03	12.03	0.1000E+08	-0.04	0.1014E+08	0.04
47	0.1037E+03	90.00	0.1003E+08	-0.21	0.1011E+08	0.20
48	0.7056E+02	57.41	0.1003E+08	-0.11	0.1011E+08	0.11
49	0.7952E+04	35.25	0.9939E+07	-2.39	0.1020E+08	2.34
50	0.1461E+04	89.98	0.9938E+07	-0.76	0.1020E+08	0.74
51	0.1835E+04	35.28	0.1001E+08	-1.14	0.1014E+08	1.12
52	0.3550E+03	89.98	0.1000E+08	-0.37	0.1014E+08	0.37
53	0.4272E+03	41.80	0.1003E+08	-0.54	0.1011E+08	0.53
54	0.1037E+03	89.99	0.1003E+08	-0.21	0.1011E+08	0.20
55	0.1143E+03	64.51	0.1004E+08	-0.25	0.1010E+08	0.25
56	0.5511E+02	90.00	0.1004E+08	-0.15	0.1010E+08	0.16
57	0.5052E+04	-28.15	0.1016E+08	-1.90	0.9986E+07	1.93
58	0.1957E+04	-45.07	0.1015E+08	-1.12	0.9986E+07	1.14
59	0.1055E+04	-28.75	0.1011E+08	-0.87	0.1003E+08	0.88
60	0.4379E+03	-45.33	0.1011E+08	-0.53	0.1003E+08	0.54
61	0.2083E+03	-23.14	0.1008E+08	-0.39	0.1006E+08	0.39
62	0.9013E+02	-35.50	0.1008E+08	-0.25	0.1006E+08	0.25

63	0.3014E+02	14.71	0.1007E+08	-0.15	0.1007E+08	0.15
64	0.1580E+02	19.75	0.1007E+08	-0.11	0.1007E+08	0.11

- TT1 - Mechanical Stress (D.C. case)
- ANG1 - Mechanical Stress Angle (D.C. case)
- TT2 - Mechanical Stress (AC, negative maximum to positive maximum)
- ANG2 - Mechanical Stress Angle (AC, negative maximum to positive maximum)
- TT3 - Mechanical Stress (AC, positive maximum to negative maximum)
- ANG3 - Mechanical Stress Angle (AC, positive maximum to negative maximum)

ELECTROMECHANICAL STRESS ANALYSIS OF FERROELECTRIC MATERIAL

ELECTRICAL STRESS DISTRIBUTION

	EZ1	EA1	EZ2	EA2	EZ3	EA3
1	0.1962E+09	-93.96	0.0000E+00	0.00	0.0000E+00	0.00
2	0.2090E+09	-90.00	0.7558E+09	36.76	0.9795E+09	50.24
3	0.2197E+09	-107.96	0.7572E+09	35.55	0.9792E+09	51.02
4	0.2217E+09	-153.07	0.7142E+09	38.05	0.1012E+10	48.79
5	0.1591E+09	-90.00	0.7145E+09	52.25	0.1012E+10	41.04
6	0.1563E+09	-94.98	0.7786E+09	37.70	0.9598E+09	50.07
7	0.1557E+09	-90.00	0.7777E+09	38.86	0.9599E+09	49.26
8	0.1114E+09	-127.45	0.7859E+09	38.38	0.9531E+09	49.73
9	0.1597E+09	-85.41	0.7833E+09	44.12	0.9532E+09	45.63
10	0.1557E+09	-90.00	0.7868E+09	37.24	0.9531E+09	50.55
11	0.1693E+09	-65.49	0.7859E+09	38.38	0.9531E+09	49.73
12	0.3347E+08	-90.00	0.8261E+09	36.20	0.9193E+09	52.29
13	0.1958E+09	-90.00	0.8227E+09	41.51	0.9186E+09	47.88
14	0.2095E+09	-85.29	0.7643E+09	36.29	0.9729E+09	50.71
15	0.2978E+09	-44.58	0.7657E+09	35.10	0.9727E+09	51.50
16	0.9350E+08	-43.62	0.8810E+09	29.98	0.8779E+09	50.12
17	0.7804E+08	-124.17	0.8738E+09	40.28	0.8703E+09	49.75
18	0.8779E+08	-154.22	0.8109E+09	44.16	0.9288E+09	45.66
19	0.3314E+08	-133.90	0.8111E+09	47.44	0.9288E+09	43.07
20	0.3816E+08	-164.75	0.8455E+09	44.97	0.8965E+09	45.03
21	0.8846E+08	-90.00	0.8455E+09	46.01	0.8965E+09	44.09
22	0.5262E+08	-134.42	0.8227E+09	41.51	0.9186E+09	47.88
23	0.4472E+08	-90.00	0.8221E+09	44.96	0.9184E+09	45.03
24	0.3164E+08	-135.57	0.8468E+09	43.32	0.8954E+09	46.53
25	0.9873E+08	-63.64	0.8466E+09	45.05	0.8953E+09	44.96

26	0.4472E+03	-90.00	0.8478E+09	40.03	0.8959E+09	49.51
27	0.5029E+08	-62.80	0.8468E+09	43.32	0.8954E+09	46.53
28	0.2175E+08	-90.00	0.8596E+09	42.52	0.8832E+09	47.37
29	0.1063E+09	-37.39	0.8594E+09	44.20	0.8830E+09	45.76
30	0.4991E+08	-28.58	0.8829E+09	39.78	0.8615E+09	50.45
31	0.4339E+08	-32.96	0.8822E+09	42.63	0.8605E+09	47.48
32	0.2503E+08	-23.59	0.8734E+09	42.95	0.8644E+09	47.20
33	0.1508E+09	-138.30	0.8733E+09	43.83	0.8642E+09	46.20
34	0.1735E+08	-164.83	0.8596E+09	45.04	0.8828E+09	44.96
35	0.6989E+07	-139.47	0.8596E+09	45.45	0.8828E+09	44.57
36	0.7976E+07	-164.12	0.8659E+09	45.03	0.8766E+09	44.97
37	0.3183E+07	-136.70	0.8659E+09	45.20	0.8766E+09	44.81
38	0.3515E+07	-160.16	0.8688E+09	45.00	0.8737E+09	45.00
39	0.1358E+07	-118.49	0.8688E+09	45.08	0.8737E+09	44.92
40	0.1302E+07	-135.01	0.8702E+09	44.98	0.8722E+09	45.02
41	0.2175E+03	-90.00	0.8702E+09	45.00	0.8722E+09	45.00
42	0.1539E+08	-137.03	0.8594E+09	44.20	0.8830E+09	45.76
43	0.1049E+08	-89.99	0.8593E+09	45.03	0.8830E+09	44.97
44	0.7419E+07	-136.73	0.8655E+09	44.62	0.8769E+09	45.37
45	0.5179E+07	-90.00	0.8655E+09	45.00	0.8769E+09	45.00
46	0.3532E+07	-128.98	0.8684E+09	44.81	0.8740E+09	45.18
47	0.2862E+07	-90.00	0.8684E+09	44.98	0.8740E+09	45.02
48	0.2308E+07	-106.30	0.8697E+09	44.90	0.8728E+09	45.10
49	0.2450E+03	-62.62	0.8697E+09	44.94	0.8728E+09	45.06
50	0.1049E+08	-89.99	0.8656E+09	43.81	0.8770E+09	46.17
51	0.1176E+08	-63.14	0.8655E+09	44.62	0.8769E+09	45.37
52	0.5180E+07	-89.99	0.8684E+09	44.43	0.8741E+09	45.56
53	0.5674E+07	-65.90	0.8684E+09	44.81	0.8740E+09	45.18

54	0.2853E+07	-89.99	0.8697E+09	44.73	0.8728E+09	45.27
55	0.2935E+07	-77.25	0.8697E+09	44.90	0.8728E+09	45.10
56	0.2215E+07	-90.00	0.8700E+09	44.87	0.8724E+09	45.13
57	0.1953E+08	-30.92	0.8700E+09	44.92	0.8724E+09	45.08
58	0.1215E+08	-21.96	0.8749E+09	44.05	0.8676E+09	45.97
59	0.3918E+07	-30.63	0.8749E+09	44.44	0.8676E+09	45.57
60	0.5745E+07	-22.33	0.8729E+09	44.55	0.8695E+09	45.44
61	0.3962E+07	-33.43	0.8729E+09	44.73	0.8695E+09	45.27
62	0.2606E+07	-27.25	0.8718E+09	44.80	0.8706E+09	45.20
63	0.1507E+07	-52.36	0.8718E+09	44.87	0.8706E+09	45.13
64	0.1125E+07	-54.87	0.8711E+09	44.92	0.8714E+09	45.08

LEGEND

- EZ1 - Electric Stress (D.C. case)
- EA1 - Electric Stress Angle (D.C. case)
- EZ2 - Electric Stress (AC, negative maximum to positive maximum)
- EA2 - Electric Stress Angle (AC, negative maximum to positive maximum)
- EZ3 - Electric Stress (AC, positive maximum to negative maximum)
- EA3 - Electric Stress Angle (AC, positive maximum to negative maximum)

FINITE ELEMENT DESIGN OF PIN-TYPE INSULATOR

NODE POTENTIAL AT DIFF NODE(V)

1	11000.00
2	11000.00
3	11000.00
4	9120.88
5	8791.67
6	8736.80
7	8681.93
8	7858.87
9	5252.17
10	2505.52
11	1202.99
12	954.43
13	918.33
14	915.04
15	913.68
16	913.45
17	913.45
18	913.34
19	913.11
20	911.46
21	911.46
22	908.17
23	893.08
24	632.60
25	359.65
26	303.13

27	293.48
28	292.10
29	290.72
30	289.34
31	279.70
32	0.00
33	0.00
34	0.00
35	0.00
36	0.00
37	0.00
38	5474.58
39	9285.50
40	8654.49
41	8366.62
42	5449.17
43	5322.15
44	2220.62
45	1054.82
46	1417.09
47	581.56
48	905.03
49	988.88
50	365.40
51	919.98
52	251.44
53	914.07

ELECTRICAL STRESS DISTRIBUTION IN PIN-TYPE INSULATOR

	EZ1	EA1	EZ2	EA2	EZ3	EA3
1	0.115E+09	5.50	0.938E+09	41.76	0.802E+09	49.24
2	0.246E+08	25.57	0.889E+09	44.62	0.853E+09	45.41
3	0.431E+08	-12.27	0.889E+09	43.23	0.853E+09	46.90
4	0.985E+07	-68.20	0.868E+09	44.54	0.874E+09	45.46
5	0.409E+07	-115.57	0.868E+09	44.93	0.874E+09	45.07
6	0.114E+09	0.00	0.932E+09	41.38	0.809E+09	49.63
7	0.185E+09	-19.32	0.932E+09	37.50	0.812E+09	54.56
8	0.743E+08	-55.51	0.861E+09	41.22	0.882E+09	48.62
9	0.630E+08	-57.45	0.861E+09	41.82	0.882E+09	48.05
10	0.531E+08	-91.98	0.841E+09	43.05	0.901E+09	46.73
11	0.360E+09	-90.00	0.683E+09	25.51	0.105E+10	53.88
12	0.362E+09	-89.73	0.683E+09	25.34	0.104E+10	53.95
13	0.402E+09	-64.20	0.795E+09	21.57	0.967E+09	60.86
14	0.202E+09	-37.59	0.766E+09	35.67	0.972E+09	51.15
15	0.205E+09	-80.47	0.782E+09	34.85	0.959E+09	52.07
16	0.173E+09	-88.45	0.779E+09	37.34	0.959E+09	50.33
17	0.357E+09	-89.73	0.685E+09	25.71	0.104E+10	53.89
18	0.355E+09	-90.00	0.685E+09	25.88	0.104E+10	53.80
19	0.355E+09	-88.63	0.691E+09	25.64	0.104E+10	54.10
20	0.253E+09	-125.70	0.665E+09	41.86	0.105E+10	46.43
21	0.205E+09	-88.70	0.762E+09	35.59	0.975E+09	51.10
22	0.133E+09	-95.96	0.760E+09	37.68	0.976E+09	49.73
23	0.148E+09	-180.00	0.790E+09	51.22	0.949E+09	40.48
24	0.105E+09	-132.14	0.788E+09	44.69	0.949E+09	45.23
25	0.800E+08	-103.75	0.818E+09	42.66	0.923E+09	46.90
26	0.765E+08	-108.42	0.818E+09	43.07	0.923E+09	46.56

27	0.740E+08	-78.86	0.840E+09	41.69	0.903E+09	47.92
28	0.703E+08	-180.00	0.833E+09	47.72	0.909E+09	42.66
29	0.500E+08	-140.36	0.832E+09	45.28	0.909E+09	44.76
30	0.398E+08	-127.44	0.841E+09	44.72	0.901E+09	45.25
31	0.404E+08	-122.28	0.841E+09	44.52	0.901E+09	45.42
32	0.370E+08	-67.31	0.860E+09	43.23	0.882E+09	46.70
33	0.153E+08	-111.39	0.860E+09	44.68	0.882E+09	45.30
34	0.145E+08	-80.86	0.865E+09	44.40	0.878E+09	45.59
35	0.388E+08	-180.00	0.850E+09	46.45	0.892E+09	43.67
36	0.284E+08	-149.58	0.850E+09	45.38	0.892E+09	44.65
37	0.259E+08	-146.37	0.852E+09	45.27	0.891E+09	44.75
38	0.254E+08	-134.34	0.852E+09	44.98	0.891E+09	45.01
39	0.190E+08	-107.11	0.858E+09	44.54	0.884E+09	45.44
40	0.185E+08	-159.81	0.858E+09	45.40	0.884E+09	44.62
41	0.679E+07	-70.22	0.869E+09	44.69	0.873E+09	45.31
42	0.292E+07	-127.98	0.869E+09	44.98	0.873E+09	45.02
43	0.230E+07	-87.26	0.870E+09	44.91	0.872E+09	45.09
44	0.244E+08	-180.00	0.858E+09	45.90	0.884E+09	44.15
45	0.184E+08	-155.43	0.858E+09	45.33	0.884E+09	44.68
46	0.193E+08	-156.64	0.857E+09	45.37	0.885E+09	44.65
47	0.196E+08	-111.63	0.857E+09	44.60	0.885E+09	45.38
48	0.206E+07	-209.30	0.871E+09	45.10	0.872E+09	44.90
49	0.557E+06	-134.99	0.871E+09	45.00	0.872E+09	45.00
50	0.409E+05	-74.41	0.871E+09	44.98	0.871E+09	45.02
51	0.229E+06	-106.32	0.871E+09	44.99	0.871E+09	45.01
52	0.169E+08	-186.41	0.863E+09	45.68	0.879E+09	44.34
53	0.746E+07	-194.64	0.868E+09	45.33	0.874E+09	44.68

54	0.408E+07	-112.52	0.868E+09	44.92	0.874E+09	45.08
55	0.451E+06	-209.14	0.871E+09	45.02	0.871E+09	44.98
56	0.127E+06	-149.58	0.871E+09	45.00	0.871E+09	45.00
57	0.911E+05	-134.94	0.871E+09	45.00	0.871E+09	45.00
58	0.985E+05	-112.62	0.871E+09	45.00	0.871E+09	45.00
59	0.159E+07	-202.38	0.871E+09	45.08	0.872E+09	44.92
60	0.701E+06	-113.20	0.871E+09	44.99	0.872E+09	45.01
61	0.110E+06	-180.00	0.871E+09	45.00	0.871E+09	45.00
62	0.408E+05	-201.82	0.871E+09	45.00	0.871E+09	45.00
63	0.169E+05	-115.59	0.871E+09	45.00	0.871E+09	45.00
64	0.291E+05	-198.44	0.871E+09	45.01	0.871E+09	44.99
65	0.130E+06	-135.01	0.871E+09	45.00	0.871E+09	45.00
66	0.758E+04	-180.00	0.871E+09	45.00	0.871E+09	45.00

LEGEND

- EZ1** - **Electric Stress (D.C. case)**
- EA1** - **Electric Stress Angle (D.C. case)**
- EZ2** - **Electric Stress (AC, negative maximum to positive maximum)**
- EA2** - **Electric Stress Angle (AC, negative maximum to positive maximum)**
- EZ3** - **Electric Stress (AC, positive maximum to negative maximum)**
- EA3** - **Electric Stress Angle (AC, positive maximum to negative maximum)**

MECHANICAL STRESS DISTRIBUTION IN PIN-TYPE INSULATOR

	TT1	TT1	TT2	ANG2	TT3	ANG3
1	0.1745E+06	-79.01	0.1166E+08	-6.47	0.8536E+07	8.47
2	0.8004E+04	-36.87	0.1049E+08	-0.76	0.9657E+07	0.81
3	0.2462E+05	-65.46	0.1049E+08	-3.54	0.9560E+07	3.80
4	0.1290E+04	46.40	0.1000E+08	-0.92	0.1014E+08	0.91
5	0.2224E+03	36.87	0.1000E+08	-0.13	0.1014E+08	0.13
6	0.1729E+06	-90.00	0.1152E+08	-7.24	0.8674E+07	9.26
7	0.4552E+06	-51.36	0.1153E+08	-14.99	0.8757E+07	19.12
8	0.7333E+05	21.03	0.9842E+07	-7.55	0.1032E+08	7.25
9	0.5259E+05	24.89	0.9838E+07	-6.35	0.1032E+08	6.09
10	0.3741E+05	86.05	0.9387E+07	-3.89	0.1077E+08	3.46
11	0.1720E+07	90.00	0.6182E+07	-38.97	0.1449E+08	17.75
12	0.1735E+07	89.46	0.6191E+07	-39.31	0.1448E+08	17.92
13	0.2141E+07	38.41	0.8392E+07	-46.85	0.1241E+08	31.71
14	0.5408E+06	35.19	0.7792E+07	-18.65	0.1252E+08	12.29
15	0.5551E+06	70.93	0.8113E+07	-20.29	0.1221E+08	14.15
16	0.3975E+06	86.91	0.8058E+07	-15.33	0.1221E+08	10.66
17	0.1690E+07	89.46	0.6228E+07	-38.58	0.1443E+08	17.77
18	0.1675E+07	90.00	0.6220E+07	-38.24	0.1444E+08	17.61
19	0.1676E+07	87.27	0.6327E+07	-38.71	0.1433E+08	18.19
20	0.8492E+06	18.60	0.5861E+07	-6.28	0.1456E+08	2.87
21	0.5603E+06	87.40	0.7704E+07	-18.81	0.1262E+08	12.20
22	0.4454E+06	78.09	0.7659E+07	-14.63	0.1263E+08	9.47
23	0.2892E+06	-90.00	0.8236E+07	12.43	0.1195E+08	-9.05
24	0.1458E+06	5.71	0.8233E+07	-0.62	0.1195E+08	0.45
25	0.8493E+05	62.51	0.8871E+07	-4.67	0.1130E+08	3.79
26	0.7752E+05	53.15	0.8869E+07	-3.85	0.1130E+08	3.13
27	0.7258E+05	67.72	0.9352E+07	-6.62	0.1081E+08	5.84
28	0.5563E+05	-90.00	0.9199E+07	5.43	0.1096E+08	-4.67

29	0.3320E+05	-11.72	0.9191E+07	0.55	0.1096E+08	-0.48
30	0.2098E+05	15.13	0.9373E+07	-0.55	0.1077E+08	0.50
31	0.2167E+05	25.43	0.9373E+07	-0.95	0.1077E+08	0.85
32	0.1819E+05	44.61	0.9823E+07	-3.54	0.1032E+08	3.39
33	0.3124E+04	47.23	0.9820E+07	-0.64	0.1032E+08	0.61
34	0.2778E+04	71.72	0.9920E+07	-1.20	0.1022E+08	1.17
35	0.1997E+05	-90.00	0.9585E+07	2.90	0.1056E+08	-2.66
36	0.1067E+05	-29.15	0.9584E+07	0.75	0.1056E+08	-0.69
37	0.8917E+04	-22.74	0.9619E+07	0.54	0.1052E+08	-0.50
38	0.8571E+04	1.33	0.9619E+07	-0.03	0.1052E+08	0.03
39	0.4800E+04	55.78	0.9772E+07	-0.92	0.1037E+08	0.88
40	0.4551E+04	-49.61	0.9772E+07	0.31	0.1037E+08	-0.77
41	0.6124E+03	50.44	0.1002E+08	-0.62	0.1012E+08	0.62
42	0.1129E+03	14.04	0.1002E+08	-0.04	0.1012E+08	0.04
43	0.7029E+02	94.53	0.1004E+08	-0.17	0.1010E+08	0.17
44	0.7931E+04	-90.00	0.9764E+07	1.30	0.1038E+08	-1.70
45	0.4516E+04	-40.86	0.9763E+07	0.67	0.1038E+08	-0.63
46	0.4967E+04	-43.28	0.9751E+07	0.74	0.1039E+08	-0.70
47	0.5093E+04	46.75	0.9751E+07	-0.81	0.1039E+08	0.77
48	0.5621E+02	-31.41	0.1006E+08	0.20	0.1008E+08	-0.20
49	0.4118E+01	0.02	0.1006E+08	0.00	0.1008E+08	0.00
50	0.2220E+01	58.82	0.1007E+08	-0.04	0.1007E+08	0.04
51	0.6956E+00	57.36	0.1007E+08	-0.01	0.1007E+08	0.01
52	0.3782E+04	-77.17	0.9893E+07	1.36	0.1026E+08	-1.31
53	0.7391E+03	-60.73	0.1000E+08	0.66	0.1014E+08	-0.65
54	0.2212E+03	44.95	0.1000E+08	-0.16	0.1014E+08	0.16
55	0.2698E+01	-31.71	0.1007E+08	0.04	0.1007E+08	-0.04

FILE: NIPU OUTPUT A1 BUET COMPUTER CENTRE, DHAKA CMSI

55	0.2150E+00	-29.15	0.1007E+08	0.00	0.1007E+08	0.00
57	0.1101E+00	0.12	0.1007E+08	0.00	0.1007E+08	0.00
58	0.1237E+00	44.77	0.1007E+08	0.00	0.1007E+08	0.00
59	0.3795E+02	-45.24	0.1006E+08	0.16	0.1008E+08	-0.16
60	0.6512E+01	43.60	0.1006E+08	-0.03	0.1008E+08	0.03
61	0.1599E+00	-90.00	0.1007E+08	0.01	0.1007E+08	-0.01
62	0.2209E-01	-46.35	0.1007E+08	0.00	0.1007E+08	0.00
63	0.3801E-02	36.82	0.1007E+08	0.00	0.1007E+08	0.00
64	0.1123E+01	-53.13	0.1007E+08	0.03	0.1007E+08	-0.03
65	0.2246E+00	-0.01	0.1007E+08	0.00	0.1007E+08	0.00
66	0.7615E-03	-90.00	0.1007E+08	0.00	0.1007E+08	0.00

LEGEND

- TT1 - Mechanical Stress (D.C. case)
- ANG1 - Mechanical Stress Angle (D.C. case)
- TT2 - Mechanical Stress (AC, negative maximum to positive maximum)
- ANG2 - Mechanical Stress Angle (AC, negative maximum to positive maximum)
- TT3 - Mechanical Stress (AC, positive maximum to negative maximum)
- ANG3 - Mechanical Stress Angle (AC, positive maximum to negative maximum)

FINITE ELEMENT DESIGN OF DISC-TYPE INSULATOR

NODE POTENTIALS AT DIFF NODES

1	0.00
2	0.00
3	0.00
4	0.00
5	0.00
6	0.00
7	0.00
8	0.00
9	0.00
10	0.00
11	5556.95
12	5903.49
13	5993.45
14	6018.50
15	6024.98
16	6028.96
17	6029.27
18	6029.34
19	6029.37
20	6029.38
21	6029.38
22	6029.38
23	6029.38
24	6029.38
25	6029.39
26	6029.41

FILE: BIS OUTPUT A1 BUET COMPUTER CENTRE. DHAKA

27	5029.45
28	5029.55
29	6031.14
30	6038.59
31	6043.54
32	6044.25
33	6044.95
34	6045.66
35	6050.63
36	6129.12
37	6265.72
38	6599.45
39	7626.07
40	11000.00
41	11000.00
42	11000.00
43	11000.00
44	11000.00
45	11000.00
46	11000.00
47	11000.00
48	11000.00
49	5377.84
50	5255.69
51	4644.95
52	2324.14
53	4651.60

54 5282.28
 55 5477.58
 56 5628.10
 57 6034.91
 58 7511.59
 59 4872.10
 60 8139.37
 61 6419.87
 62 6058.58
 63 6031.77
 64 6025.91
 65 6027.80
 66 6028.22
 67 6265.72
 68 6029.39
 69 5029.37
 70 5029.41
 71 5029.38
 72 5029.38

MECHANICAL STRESS DISTRIBUTION IN DISC-TYPE INSULATOR

	TT1	ANG1	TT2	ANG2	TT3	ANG3
1	0.163E+07	90.00	0.144E+08	17.47	0.626E+07	-37.56
2	0.156E+07	87.28	0.144E+08	16.67	0.622E+07	-35.93
3	0.156E+07	90.00	0.143E+08	17.22	0.632E+07	-36.41
4	0.125E+07	74.77	0.144E+08	13.21	0.615E+07	-28.21
5	0.123E+07	90.00	0.139E+08	15.91	0.566E+07	-30.87
6	0.632E+06	0.08	0.140E+08	0.01	0.635E+07	-0.02
7	0.633E+06	0.00	0.140E+08	0.00	0.635E+07	0.00
8	0.178E+07	87.45	0.147E+08	17.39	0.603E+07	-39.46
9	0.185E+07	90.00	0.146E+08	18.16	0.608E+07	-41.11

10	0.187E+07	77.55	0.151E+08	15.49	0.557E+07	-38.77
11	0.224E+07	90.00	0.150E+08	19.21	0.580E+07	-47.31
12	0.255E+07	48.85	0.170E+08	10.10	0.394E+07	-37.59
13	0.255E+07	-48.71	0.170E+08	-10.06	0.394E+07	37.48
14	0.534E+06	0.08	0.140E+08	0.01	0.634E+07	-0.02
15	0.124E+07	-90.00	0.139E+08	-15.92	0.665E+07	30.92
16	0.224E+07	-90.00	0.150E+08	-19.20	0.581E+07	47.24
17	0.186E+07	-77.09	0.151E+08	-15.36	0.556E+07	38.42
18	0.126E+07	-74.30	0.144E+08	-13.14	0.613E+07	28.18
19	0.158E+07	-90.00	0.143E+08	-17.28	0.631E+07	36.66
20	0.184E+07	-90.00	0.146E+08	-18.11	0.609E+07	40.85
21	0.172E+07	-85.85	0.148E+08	-16.87	0.602E+07	38.20
22	0.158E+07	-85.67	0.145E+08	-16.40	0.614E+07	35.89
23	0.169E+07	-90.00	0.145E+08	-17.66	0.621E+07	38.51
24	0.172E+07	-90.00	0.145E+08	-17.75	0.618E+07	38.94
25	0.163E+07	-86.72	0.145E+08	-16.77	0.613E+07	36.93
26	0.169E+07	-86.78	0.146E+08	-16.98	0.608E+07	37.94
27	0.178E+07	-90.00	0.146E+08	-17.95	0.613E+07	39.97
28	0.163E+07	-90.00	0.144E+08	-17.45	0.626E+07	37.50
29	0.141E+07	-80.45	0.144E+08	-14.80	0.614E+07	32.04
30	0.179E+07	-81.53	0.149E+08	-16.14	0.579E+07	38.42
31	0.203E+07	-90.00	0.148E+08	-18.58	0.594E+07	44.01
32	0.140E+07	-90.00	0.141E+08	-16.62	0.647E+07	33.72
33	0.834E+06	-43.79	0.142E+08	-6.72	0.617E+07	13.89
34	0.216E+07	-61.79	0.161E+08	-12.56	0.473E+07	38.09
35	0.175E+07	32.48	0.163E+08	6.14	0.443E+07	-19.08
36	0.138E+07	73.71	0.135E+08	19.58	0.710E+07	-35.46

37	0.706E+06	-90.00	0.130E+08	-12.98	0.738E+07	21.38
38	0.501E+06	-65.10	0.130E+08	-8.31	0.729E+07	13.74
39	0.431E+06	-63.11	0.128E+08	-7.51	0.745E+07	12.18
40	0.315E+06	-5.99	0.128E+08	-0.65	0.741E+07	1.04
41	0.159E+06	42.20	0.108E+08	10.02	0.938E+07	-11.33
42	0.227E+05	21.04	0.108E+08	0.72	0.935E+07	-0.81
43	0.226E+05	21.77	0.102E+08	4.05	0.994E+07	-4.15
44	0.105E+04	57.98	0.102E+08	0.43	0.993E+07	-0.44
45	0.145E+04	19.92	0.101E+08	1.04	0.100E+08	-1.04
46	0.643E+02	69.54	0.101E+08	0.13	0.100E+08	-0.13
47	0.993E+02	14.68	0.101E+08	0.27	0.101E+08	-0.27
48	0.532E+01	67.01	0.101E+08	0.05	0.101E+08	-0.05
49	0.759E+01	20.24	0.101E+08	0.08	0.101E+08	-0.08
50	0.630E+00	75.15	0.101E+08	0.02	0.101E+08	-0.02
51	0.652E+00	64.31	0.101E+08	0.02	0.101E+08	-0.02
52	0.493E+06	-69.53	0.121E+08	-13.62	0.825E+07	19.02
53	0.189E+06	-56.69	0.111E+08	-9.78	0.910E+07	11.61
54	0.641E+05	-70.14	0.111E+08	-3.71	0.907E+07	4.41
55	0.920E+04	-35.85	0.105E+08	-0.79	0.963E+07	0.85
56	0.888E+04	-28.85	0.105E+08	-0.63	0.963E+07	0.68
57	0.238E+04	68.85	0.103E+08	0.75	0.987E+07	-0.78
58	0.166E+04	-19.04	0.103E+08	-0.18	0.987E+07	0.19
59	0.562E+03	83.11	0.102E+08	0.43	0.998E+07	-0.44
60	0.400E+03	-55.04	0.102E+08	-0.25	0.998E+07	0.26
61	0.353E+02	81.25	0.101E+08	0.13	0.101E+08	-0.13
62	0.154E+02	-6.31	0.101E+08	-0.01	0.101E+08	0.01
63	0.688E+01	85.52	0.101E+08	0.05	0.101E+08	-0.05
64	0.378E+01	-47.27	0.101E+08	-0.02	0.101E+08	0.02

65	0.534E+00	61.57	0.101E+08	0.02	0.101E+08	-0.02
66	0.170E+00	-49.54	0.101E+08	0.00	0.101E+08	0.00
67	0.258E-01	35.05	0.101E+08	0.00	0.101E+08	0.00
68	0.235E-02	-9.53	0.101E+08	0.00	0.101E+08	0.00
69	0.127E-02	32.78	0.101E+08	0.00	0.101E+08	0.00
70	0.105E-03	22.62	0.101E+08	0.00	0.101E+08	0.00
71	0.739E-04	77.32	0.101E+08	0.00	0.101E+08	0.00
72	0.658E+04	-90.00	0.104E+08	-1.56	0.979E+07	1.63
73	0.110E+04	-90.00	0.102E+08	-0.65	0.996E+07	0.66
74	0.100E+02	-45.19	0.101E+08	-0.08	0.101E+08	0.08
75	0.172E+01	43.56	0.101E+08	0.01	0.101E+08	-0.01
76	0.297E+00	-53.00	0.101E+08	-0.01	0.101E+08	0.01
77	0.591E-01	0.63	0.101E+08	0.00	0.101E+08	0.00
78	0.189E-02	-26.78	0.101E+08	0.00	0.101E+08	0.00
79	0.113E-03	-36.87	0.101E+08	0.00	0.101E+08	0.00
80	0.550E-04	-10.39	0.101E+08	0.00	0.101E+08	0.00
81	0.586E-04	-30.51	0.101E+08	0.00	0.101E+08	0.00
82	0.153E-04	61.93	0.101E+08	0.00	0.101E+08	0.00
83	0.451E-05	-36.87	0.101E+08	0.00	0.101E+08	0.00
84	0.902E-05	90.00	0.101E+08	0.00	0.101E+08	0.00
85	0.902E-04	-90.00	0.101E+08	0.00	0.101E+08	0.00
86	0.442E-04	-90.00	0.101E+08	0.00	0.101E+08	0.00
87	0.721E-05	0.00	0.101E+08	0.00	0.101E+08	0.00
88	0.000E+00	90.00	0.101E+08	0.00	0.101E+08	0.00
89	0.000E+00	90.00	0.101E+08	0.00	0.101E+08	0.00
90	0.000E+00	90.00	0.101E+08	0.00	0.101E+08	0.00
91	0.000E+00	90.00	0.101E+08	0.00	0.101E+08	0.00

FILE: BIS OUTPUT A1 BUET COMPUTER CENTRE, DHAKA CMS:

92	0.000E+00	90.00	0.101E+08	0.00	0.101E+08	0.00
93	0.000E+00	90.00	0.101E+08	0.00	0.101E+08	0.00

LEGEND

- TT1 - Mechanical Stress (D.C. case)
- ANG1 - Mechanical Stress Angle (D.C. case)
- TT2 - Mechanical Stress (AC, negative maximum to positive maximum)
- ANG2 - Mechanical Stress Angle (AC, negative maximum to positive maximum)
- TT3 - Mechanical Stress (AC, positive maximum to negative maximum)
- ANG3 - Mechanical Stress Angle (AC, positive maximum to negative maximum)

ELECTRICAL STRESS DISTRIBUTION IN DISC-TYPE INSULATOR

	EZ1	EA1	EZ2	EA2	EZ3	EA3
1	0.351E+09	-90.00	0.104E+10	53.73	0.687E+09	26.22
2	0.343E+09	88.64	0.104E+10	53.34	0.685E+09	27.03
3	0.343E+09	-90.00	0.104E+10	53.61	0.590E+09	26.80
4	0.308E+09	82.39	0.104E+10	51.60	0.681E+09	30.89
5	0.305E+09	-90.00	0.102E+10	52.96	0.708E+09	29.57
6	0.218E+09	45.04	0.103E+10	45.01	0.692E+09	44.99
7	0.218E+09	45.00	0.103E+10	45.00	0.692E+09	45.00
8	0.366E+09	88.72	0.105E+10	53.59	0.574E+09	25.27
9	0.374E+09	-90.00	0.105E+10	54.08	0.677E+09	24.45
10	0.376E+09	83.78	0.107E+10	52.75	0.648E+09	25.61
11	0.411E+09	-90.00	0.106E+10	54.61	0.661E+09	21.35
12	0.439E+09	69.43	0.113E+10	50.05	0.545E+09	26.20
13	0.439E+09	20.64	0.113E+10	39.97	0.545E+09	53.74
14	0.219E+09	45.04	0.103E+10	45.01	0.691E+09	44.99
15	0.305E+09	0.00	0.102E+10	37.04	0.708E+09	50.46
16	0.411E+09	0.00	0.106E+10	35.40	0.662E+09	58.62
17	0.374E+09	6.45	0.107E+10	37.32	0.648E+09	54.21
18	0.308E+09	7.85	0.104E+10	38.43	0.580E+09	59.09
19	0.345E+09	0.00	0.104E+10	36.36	0.689E+09	53.33
20	0.372E+09	0.00	0.105E+10	35.94	0.677E+09	55.42
21	0.360E+09	2.07	0.105E+10	36.56	0.674E+09	54.10
22	0.345E+09	2.15	0.105E+10	36.80	0.580E+09	62.95
23	0.357E+09	0.00	0.104E+10	36.17	0.684E+09	54.26
24	0.360E+09	0.00	0.104E+10	36.12	0.683E+09	54.47
25	0.351E+09	1.64	0.105E+10	36.51	0.680E+09	53.46

26	0.357E+09	1.61	0.105E+10	36.51	0.677E+09	63.97
27	0.365E+09	0.00	0.105E+10	36.02	0.680E+09	64.98
28	0.351E+09	0.00	0.104E+10	36.27	0.687E+09	63.75
29	0.326E+09	4.77	0.104E+10	37.60	0.680E+09	61.02
30	0.367E+09	4.24	0.106E+10	36.93	0.661E+09	64.21
31	0.391E+09	0.00	0.106E+10	35.66	0.669E+09	67.01
32	0.325E+09	0.00	0.103E+10	36.69	0.699E+09	61.86
33	0.251E+09	23.10	0.104E+10	41.64	0.682E+09	51.95
34	0.404E+09	14.11	0.110E+10	38.72	0.597E+09	64.05
35	0.364E+09	61.24	0.111E+10	48.07	0.578E+09	35.46
36	0.322E+09	-261.8	0.101E+10	54.84	0.732E+09	27.27
37	0.231E+09	0.00	0.989E+09	38.51	0.746E+09	55.69
38	0.194E+09	12.45	0.990E+09	40.84	0.741E+09	51.87
39	0.180E+09	13.44	0.983E+09	41.20	0.749E+09	51.09
40	0.154E+09	42.00	0.984E+09	44.68	0.747E+09	45.52
41	0.113E+09	-246.100	0.903E+09	50.01	0.841E+09	39.34
42	0.414E+08	55.52	0.902E+09	45.36	0.840E+09	44.59
43	0.412E+08	-235.9	0.877E+09	47.02	0.865E+09	42.93
44	0.891E+07	73.99	0.877E+09	45.22	0.865E+09	44.78
45	0.105E+08	-234.9	0.873E+09	45.52	0.870E+09	44.48
46	0.220E+07	79.77	0.873E+09	45.06	0.870E+09	44.94
47	0.274E+07	-232.3	0.871E+09	45.14	0.871E+09	44.85
48	0.633E+06	-258.5	0.871E+09	45.03	0.871E+09	44.97
49	0.756E+06	-235.1	0.871E+09	45.04	0.871E+09	44.96
50	0.218E+06	-262.6	0.871E+09	45.01	0.871E+09	44.99
51	0.222E+06	-257.2	0.871E+09	45.01	0.871E+09	44.99
52	0.193E+09	-10.23	0.953E+09	38.19	0.788E+09	54.51
53	0.119E+09	-16.65	0.915E+09	40.11	0.828E+09	50.81

54	0.595E+08	9.93	0.914E+09	43.14	0.827E+09	47.21
55	0.263E+08	27.08	0.890E+09	44.61	0.852E+09	45.43
56	0.259E+08	30.57	0.890E+09	44.69	0.852E+09	45.34
57	0.134E+08	79.42	0.880E+09	45.38	0.863E+09	44.61
58	0.112E+08	35.48	0.880E+09	44.91	0.863E+09	45.10
59	0.651E+07	36.56	0.875E+09	45.22	0.867E+09	44.78
60	0.349E+07	17.48	0.875E+09	44.87	0.867E+09	45.13
61	0.165E+07	-265.6	0.872E+09	45.06	0.870E+09	44.94
62	0.108E+07	41.85	0.872E+09	45.00	0.870E+09	45.00
63	0.720E+06	-267.8	0.872E+09	45.03	0.871E+09	44.97
64	0.534E+06	21.36	0.872E+09	44.99	0.871E+09	45.01
65	0.201E+06	-255.8	0.871E+09	45.01	0.871E+09	44.99
66	0.113E+06	20.23	0.871E+09	45.00	0.871E+09	45.00
67	0.441E+05	-242.5	0.871E+09	45.00	0.871E+09	45.00
68	0.133E+05	40.24	0.871E+09	45.00	0.871E+09	45.00
69	0.930E+04	-241.4	0.871E+09	45.00	0.871E+09	45.00
70	0.282E+04	56.31	0.871E+09	45.00	0.871E+09	45.00
71	0.236E+04	-253.7	0.871E+09	45.00	0.871E+09	45.00
72	0.223E+08	0.00	0.883E+09	44.22	0.859E+09	45.82
73	0.912E+07	0.00	0.876E+09	44.58	0.866E+09	45.33
74	0.869E+06	-22.40	0.871E+09	44.96	0.871E+09	45.04
75	0.360E+06	66.78	0.871E+09	45.01	0.871E+09	44.99
76	0.150E+06	-18.50	0.871E+09	44.99	0.871E+09	45.01
77	0.567E+05	45.32	0.871E+09	45.00	0.871E+09	45.00
78	0.119E+05	-31.61	0.871E+09	45.00	0.871E+09	45.00
79	0.291E+04	26.57	0.871E+09	45.00	0.871E+09	45.00
80	0.204E+04	39.81	0.871E+09	45.00	0.871E+09	45.00
81	0.210E+04	29.74	0.871E+09	45.00	0.871E+09	45.00

82	0.107E+04	-255.9	0.871E+09	45.00	0.871E+09	45.00
83	0.583E+03	26.57	0.871E+09	45.00	0.871E+09	45.00
84	0.261E+03	-90.00	0.871E+09	45.00	0.871E+09	45.00
85	0.261E+04	0.00	0.871E+09	45.00	0.871E+09	45.00
86	0.182E+04	0.00	0.871E+09	45.00	0.871E+09	45.00
87	0.737E+03	-45.00	0.871E+09	45.00	0.871E+09	45.00
88	0.000E+00	-90.00	0.871E+09	45.00	0.871E+09	45.00
89	0.000E+00	-90.00	0.871E+09	45.00	0.871E+09	45.00
90	0.000E+00	-90.00	0.871E+09	45.00	0.871E+09	45.00
91	0.000E+00	-90.00	0.871E+09	45.00	0.871E+09	45.00
92	0.000E+00	-90.00	0.871E+09	45.00	0.871E+09	45.00
93	0.000E+00	-90.00	0.871E+09	45.00	0.871E+09	45.00

LEGEND

- EZ1 - Electric Stress (D.C. case)
- EA1 - Electric Stress Angle (D.C. case)
- EZ2 - Electric Stress (AC, negative maximum to positive maximum)
- EA2 - Electric Stress Angle (AC, negative maximum to positive maximum)
- EZ3 - Electric Stress (AC, positive maximum to negative maximum)
- EA3 - Electric Stress Angle (AC, positive maximum to negative maximum)

REFERENCES

- [01] M. Ieda, "Dielectric Breakdown Process of Polymer" IEEE Trans. Vol. EI-15 PP - 206-224, 1980
- [02] P.K. Mukherjee and C.K. Roy, "Computation of Fields in and around Insulators by Fictitious Point Charge Method", IEEE Trans, Vol. EI-13 No. 1, 1978
- [03] D.D. Chang, T.S. Sudarshan and J.E Thompson, "Analysis of Electric Stress Distribution in Cavities Embded within Dielectric Structures" IEEE Trans, Vol. EI-21, No. 2, 1986
- [04] Takeshi Takashima and Ryoze Ishibashi, "Electric Fields in Dielectric Multilayers Calculated by Digital Computers" IEEE Trans. Vol. EI-13, No. 1, 1978
- [05] Tadasu Takuma, "Field behaviour near singular Points in Composite Dielectric Arrangements", IEEE Trans. Vol. EI-13 No. 6, 1978
- [06] T. Takada and T. Sakai, "Measurement of Electric Fields at a Dielectric/Electrode Interface Using an Acqustic Tranducer Technique", IEEE Trans. Vol. EI-18, No. 6, 1983
- [07] Hen Kun, "Computation of Electric Fields and Study of Optimal Corona Suspension for Bushing Type Insulators", IEEE Trans, Vol. EI-21, No. 1, 1986
- [08] M. Abdel Salam and E.K. Stanek, "Optimizing Field Stress on High Voltage Insulators" IEEE Trans, Vol. EI-22 No. 1, 1987
- [09] Z. Stih, "High Voltage Insulating System Design by Application of Electrode and Insulator Contour Optimization", IEEE Trans. Vol. EI-21 No. 4, 1986
- [10] R.K. Begg, "Calcalaton of Electromechanical Stress Distribution in Insulators Using Finite Element Method" MSc Thesis, Dept. of Electrical & Electronic Engg., BUET, Dhaka May, 1987.
- [11] J.A. Stratton, "Electromagnetic Theory" McGraw Hill Book Co. New York and London, 1941

- [12] K. Itaka and H. Hara, "Optimization of Three Dimensional Electrode Contour Based on Surface charge Method and its Application to Insulator Design", IEE Trans Vol. PAS-102, No. 6, 1983
- [13] A.J. Dekker "Electrical Engineering Material" Prentice Hall of India, New Delhi, 1984
- [14] Takeo FuruKawa, "Piezoelectricity and Pyroelectricity in Polymers", IEEE Trans. Vol. EI-24, No. 3, 1989
- [15] Y. Wada, "Ferro, Piezo and Pyroelectricity" IEEE Trans. Vol. EI-22, No. 3, 1987
- [16] Kenji Morita and Takashi Imakoma", Long Term performance of Ceramic Insulators", IEEE Thailand, HVPS, Bangkok Thailand, 1984
- [17] T. Imakoma, Y Suzuki and K. Arakawa, "Insulator Pollution" Research Paper, NGK Insulators Ltd. Japan
- [18] K. Naito, K. Morita, Y Hasegawa and T. Imakoma, "Improvement of the dc Voltage Insulation Efficiency of Suspension Insulators Under Contaminated Conditions" IEEE Trans. Vol 23, No. 6, 1988.
- [19] Test Report of W.S. Insulators (India) carried by the Swedish State Power Board Materials Laboratory. No. 43E.83 dated 16.9.1983.

